



## Supporting Information

### **Covalent Template-Directed Synthesis of a Spoked 18-Porphyrin Nanoring**

*M. A. Majewski, W. Stawski, J. M. Van Raden, M. Clarke, J. Hart, J. N. O'Shea, A. Saywell\*,  
H. L. Anderson\**

## Table of Contents

Section 1. General Methods	S2
Section 2. Synthetic Procedures	S3
Section 3. Comparison of UV-vis-NIR Spectra	S10
Section 4. NMR and Mass Spectra	S11
Section 5. STM Studies	S35
Section 6. Calculated Molecular Geometries	S39
Section 7. References	S50

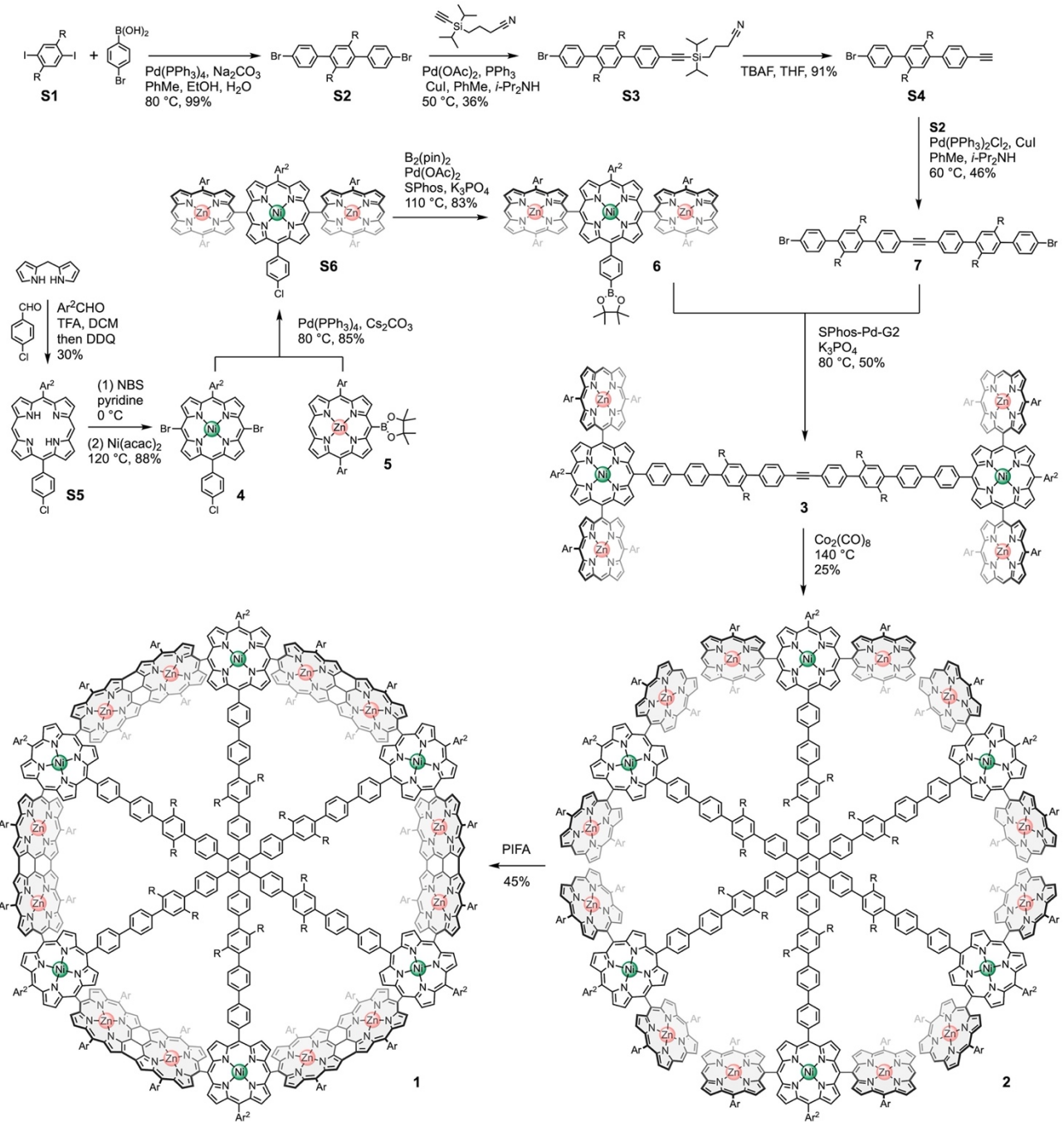
## 1. General Methods

Dichloromethane, toluene and DMF for reactions were obtained from an MBraun MBSPS-5-BenchTop solvent purification system (SPS) under nitrogen. Chloroform-*d* for NMR was stored over K<sub>2</sub>CO<sub>3</sub> and passed through a short neutral alumina plug prior to use. Bis(pinacolato)diboron was recrystallized from warm pentane. All other reagents and solvents were obtained from commercial suppliers and used as received unless otherwise stated. 1,4-Diido-2,5-dioctylbenzene **S1**, 3,5-bis(trihexylsilyl)benzaldehyde and 5-(4,4,5,5-tetramethyl-1,3,2-dioxaborolan-2-yl)-10,20-bis(3,5-dioctyloxyphenyl)porphyrinato zinc(II) **5** were prepared as described in the literature.<sup>[1-3]</sup>

Thin-layer chromatography (TLC) was carried out using commercially available (Merck) aluminum sheets precoated with silica gel with fluorescence indicator and visualized under UV light at 254 or 360 nm. Purification by column chromatography was carried out on silica gel (SiO<sub>2</sub>, 60 Å, 40–63 µm, Merck). Size exclusion chromatography (SEC) was performed on gravity columns filled with Bio Beads S-X1. Analytical GPC was carried out using Jaigel-3H-A (8 × 500 mm) and Jaigel-4H-A (8 × 500 mm) columns in THF + 1% pyridine as eluent with a flow rate of 1.0 mL/min. Semipreparative GPC was carried out on a Shimadzu recycling GPC system equipped with a LC-20 AD pump, SPD20A UV detector and a set of JAIGEL 3H (20 × 600 mm) and JAIGEL 4H (20 × 600 mm) columns in toluene + 1% pyridine as the eluent at a flow rate of 3.5 mL/min. Pyridine after separations was removed fully on a rotary evaporator by adding toluene and evaporating to dryness and repeating the process four times.

<sup>1</sup>H and <sup>13</sup>C NMR spectra were recorded on either a Bruker AVIII HD 400, a Bruker AVIII HD 500, or a Bruker AVIII 600 with a broadband cryo-probe. Chemical shift values are quoted in ppm and coupling constants (*J*, reported <sup>3</sup>*J*<sub>H-H</sub> if not indicated differently) in Hertz to the nearest 0.1 Hz. Multiplicity is described as follows: s – singlet, d – doublet, t – triplet, m – multiplet, br. – broadened. <sup>1</sup>H and <sup>13</sup>C NMR spectra are referenced against the residual solvent peak (CHCl<sub>3</sub> δ<sub>H</sub> = 7.26 ppm, CDCl<sub>3</sub> δ<sub>C</sub> = 77.16 ppm). UV-vis-NIR measurements were carried out in a 1 cm path length glass cuvette at 298 K using either a Perkin Lambda 20 or a Jasco V770 spectrophotometer (for NIR-absorbing compounds). Mass spectra were recorded using MALDI-TOF method using Bruker Autoflex instrument with DCTB as a matrix. Calibration was performed before each measurement using Peptide Standard II for the 700–3500 Da Protein Standard I for the 5–20 kDa window (Bruker). Mass spectra of compounds with molecular weight up to 3.5 kDa were measured in a reflectron mode whereas for larger mass a linear mode was used.

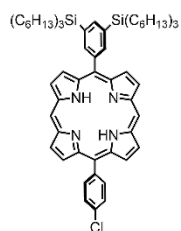
## 2. Synthetic Procedures



**Scheme S1.** Summary of synthetic route. ( $\text{Ar} = 3,5\text{-bis(octyloxy)phenyl}$ ,  $\text{Ar}^2 = 3,5\text{-bis(tri-}n\text{-hexylsilyl)phenyl}$ ,  $\text{R} = n\text{-C}_8\text{H}_{17}$ .)

### Synthesis of 5-(3,5-bis(trihexylsilyl)phenyl)-15-(4-chlorophenyl)porphyrin S5.

3,5-Bis(trihexylsilyl)benzaldehyde<sup>[2]</sup> (1.52 g, 1 equiv., 2.26 mmol), 4-chlorobenzaldehyde (1.27 g, 4 equiv., 9.06 mmol) and dipyrromethane (1.65 g, 5 equiv., 11.3 mmol) were dissolved in dichloromethane (1.5 L). The solution was purged with nitrogen, then trifluoroacetic acid (3.1 g, 2.1 mL, 12 equiv., 27.2 mmol) was added and the mixture was stirred at room temperature for 3 h in the dark. DDQ (3.85 g, 7.5 equiv., 17.0 mmol) was added and stirring was continued for 40 min. Finally, triethylamine (8.02 g, 11.0 mL, 35 equiv., 79.2 mmol) was added and the mixture was stirred for an additional 30 min. The solution was concentrated and passed through two silica plugs using dichloromethane/petroleum ether (1:4). Solvents were removed giving a mixture of different porphyrins. The crude mixture was purified on silica gel, first with



DCM/PE, 1:10 to separate bis-THS condensed byproduct, then the desired product was eluted using DCM/PE, 1:5, followed by another byproduct (bis(chlorophenyl)porphyrin) eluted in DCM. Organic fractions were concentrated, precipitated from DCM/methanol on a rotary evaporator and dried, yielding **S5** as a purple semisolid (710 mg, 30%).

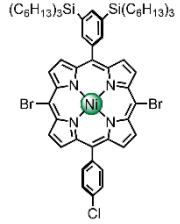
**<sup>1</sup>H NMR** (400 MHz, CDCl<sub>3</sub>, 298 K): δ<sub>H</sub> 10.34 (s, 2H, *meso*-H), 9.43 (d, *J* = 4.4 Hz, 2H, β-H), 9.41 (d, *J* = 4.4 Hz, 2H, β-H), 9.10 (d, *J* = 4.4 Hz, 2H, β-H), 9.07 (d, *J* = 4.4 Hz, 2H, β-H), 8.36 (d, *J* = 1.2 Hz, 2H, *o*-Ph), 8.23 (d, *J* = 8.2 Hz, 2H, Ph(Cl)-H), 8.03 (t, *J* = 1.2 Hz, 1H, *p*-Ph), 7.81 (d, *J* = 8.2 Hz, 2H, Ph(Cl)-H), 1.51 (p, 12H, overlapping with H<sub>2</sub>O, CH<sub>2</sub>), 1.39 (p, 12H, CH<sub>2</sub>), 1.32 (m, 24H, CH<sub>2</sub>), 0.95 (m, 12H, CH<sub>2</sub>), 0.88 (t, *J* = 6.9 Hz, 18H, CH<sub>3</sub>), -3.08 (s, 2H, NH).

**<sup>13</sup>C NMR** (151 MHz, CDCl<sub>3</sub>) δ<sub>C</sub> 147.5, 146.9, 145.3, 145.2, 141.0, 140.0, 139.4, 139.3, 135.8, 135.4, 134.2, 131.8, 131.5, 131.3, 130.6, 127.2, 120.8, 117.1, 105.3, 33.5, 31.6, 24.0, 22.6, 14.1, 12.7.

**HRMS (MALDI):** *m/z* calcd for C<sub>68</sub>H<sub>97</sub>ClN<sub>4</sub>Si<sub>2</sub>: 1060.694 [M]<sup>+</sup>; found: 1060.505.

#### **Synthesis of 5-(3,5-bis(trihexylsilyl)phenyl)-15-(4-chlorophenyl)porphyrinato nickel(II) **4**.**

Porphyrin **S5** (1.29 g, 1 equiv., 1.22 mmol) was dissolved in chloroform (235 mL) and pyridine (12 mL), then NBS (432 mg, 2 equiv., 2.43 mmol) was added as a CHCl<sub>3</sub>/pyridine solution (12 mL + 0.6 mL) and the mixture was stirred for 3 h at 0 °C. The resulting crude was subjected to a short chromatography column in chloroform. The first fraction was collected and evaporated to leave a dark green solid and was used without further purification. The crude product and nickel acetylacetone dihydrate (2.11 g, 6 equiv., 7.21 mmol) were dissolved in xylenes (120 mL), purged with argon, and heated at 120 °C on an oil bath for 4 h. The crude product was passed through a short silica plug in DCM and precipitated from DCM and MeOH on a rotary evaporator to give a red residue. Purification by column chromatography using DCM/PE (1:10), evaporation of organic fractions and additional wash with MeOH gave **4** as a red semisolid (1.35 g, 88%).

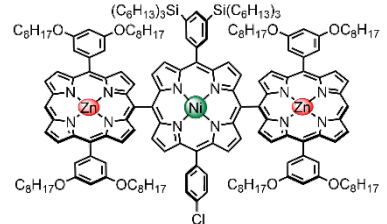


**<sup>1</sup>H NMR** (400 MHz, CDCl<sub>3</sub>, 298 K): δ<sub>H</sub> 9.46 (d, *J* = 4.9 Hz, 2H, β-H), 9.44 (d, *J* = 4.9 Hz, 2H, β-H), 8.72 (d, *J* = 4.9 Hz, 2H, β-H), 8.68 (d, *J* = 4.9 Hz, 2H, β-H), 8.01 (d, *J* = 1.1 Hz, 2H, *o*-Ph), 7.92 (t, *J* = 1.1 Hz, 1H, *p*-Ph), 7.87 (d, *J* = 8.3 Hz, 2H, Ph(Cl)-H), 7.68 (d, *J* = 8.3 Hz, 2H, Ph(Cl)-H), 1.47–1.26 (overlapping m, 60H, CH<sub>2</sub>), 0.90–0.84 (m, 18H, CH<sub>3</sub>).

**<sup>13</sup>C NMR** (151 MHz, CDCl<sub>3</sub>, 298 K): δ<sub>C</sub> 144.0, 142.9, 142.8, 142.7, 139.7, 139.6, 138.5, 138.0, 135.6, 134.6, 134.5, 134.0, 133.7, 133.5, 133.2, 127.3, 121.5, 118.1, 102.8, 33.5, 31.6, 24.0, 22.6, 14.1, 12.6.

**HRMS (MALDI):** *m/z* calcd for C<sub>68</sub>H<sub>93</sub>Br<sub>2</sub>ClN<sub>4</sub>NiSi<sub>2</sub>: 1272.434 [M]<sup>+</sup>; found 1272.474.

**Synthesis of porphyrin trimer **S6**.** 5-(4,4,5,5-Tetramethyl-1,3,2-dioxaborolan-2-yl)-10,20-bis(3,5-diocyloxyphenyl)porphyrinato zinc(II) **5**<sup>[3]</sup> (170 mg, 2.2 equiv., 0.15 mmol), **4** (85 mg, 1.0 equiv., 67 μmol) and cesium carbonate (0.13 g, 6 equiv., 0.40 mmol) were placed in a dry Schlenk vessel and dried under vacuum at 40 °C for 1 h, then purged with argon 5 times. Tetrakis(triphenylphosphine)palladium (23 mg, 0.3 equiv., 20 μmol), toluene (12.0 mL) and DMF (6.00 mL) were added and the mixture was purged with argon. The reaction was heated at 80 °C on an oil bath for 18 h under argon. After completion, it was passed through a short silica gel plug in 10% EtOAc in DCM and evaporated. The crude was subjected to column chromatography in DCM/PE (1:2), followed by SEC column in 1% pyridine in toluene to give **S6** as a red solid (180 mg, 85%).



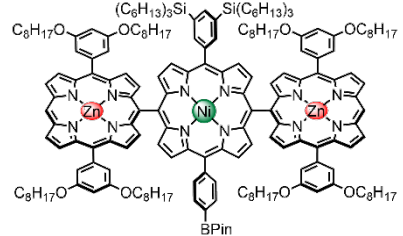
**<sup>1</sup>H NMR** (400 MHz, CDCl<sub>3</sub>, 298 K): δ<sub>H</sub> 10.38 (s, 2H, *meso*-H), 9.49 (d, *J* = 4.4 Hz, 4H, Zn-β-H), 9.28 (d, *J* = 4.4 Hz, 4H, Zn-β-H), 8.93 (d, *J* = 4.4 Hz, 4H, Zn-β-H), 8.56 (d, *J* = 5.0 Hz, 2H, Ni-β-H), 8.52 (d, *J* = 5.0 Hz, 2H, Ni-β-H), 8.30 (d, *J* = 4.4 Hz, 4H, Zn-β-H), 8.12 (two overlapping d, 4H, Ni-β-H and *o*-Ph-Ni), 8.08 (d, *J* = 5.0 Hz, 2H, Ni-β-

H), 7.99 (d,  $J$  = 8.9 Hz, 2H, Ph(Cl)-H), 7.72 (s, 1H, *p*-Ph-Ni), 7.52 (d,  $J$  = 8.9 Hz, 2H, Ph(Cl)-H), 7.43 (bd, 8H, *o*-Ph-Zn), 6.86 (t,  $J$  = 2.2 Hz, 4H, *p*-Ph-Zn), 4.10 (bt, 16H, OOOct-CH<sub>2</sub>), 1.83 (m, 16H, OOOct-CH<sub>2</sub>), 1.46 (m, 16H, OOOct-CH<sub>2</sub>), 1.37–1.11 (overlapping m, 74 H, -CH<sub>2</sub>), 1.12 (m, 16H, -CH<sub>2</sub>), 1.05–0.95 (overlapping m, 22H, -CH<sub>2</sub>), 0.81 (t,  $J$  = 6.7 Hz, 24H, OOOct-CH<sub>3</sub>), 0.70 (m, 12H, THS-CH<sub>2</sub>), 0.47 (t,  $J$  = 6.8 Hz, 18H, THS-CH<sub>3</sub>)

**<sup>13</sup>C NMR** (151 MHz, CDCl<sub>3</sub>)  $\delta$  158.5, 154.2, 150.7, 150.1, 149.8, 147.8, 147.8, 144.4, 143.5, 142.8, 139.7, 139.6, 139.4, 139.1, 135.2, 134.8, 134.7, 134.2, 133.7, 132.8, 132.4, 132.4, 132.0, 131.6, 127.1, 122.4, 121.5, 119.2, 119.1, 117.9, 114.5, 114.4, 106.9, 101.2, 68.5, 33.4, 31.9, 31.5, 29.5 (two overlapping peaks), 29.4, 26.3, 24.0, 22.8, 22.5, 14.2, 14.0, 12.6.

**HRMS (MALDI)**: *m/z* calcd for C<sub>196</sub>H<sub>259</sub>CIN<sub>12</sub>NiO<sub>8</sub>Si<sub>2</sub>Zn<sub>2</sub>: 3185.739 [M]<sup>+</sup>; found 3185.411.

**Synthesis of porphyrin trimer 6.** Porphyrin trimer **S6** (450 mg, 1 equiv., 141  $\mu$ mol), bis(pinacolato)diboron (358 mg, 10 equiv., 1.41 mmol), Pd(OAc)<sub>2</sub> (31.6 mg, 1 equiv., 141  $\mu$ mol), potassium phosphate (239 mg, 8 equiv., 1.13 mmol) and SPhos (116 mg, 2 equiv., 282  $\mu$ mol) were placed in a dry flask, degassed and purged with argon 3 times. Then dry 1,4-dioxane (20.0 mL) was added, followed by degassing by three freeze-pump-thaw cycles and the mixture was stirred at 110 °C for 16 h. After removing the solvent in vacuo, the residue was dissolved in chloroform, washed with brine 3 times, dried over anhydrous Na<sub>2</sub>SO<sub>4</sub> and evaporated. The crude material was subjected to column chromatography in 2:3 DCM/PE with 1% pinacol added to separate fraction containing deborylated compound, then in DCM separate the main fraction, which was then recrystallized from DCM/MeOH and subjected to SEC chromatography in THF. The main fraction was collected, solvent was removed and recrystallization from DCM/MeOH provided **6** as a red solid (385 mg, 83%).

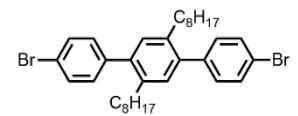


**<sup>1</sup>H NMR** (400 MHz, CDCl<sub>3</sub>, 298 K):  $\delta$ <sub>H</sub> 10.38 (s, 2H, meso-H), 9.49 (d,  $J$  = 4.4 Hz, 4H, Zn- $\beta$ -H), 9.27 (d,  $J$  = 4.4 Hz, 4H, Zn- $\beta$ -H), 8.93 (d,  $J$  = 4.5 Hz, 4H, Zn- $\beta$ -H), 8.55 (d,  $J$  = 5.1 Hz, 2H, Ni- $\beta$ -H), 8.54 (d,  $J$  = 5.1 Hz, 2H, Ni- $\beta$ -H), 8.31 (d,  $J$  = 4.5 Hz, 4H, Zn- $\beta$ -H), 8.12 (two overlapping d, 4H, Ni- $\beta$ -H and *o*-Ph-Ni), 8.05 (two overlapping d, 4H, Ni- $\beta$ -H and Ph(BPin)-H), 7.97 (d,  $J$  = 8.6 Hz, 2H, Ph(BPin)-H), 7.72 (s, 1H, *p*-Ph-Ni), 7.43 (m, 8H, *o*-Ph-Zn), 6.85 (t,  $J$  = 2.3 Hz, 4H, *p*-Ph-Zn), 4.10 (bt, 16H, OCH<sub>2</sub>), 1.86–1.79 (m, 16H, CH<sub>2</sub>), 1.50–1.42 (m, 16H, CH<sub>2</sub>), 1.37–1.20 (m, 72H, CH<sub>2</sub>), 1.31 (s, 12H, Bpin), 1.19–1.09 (m, 12H, CH<sub>2</sub>), 1.03–0.96 (m, 24H, CH<sub>2</sub>), 0.82 (t,  $J$  = 6.7 Hz, 24H, OOOct-CH<sub>3</sub>), 0.73–0.65 (m, 12H, CH<sub>2</sub>), 0.47 (t,  $J$  = 6.8 Hz, 18H, THS-CH<sub>3</sub>).

**<sup>13</sup>C NMR** (151 MHz, CDCl<sub>3</sub>)  $\delta$ <sub>C</sub> 158.5, 154.3, 150.7, 150.1, 149.9, 147.7, 144.5, 144.1, 143.4, 143.0, 139.6, 139.3, 139.3, 135.1, 134.7, 134.6, 133.8, 133.4, 133.2, 132.8, 132.4, 132.3, 132.0, 122.3, 121.5, 120.8, 118.9, 118.1, 114.52, 114.47, 106.9, 101.2, 84.1, 68.5, 33.4, 32.0, 31.5, 29.6, 29.4, 26.3, 25.1, 24.0, 22.8, 22.5 (two overlapping peaks), 14.2, 14.0, 12.6. Two aromatic peaks are not visible, they either overlap with some others or correspond to quaternary carbons and are very weak.

**HRMS (MALDI)**: *m/z* calcd for C<sub>202</sub>H<sub>271</sub>BN<sub>12</sub>NiO<sub>10</sub>Si<sub>2</sub>Zn<sub>2</sub>: 3277.863 [M]<sup>+</sup>; found 3277.932.

**Synthesis of 4,4"-dibromo-2',5'-dioctyl-1,1':4',1"-terphenyl S2.** 1,4-Diido-2,5-dioctylbenzene **S1**<sup>[1]</sup> (1.00 g, 1 equiv., 1.80 mmol), (4-bromophenyl)boronic acid (1.09 g, 3 equiv., 5.41 mmol) and sodium carbonate (765 mg, 4 equiv., 7.22 mmol) were dissolved in a mixture of toluene (20.0 mL), ethanol (4.00 mL) and water (4.00 mL), then degassed via three freeze-pump-thaw cycles. Pd(PPh<sub>3</sub>)<sub>4</sub> (104 mg, 0.05 equiv., 90.2  $\mu$ mol) was then added and the reaction stirred at 80 °C for 18 h. The crude mixture was allowed to cool, extracted with DCM from water, washed with brine, dried over anhydrous Na<sub>2</sub>SO<sub>4</sub>, evaporated and subjected to column chromatography in PE 40/60, after evaporation providing **S2** as a white solid (1.10 g, 99%).



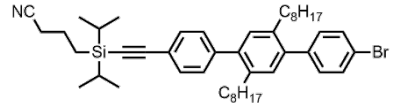
**<sup>1</sup>H NMR** (400 MHz, CDCl<sub>3</sub>, 298 K):  $\delta$ <sub>H</sub> 7.55 (d,  $J$  = 8.1 Hz, 4H, Ph), 7.22 (d,  $J$  = 8.1 Hz, 4H, Ph), 7.07 (s, 2H, Ph), 2.51 (t,  $J$  = 8.1 Hz, 4H, -CH<sub>2</sub>), 1.46–1.40 (m, 4H, -CH<sub>2</sub>), 1.29–1.17 (m, 20H, -CH<sub>2</sub>), 0.86 (t,  $J$  = 6.8 Hz, 6H, -CH<sub>3</sub>).

<sup>13</sup>C NMR (150 MHz, CDCl<sub>3</sub>, 298 K): δ<sub>C</sub> 140.7, 139.8, 137.5, 131.2, 131.0, 130.8, 121.0, 32.5, 31.8, 31.4, 29.5, 29.2, 29.1, 22.6, 14.1.

HRMS (MALDI): *m/z* calcd for C<sub>34</sub>H<sub>44</sub>Br<sub>2</sub>: 610.180 [M]<sup>+</sup>; found 610.233.

**Synthesis of 4-((4"-bromo-2',5'-dioctyl-[1,1':4',1"-terphenyl]-4-yl)ethynyl)diisopropylsilylbutanenitrile S3.**

An oven dried and argon flushed Schlenk tube was charged with **S2** (400 mg, 1.0 equiv., 653 μmol), dry toluene (4.00 mL) and iPr<sub>2</sub>NH (4.00 mL) and the mixture was degassed by argon bubbling for 10 min. Then 4-(ethynyl)diisopropylsilylbutanenitrile (0.15 g, 0.17 mL, 1.1 equiv., 0.73 mmol), palladium(II) acetate (16.1 mg, 0.11 equiv., 71.8 μmol), triphenylphosphine (54.8 mg, 0.32 equiv., 209 μmol) and copper(I) iodide (37.3 mg, 0.3 equiv., 196 μmol) were added and the mixture was bubbled again for 5 min. The solution was stirred at 50 °C for 2.5 h, then allowed to cool, diluted with ethylacetate (60 mL), washed with brine and water, the organic phase dried over anhydrous Na<sub>2</sub>SO<sub>4</sub> and evaporated. Column chromatography in DCM/PE (1:2) gave **S3** as yellow-white oily solid (175 mg, 36%), accompanied by recovered **S2** (130 mg) in the first fraction.

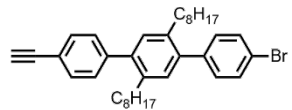


<sup>1</sup>H NMR (400 MHz, CDCl<sub>3</sub>, 298 K): δ<sub>H</sub> 7.56 (d, *J* = 8.3 Hz, 2H, Ph), 7.53 (d, *J* = 8.3 Hz, 2H, Ph), 7.30 (d, *J* = 8.3 Hz, 2H, Ph), 7.23 (d, *J* = 8.3 Hz, 2H, Ph), 7.07 (s, 2H, Ph), 2.52 (m, 4H, alkyl), 2.45 (t, *J* = 7.0 Hz, 2H, alkyl), 1.90 (m, 2H, alkyl), 1.44 (m, 4H, alkyl), 1.27–1.09 (overlapping m, 36H, alkyl), 0.88–0.83 (m, 6H, alkyl).

<sup>13</sup>C NMR (151 MHz, CDCl<sub>3</sub>) δ<sub>C</sub> 142.4, 140.8, 140.3, 139.8, 137.54, 137.52, 131.8, 131.2, 131.0, 130.79, 130.76, 129.3, 121.4, 121.0, 119.8, 107.9, 89.5, 32.5, 31.8, 31.4, 31.3, 29.47, 29.45, 29.3, 29.2, 29.1, 29.1, 22.7, 22.6, 21.4, 20.8, 18.2, 18.0, 14.1, 11.8, 9.7.

**Synthesis of 4-bromo-4"-ethynyl-2',5'-dioctyl-1,1':4',1"-terphenyl S4.**

Terphenyl **S3** was dissolved in dry THF (6.00 mL) and TBAF in THF (1.0 M, 310 mg, 1.18 mL, 5 equiv., 1.18 mmol) was added. The reaction mixture was stirred at room temperature for 15 min and checked via TLC, after completion quenched with water (3 mL) and extracted with AcOEt, dried over anhydrous Na<sub>2</sub>SO<sub>4</sub> and evaporated. Column chromatography in DCM/PE (1:6) gave pure **S4** as yellowish oil that solidified after few hours (120 mg, 91%).



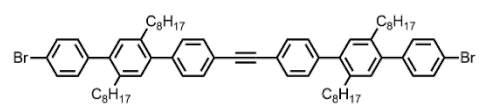
<sup>1</sup>H NMR (400 MHz, CDCl<sub>3</sub>, 298 K): δ<sub>H</sub> 7.56 (d, *J* = 8.4 Hz, 2H, Ph), 7.54 (d, *J* = 8.4 Hz, 2H, Ph), 7.31 (d, *J* = 8.5 Hz, 2H, Ph), 7.23 (d, *J* = 8.3 Hz, 2H, Ph), 7.08 (s, 1H, Ph), 7.07 (s, 1H, Ph), 3.12 (s, 1H, acet.), 2.53 (m, 4H, -CH<sub>2</sub>), 1.44 (m, 4H, CH<sub>2</sub>), 1.28–1.16 (overlapping m, 20H, -CH<sub>2</sub>), 0.86 (two overlapping t, *J* = 6.8 Hz, 6H, -CH<sub>3</sub>).

<sup>13</sup>C NMR (151 MHz, CDCl<sub>3</sub>, 298 K): δ<sub>C</sub> 142.5, 140.7, 140.3, 139.8, 137.5, 137.5, 131.8, 131.2, 131.0, 130.8, 130.7, 129.3, 120.9, 120.5, 83.6, 32.5, 31.8, 31.4, 29.4, 29.2, 29.1, 22.6, 14.1.

HRMS (MALDI): *m/z* calcd for C<sub>36</sub>H<sub>45</sub>Br, 556.270 [M]<sup>+</sup>; found 556.346

**Synthesis of 1,2-bis(4"-bromo-2',5'-dioctyl-[1,1':4',1"-terphenyl]-4-yl)ethyne 7.**

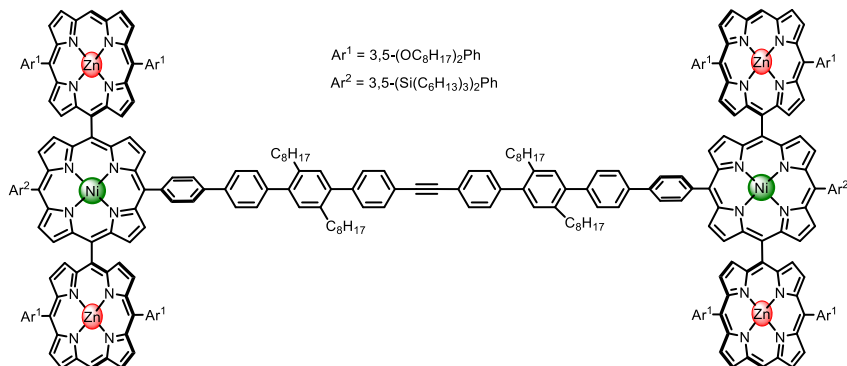
An oven dried and argon flushed Schlenk tube was charged with **S2** (54.9 mg, 5 equiv., 89.7 μmol), dry toluene (0.50 mL) and iPr<sub>2</sub>NH (0.50 mL) and the mixture was degassed by argon bubbling for 10 min. Then **S4** (10.0 mg, 1 equiv., 17.9 μmol), bis(triphenylphosphine)palladium(II) dichloride (2.52 mg, 0.2 equiv., 3.59 μmol) and copper(I) iodide (0.68 mg, 0.2 equiv., 3.59 μmol) were added and the mixture was bubbled again for 5 min. The solution was stirred at 60 °C for 1 h on an oil bath, diluted with AcOEt, washed with brine, water, organic phase was dried over anhydrous Na<sub>2</sub>SO<sub>4</sub> and evaporated. Column chromatography was then performed in pure PE, then switching to DCM/PE (1:2) which gave **7** as a white solid (9 mg, 46%), accompanied by recovered **6** in first fraction (in PE).



**<sup>1</sup>H NMR** (400 MHz, CDCl<sub>3</sub>, 298 K): δ<sub>H</sub> 7.60 (d, *J* = 8.3 Hz, 4H, Ph), 7.56 (d, *J* = 8.3 Hz, 4H, Ph), 7.35 (d, *J* = 8.3 Hz, 4H, Ph), 7.23 (d, *J* = 8.3 Hz, 4H, Ph), 7.10 (s, 2H, Ph), 7.08 (s, 2H, Ph), 2.56 (m, 8H, -CH<sub>2</sub>), 1.47 (m, 8H, -CH<sub>2</sub>), 1.29–1.09 (m, 40H, -CH<sub>2</sub>), 0.86 (overlapping t, 12H, -CH<sub>3</sub>).

**<sup>13</sup>C NMR** (151 MHz, CDCl<sub>3</sub>, 298 K): δ<sub>C</sub> 141.9, 140.8, 140.5, 139.8, 137.6, 137.5, 131.3, 131.2, 131.0, 130.8, 129.4, 121.8, 121.0, 89.7, 32.63, 32.58, 31.9, 31.4, 29.52, 29.49, 29.3, 29.2, 22.7, 14.1.

**HRMS (MALDI)**: *m/z* calcd for C<sub>70</sub>H<sub>88</sub>Br<sub>2</sub>: 1086.525 [M]<sup>+</sup>; found: 1086.471.



**Synthesis of hexaporphyrin tolan 3.** Tolan **7** (22.0 mg, 1 equiv., 20.2 μmol), porphyrin trimer **6** (199 mg, 3 equiv., 60.6 μmol) and SPhos-Pd-G2 (14.6 mg, 1 equiv., 20.2 μmol), were placed in a dry Schlenk and dried under high vacuum for 30 min, then dry 1,4-dioxane (6.0 mL) was added. A degassed, aqueous solution of potassium phosphate (2.0 M, 0.3 mL, 30 equiv., 606 μmol) was then added and the mixture was subjected to degassing by four freeze-pump-thaw cycles. The reaction mixture was heated under argon at 80 °C on an oil bath for 16 h, extracted with DCM/H<sub>2</sub>O, the organic phase was dried over anhydrous Na<sub>2</sub>SO<sub>4</sub> and evaporated. The crude mixture was subjected to column chromatography (DCM/PE, 1:1, after elution of smaller by-products change to DCM), followed by preparative GPC separation (1% pyridine in toluene), evaporation of all solvents and precipitation from DCM/MeOH on a rotary evaporator to yield **3** as a red solid (73 mg, 50%).

**<sup>1</sup>H NMR** (600 MHz, CDCl<sub>3</sub>, 298 K): δ<sub>H</sub> 10.36 (s, 4H), 9.48 (d, *J* = 4.3 Hz, 8H), 9.27 (d, *J* = 4.3 Hz, 8H), 8.93 (d, *J* = 4.3 Hz, 8H), 8.64 (d, *J* = 5.1 Hz, 4H), 8.56 (d, *J* = 5.1 Hz, 4H), 8.31 (d, *J* = 4.3 Hz, 8H), 8.19–8.10 (overlapping t,d,d, 12H), 8.05 (d, *J* = 5.1 Hz, 4H), 7.85 (d, *J* = 8.8 Hz, 4H), 7.77 (d, *J* = 8.8 Hz, 4H), 7.75 (s, 2H), 7.57 (d, *J* = 8.8 Hz, 4H), 7.45 (d, *J* = 2.3 Hz, 16H), 7.43 (d, *J* = 8.8 Hz, 4H), 7.33 (d, *J* = 8.8 Hz, 4H), 7.14 (s, 2H), 7.10 (s, 2H), 6.87 (t, *J* = 2.3 Hz, 8H), 4.14–4.09 (overlapping m, 32H), 2.56 (overlapping m, 8H), 1.85 (p, *J* = 6.8 Hz, 32H), 1.52–1.43 (overlapping, 32H), 1.39–1.19 (overlapping m, 168H), 1.19–1.08 (overlapping m, 60H), 1.08–0.98 (overlapping m, 48H), 0.86–0.79 (m, 48H), 0.76–0.71 (overlapping m, 32H), 0.52 (t, *J* = 7.1 Hz, 36H).

<sup>1</sup>H signals assignment – see Fig. S26.

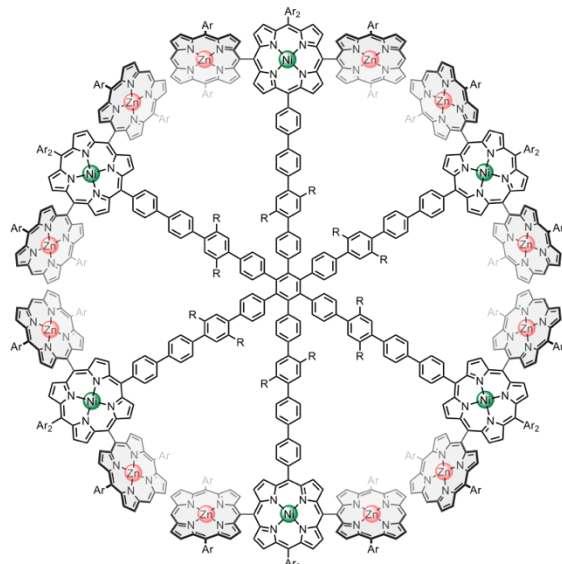
**<sup>13</sup>C NMR** (151 MHz, CDCl<sub>3</sub>) δ 158.4, 154.2, 150.6, 150.0, 149.8, 147.9, 144.7, 143.5, 143.4, 143.1, 142.1, 141.2, 140.7, 140.3, 140.1, 139.6, 139.3, 139.1, 137.8, 137.6, 136.1, 135.1, 134.6, 134.3, 133.7, 132.7, 132.3, 131.9, 131.4, 131.1, 130.9, 130.0, 129.5, 126.9, 125.4, 122.5, 122.2, 121.8, 121.4, 120.4, 119.2, 117.8, 114.6, 114.5, 106.8, 101.0, 89.8, 68.5, 33.4, 32.8, 31.9, 31.9, 31.5, 29.63, 29.59, 29.55, 29.54, 29.53, 29.4, 29.3, 29.24, 29.20, 26.3, 24.0, 22.8, 22.7, 22.5, 14.2, 14.0, 12.6. Seven alkyl peaks are not resolved as they overlap with other peaks in the alkyl region.

**MS (MALDI)**: *m/z* calcd for C<sub>462</sub>H<sub>606</sub>N<sub>24</sub>Ni<sub>2</sub>O<sub>16</sub>Si<sub>4</sub>Zn<sub>4</sub>: 7243.235 [M]<sup>+</sup>; found: 7245.023.

**UV-vis:** (CH<sub>2</sub>Cl<sub>2</sub>, 298 K) λ, log ε: 411 (6.07), 463 (5.91), 551 (5.49).

**Synthesis of 18-porphyrin radial oligomer 2.** Tolan **3** (23 mg, 1 equiv., 3.18  $\mu$ mol) and octacarbonylcobalt(II)\* (1.1 mg, 1.0 equiv, 3.18  $\mu$ mol) were placed in a dry 1 mL pressure tube with Teflon cap, atmosphere was changed to argon, dry toluene (90  $\mu$ L) was added. The tube was sealed under stream of argon, pre-stirred for 15 min and then heated at 140 °C on an oil bath for 16 h. After completion, the crude mixture was passed through a short silica plug in DCM and evaporated, then subjected to GPC separation (1% pyridine in toluene) followed by evaporation of all solvents and precipitation from DCM/MeOH on a rotary evaporator to yield cyclotrimer **2** as a dark red solid (5.75 mg, 25%).

\*Note:  $\text{Co}_2(\text{CO})_8$  is not stable in the air and care must be taken when handling and storing the chemical – it has to be orange/brown. A black/violet color indicates substantial decomposition and the use of the catalyst of that quality was found not to lead to formation of the desired product. We recommend storing this compound in separate vials under argon in a freezer to avoid decomposition of the whole package.



**$^1\text{H NMR}$**  (600 MHz,  $\text{CD}_2\text{Cl}_2$ ):  $\delta_{\text{H}}$  10.20 (s, 12H), 9.33 (d,  $J$  = 4.6 Hz, 24H), 9.15 (d,  $J$  = 4.6 Hz, 24H), 8.87 (d,  $J$  = 4.5 Hz, 24H), 8.61 (d,  $J$  = 5.0 Hz, 12H), 8.58 (d,  $J$  = 5.0 Hz, 12H), 8.28 (d,  $J$  = 4.5 Hz, 24H), 8.18 (s, 12H), 8.12 (d,  $J$  = 4.9 Hz, 12H), 8.10–8.05 (overlapping d and t, 24H), 7.82 (s, 6H), 7.75 (d,  $J$  = 8.4 Hz, 12H), 7.62 (d,  $J$  = 8.4 Hz, 12H), 7.24 (d,  $J$  = 6.6 Hz, 48H), 7.22 (overlapping d, 12H), 6.91 (d,  $J$  = 8.4 Hz, 12H), 6.87 (s, 6H), 6.79 (overlapping s and d, 18H), 6.62 (t,  $J$  = 2.3 Hz, 24H), 3.91 (m, 48H), 3.85 (m, 48H), 2.37 (m, 12H), 2.22 (m, 12H), 1.72 (p,  $J$  = 6.9 Hz, 48H), 1.58 (p,  $J$  = 7.5 Hz, 48H), 1.38 (overlapping p,  $J$  = 7.5 Hz, 48H), 1.33–1.20 (overlapping m, 348H), 1.20–1.14 (overlapping m, 96H), 1.14–0.97 (overlapping m, 360H), 0.95–0.83 (overlapping m, 96H), 0.83–0.74 (overlapping m and t, 144H), 0.63 (t,  $J$  = 7.1 Hz, 72H, OOct - $\text{CH}_3$ ), 0.49 (t,  $J$  = 7.1 Hz, 108H, THS - $\text{CH}_3$ ).

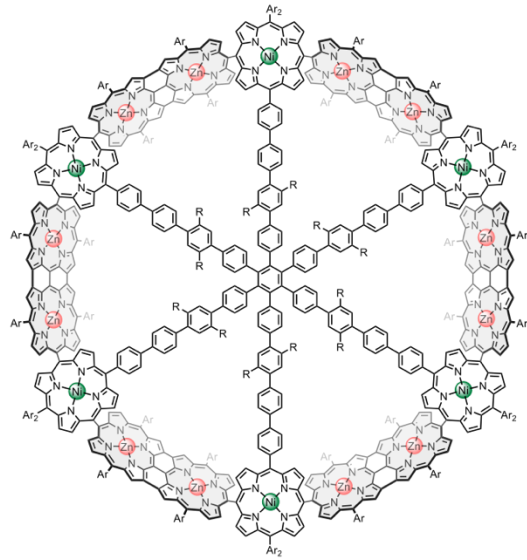
$^1\text{H}$  signals assignment – see Fig. S33.

**$^{13}\text{C NMR}$**  (151 MHz,  $\text{CD}_2\text{Cl}_2$ , 298 K):  $\delta_{\text{C}}$  158.1, 153.9, 150.4, 149.8, 149.6, 147.6, 144.1, 143.3, 143.0, 141.29, 141.27, 140.7, 140.6, 139.9, 139.0, 138.9, 138.6, 137.4, 137.1, 135.2, 134.2, 133.3, 132.5, 132.1, 131.7, 131.2, 130.5, 129.7, 127.5, 126.4, 125.2, 122.3, 121.3, 120.5, 118.8, 117.6, 114.5, 114.4, 106.6, 100.9, 68.4, 68.3, 33.3, 32.4, 31.9, 31.8, 31.7, 31.6, 31.4, 29.7, 29.34, 29.24, 29.21, 29.17, 29.13, 29.04, 28.95, 25.6, 25.9, 23.8, 22.6, 22.44, 22.37, 13.8, 13.7, 13.64, 13.61, 12.4. Two of the alkyl signals are not resolved due to overlapping with other signals. Seven aromatic signals are not visible too due to low signal to noise ratio which results from line broadening and aggregation, even though we recorded the spectrum for a long time using a cryoprobe (Fig. S35). To compensate for that, we recorded a series of 2D experiments (see Fig. S37–S41).

**MS (MALDI):**  $m/z$  calcd for  $\text{C}_{1386}\text{H}_{1818}\text{N}_{72}\text{Ni}_6\text{O}_{48}\text{Si}_{12}\text{Zn}_{12}$ : 21729.705 [ $M]^+$ ; found: 21738.003.

**UV-vis:** ( $\text{CH}_2\text{Cl}_2$ , 298 K)  $\lambda$ ,  $\log \epsilon$ : 412 (6.33), 464 (6.18), 552 (5.78).

**Synthesis of nanoring 1.** Porphyrin octadecamer **2** (10.0 mg, 0.46  $\mu$ mol, 1 equiv.) was dissolved in dry, degassed DCM (39 mL) under inert gas atmosphere and the solution was cooled to  $-78^{\circ}\text{C}$ . A solution of bis(trifluoroacetoxy)iodobenzene (PIFA, 2.97 mg, 6.9  $\mu$ mol, 15 equiv.) in dry, degassed DCM (1 mL) was added. The cooling bath was removed and the mixture was stirred at room temperature for 2.5 h which was followed by a color change from orange to turquoise. After quenching the reaction by adding a suspension of NaBH<sub>4</sub> (1.0 mg, 27.6  $\mu$ mol, 60 equiv.) in MeOH (0.3 mL), the solvents were evaporated and the solid residue was washed with methanol. Separation by GPC (1% pyridine in toluene) followed by evaporation of all solvents and precipitation from DCM/MeOH on a rotary evaporator and filtration gave nanoring **1** as a turquoise solid (4.5 mg, 45%).



**<sup>1</sup>H NMR** (600 MHz, CDCl<sub>3</sub> + 1% pyridine-*d*<sub>5</sub>, 298 K):  $\delta_{\text{H}}$  9.14 (br., 12H), 8.82 (br., 12H), 8.30 (br., 12H), 8.25 (br., 12H), 7.89 (overlapping s and d\*, 18H), 7.76 (s, 6H), 7.73 (two overlapping d\*, 24H), 7.43 (br. d, 24H), 7.35 (d\*, 12H), 7.10 (br., 24H), 7.00 (br., 18H), 6.94 (br., 24H), 6.90 (br., 12H), 6.79 (br., 48H), 6.58 (br., 24H), 3.99 (m, 48H), 3.94 (m, 48H), 2.47 (m, 12H), 2.36 (m, 12H), 1.78 (m, 48H), 1.69 (m, 48H), 1.57–0.96 (overlapping m, 720H), 0.91–0.78 (overlapping m, 324H), 0.78 – 0.67 (overlapping t, 216H).

\*The *para*-phenylene signals from the template core become more resolved when the spectrum is measured in C<sub>2</sub>D<sub>2</sub>Cl<sub>4</sub> at 100 °C (Fig. S44). Partial <sup>1</sup>H signals assignment – see Fig. S42. Due to substantial broadening and overlapping of signals it was not possible to assign all of them.

**<sup>13</sup>C NMR** (from <sup>1</sup>H-<sup>13</sup>C HSQC experiment, 151 MHz, CDCl<sub>3</sub> + 1% pyridine-*d*<sub>5</sub>, 298 K):  $\delta_{\text{C}}$  139.8, 139.4, 133.9, 132.7, 131.6, 131.0, 130.8, 130.7, 129.8, 127.8, 126.9, 126.4, 112.9, 112.2, 100.4, 68.2, 40.1, 36.8, 32.9, 32.7, 31.7, 29.6, 29.3, 27.4, 26.5, 26.2, 24.0, 22.6, 20.1, 19.4, 14.1, 12.7. We did not manage to measure <sup>13</sup>C NMR spectrum directly due to substantial line broadening and aggregation. Instead, we measured a <sup>1</sup>H-<sup>13</sup>C HSQC NMR spectrum.

**HRMS (MALDI):** *m/z* calcd for C<sub>1386</sub>H<sub>1782</sub>N<sub>72</sub>Ni<sub>6</sub>O<sub>48</sub>Si<sub>12</sub>Zn<sub>12</sub>: 21693.424 [M]<sup>+</sup>; found: 21693.111.

**UV-vis-NIR:** (CH<sub>2</sub>Cl<sub>2</sub>, 298 K)  $\lambda$ , log  $\varepsilon$ : 413 (5.64), 618 (5.55), 934 (4.77), 1054 (4.93).

### 3. Comparison of UV-vis-NIR spectra

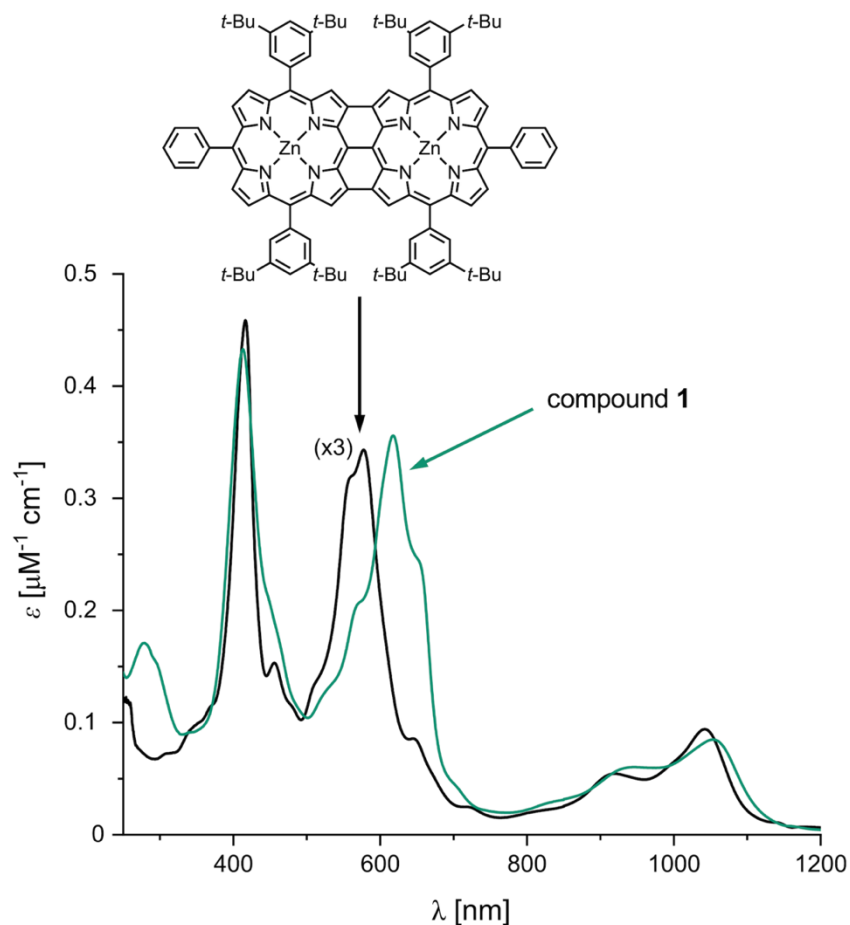


**Figure S1.** Comparison of the UV-vis-NIR spectrum of porphyrin 18-mer **1** (green line) with that of an edge-fused porphyrin dimer (black line), both spectra recorded in  $\text{CH}_2\text{Cl}_2$  at 298 K.

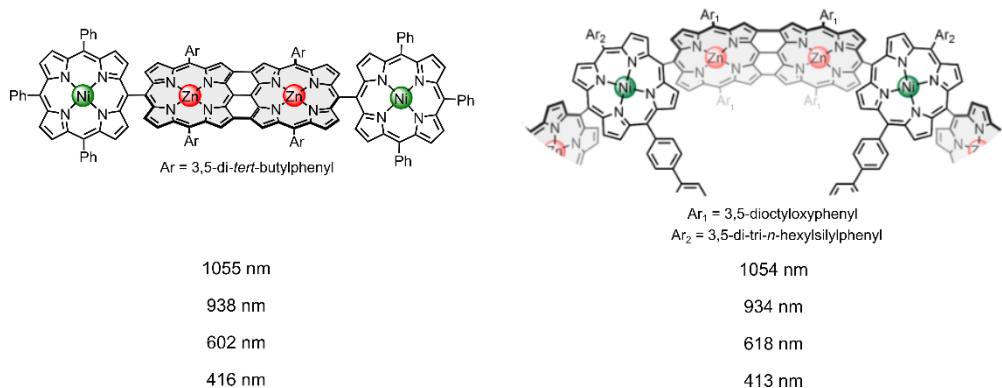


**Figure S2.** Comparison between the observed absorption maxima for **1** (right) and for a known linear tetramer (left).<sup>[4]</sup>

#### 4. NMR and Mass Spectra

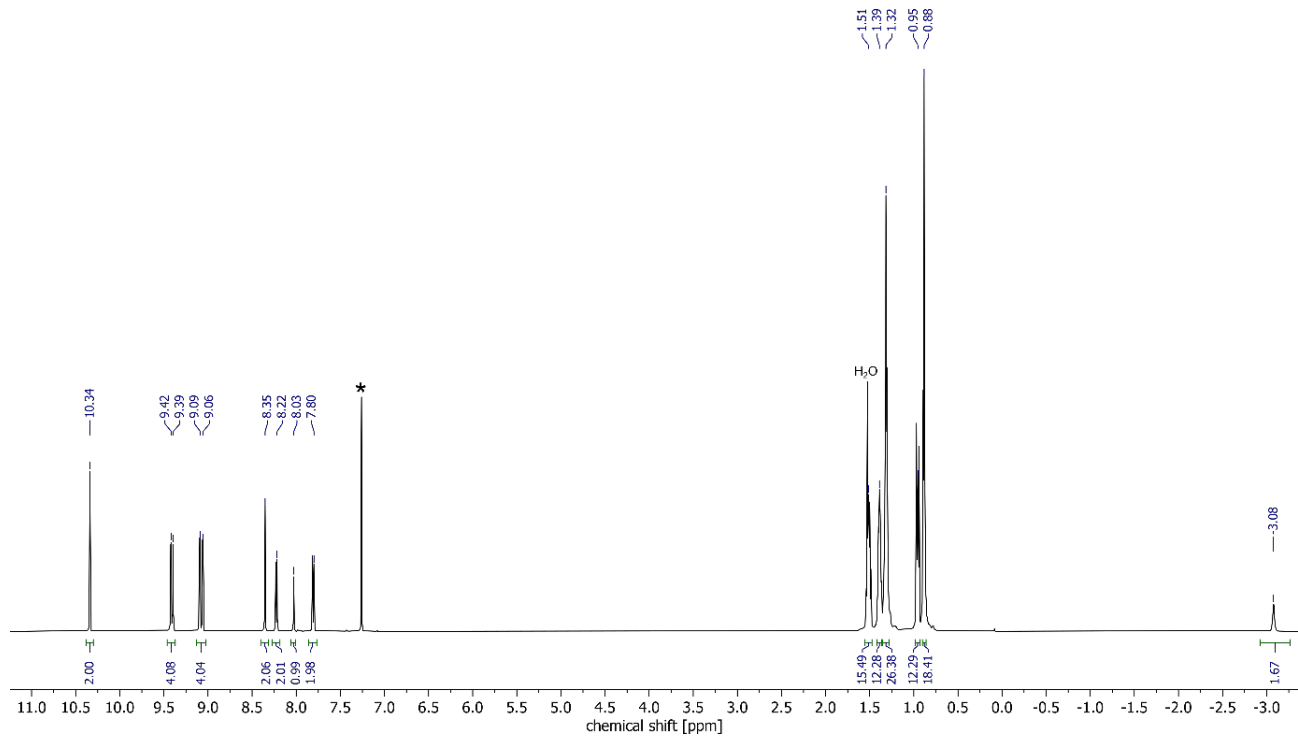


Figure S3. <sup>1</sup>H NMR spectrum of S5,  $\text{CDCl}_3$ , 600 MHz, 298 K.

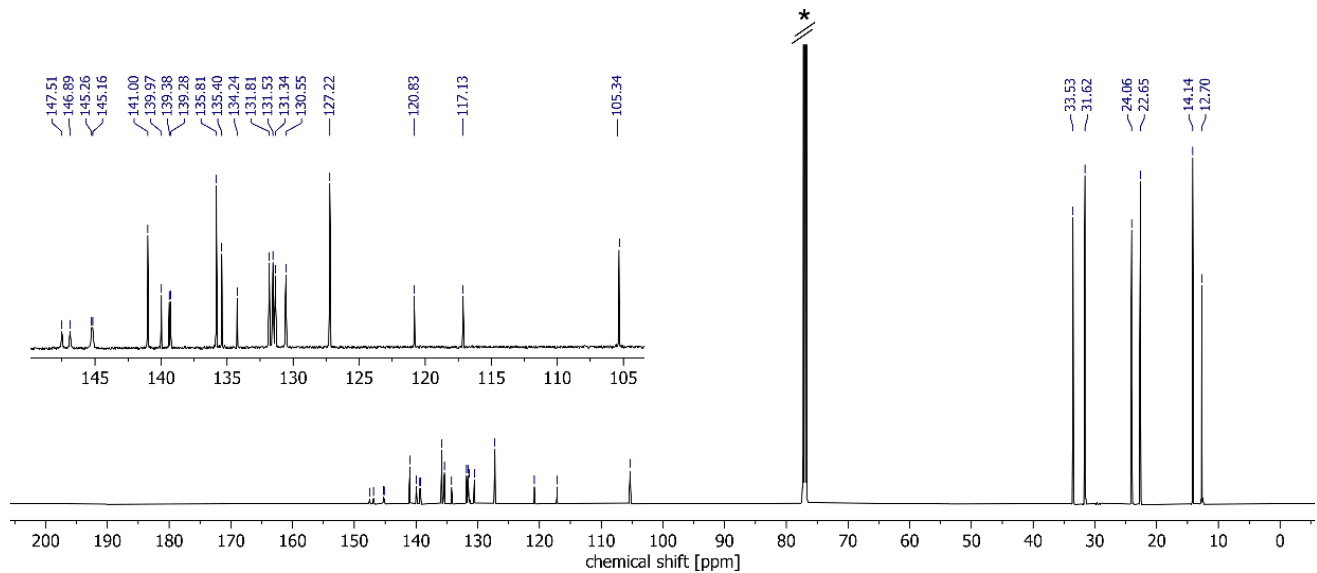
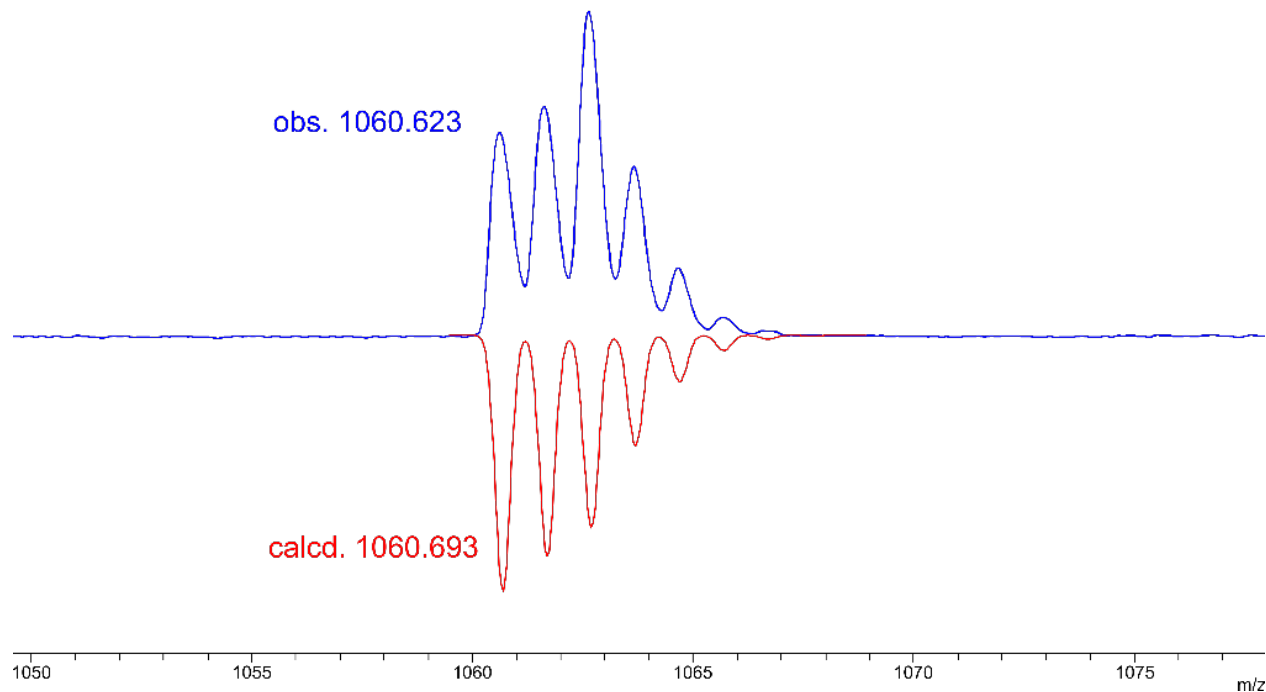
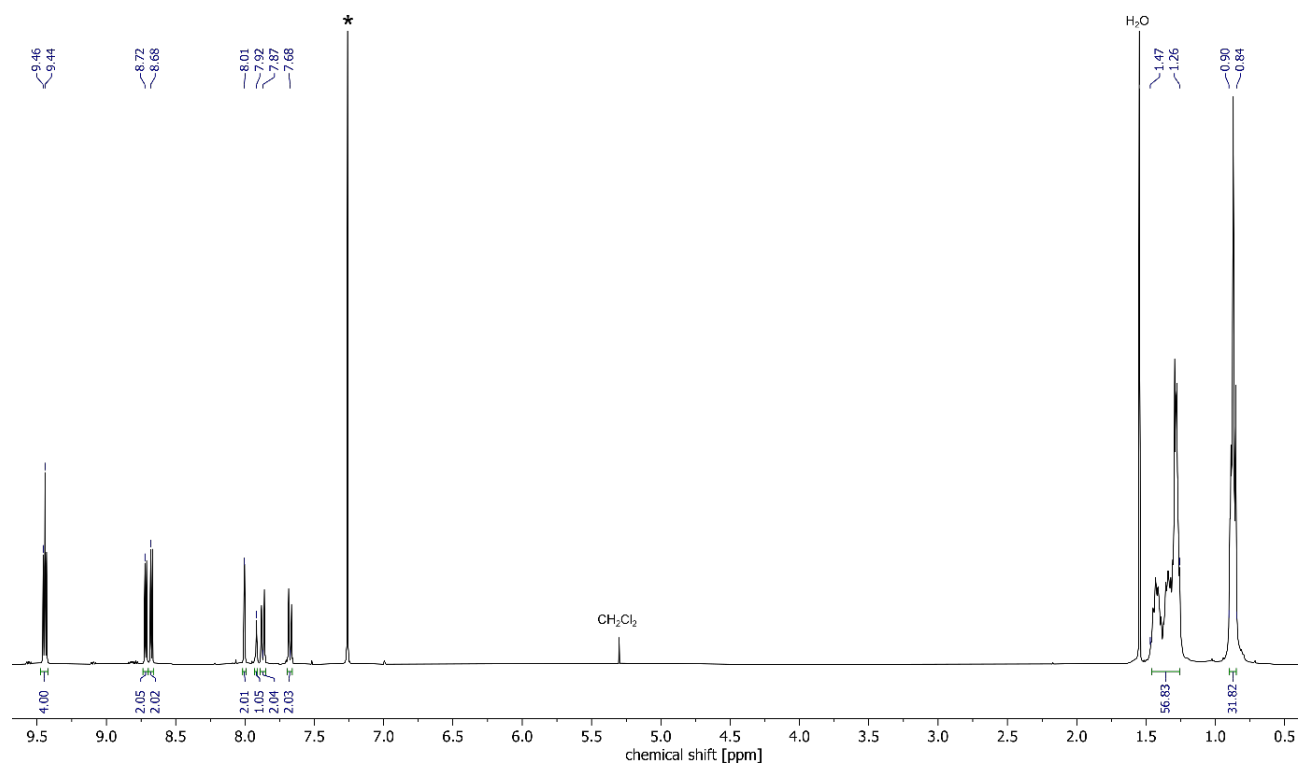


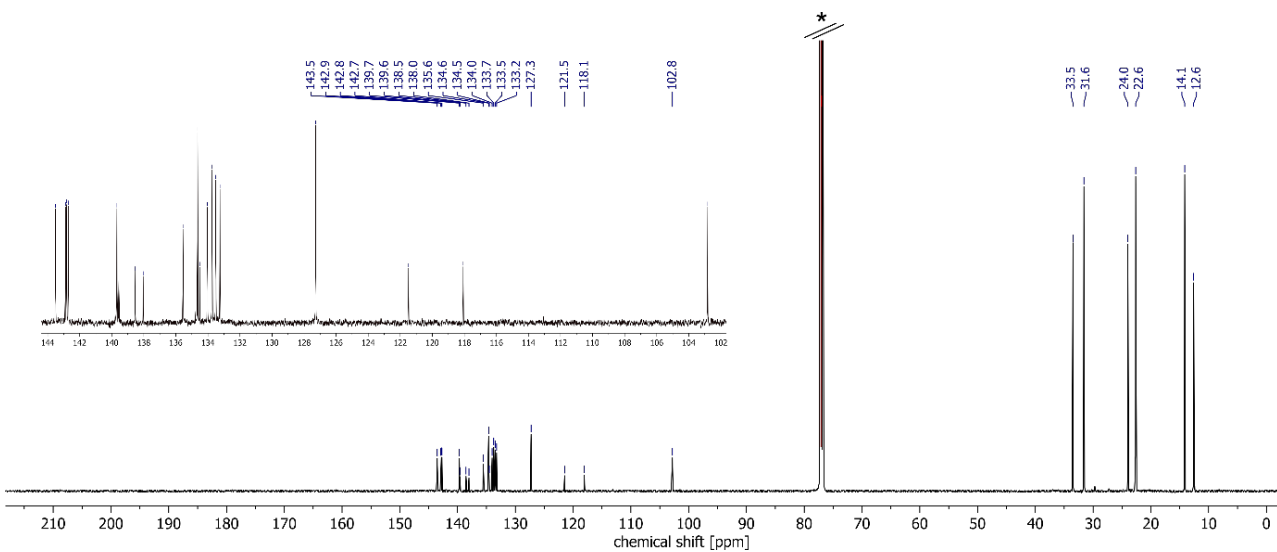
Figure S4. <sup>13</sup>C NMR spectrum of S5,  $\text{CDCl}_3$ , 151 MHz, 298 K.



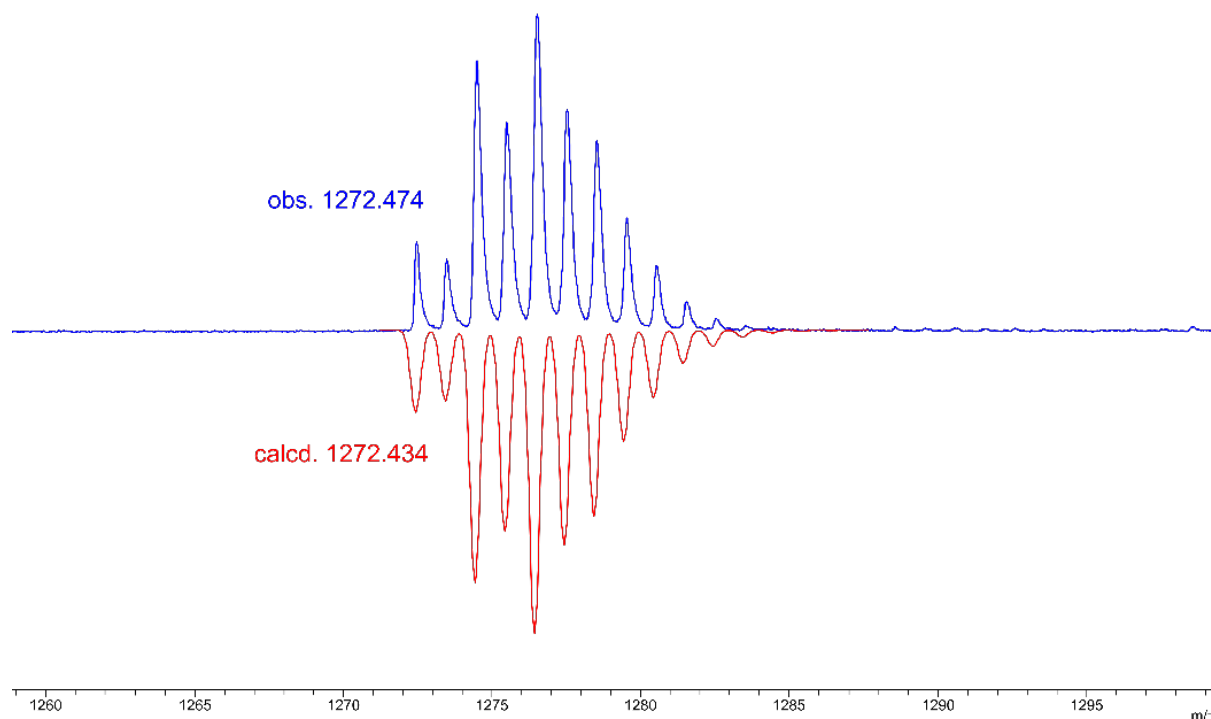
**Figure S5.** Selected region of a calculated (red) and recorded (blue) MALDI mass spectra of **S5**, DCTB matrix.



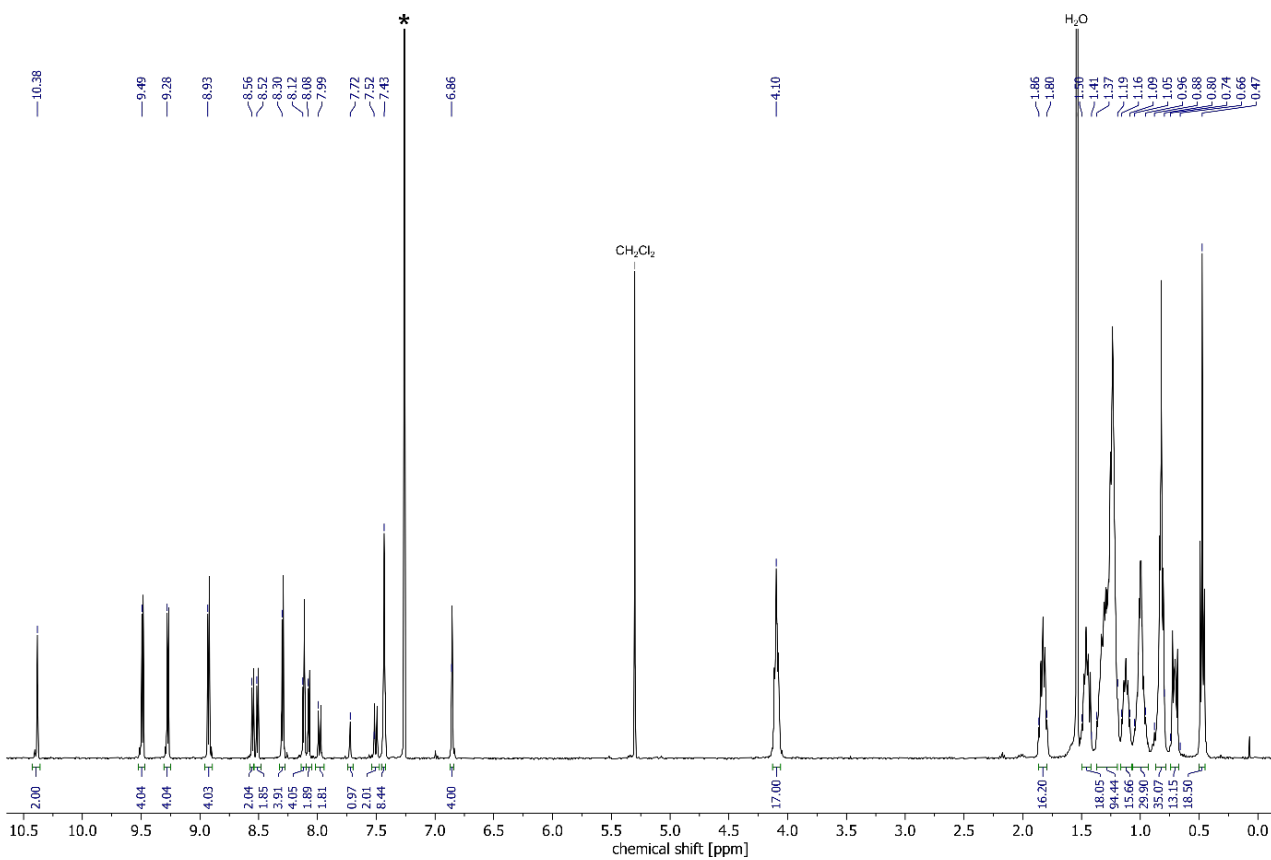
**Figure S6.**  $^1\text{H}$  NMR spectrum of **4**,  $\text{CDCl}_3$ , 600 MHz, 298 K.



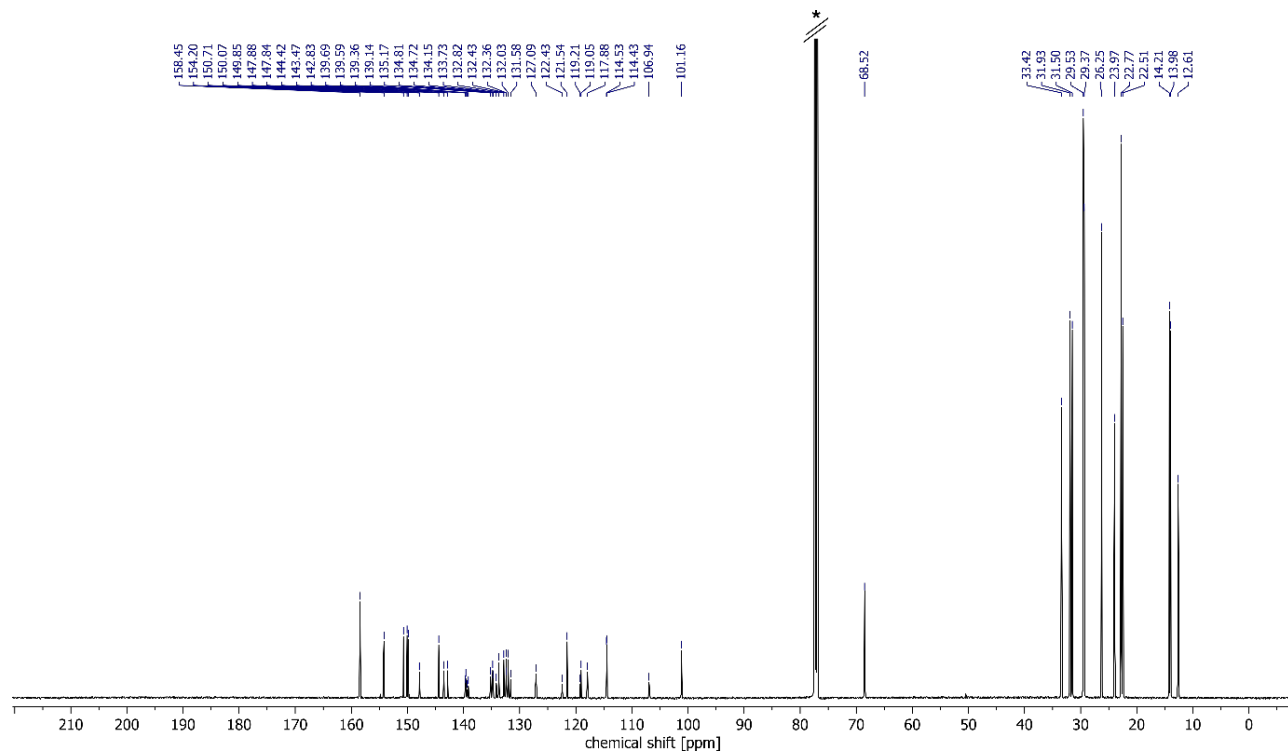
**Figure S7.**  $^{13}\text{C}$  NMR spectrum of **4**,  $\text{CDCl}_3$ , 151 MHz, 298 K.



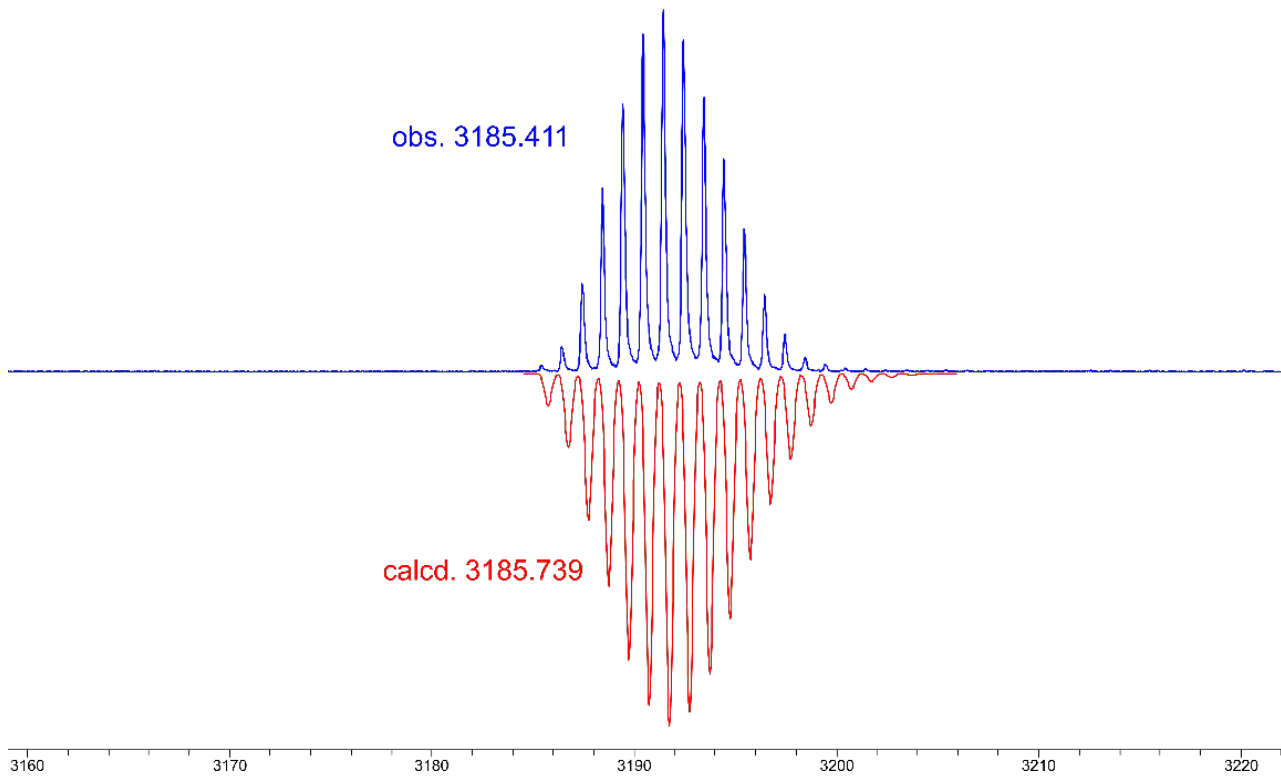
**Figure S8.** Selected region of a calculated (red) and recorded (blue) MALDI mass spectra of **4**, DCTB matrix.



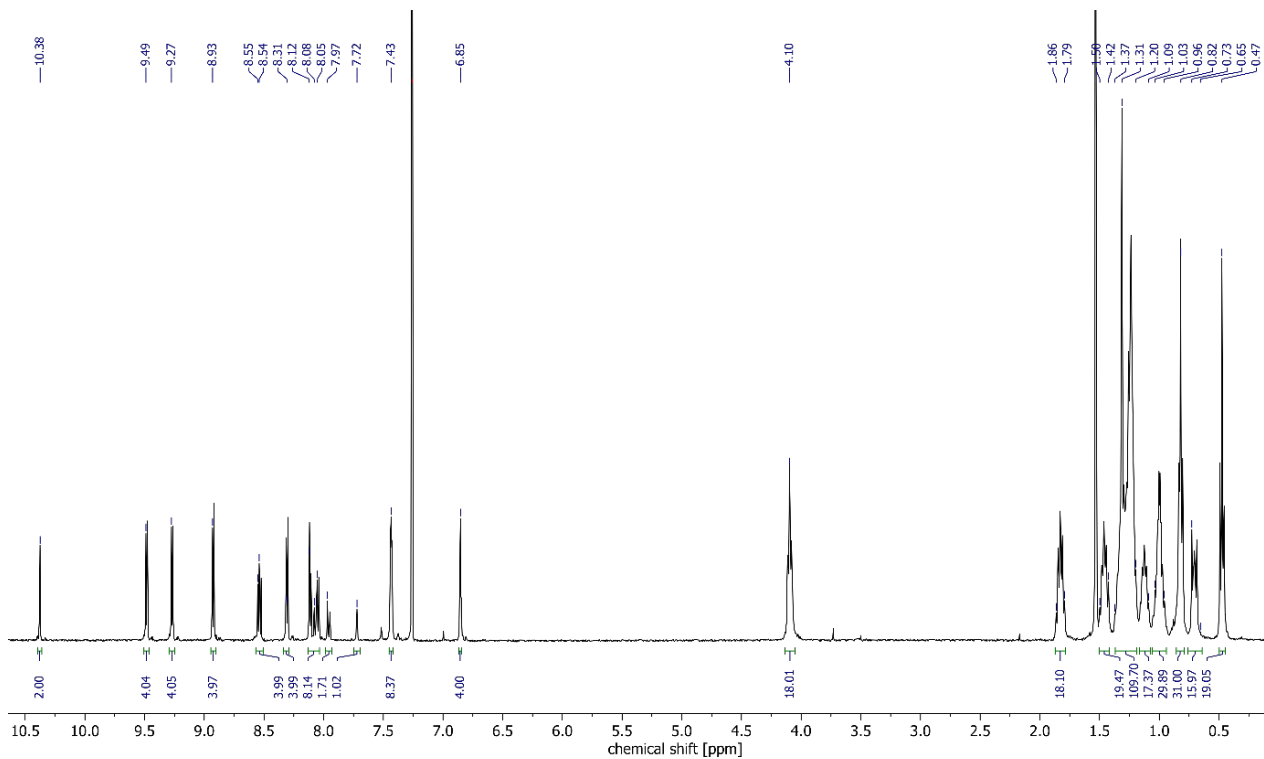
**Figure S9.**  $^1\text{H}$  NMR spectrum of **S6**,  $\text{CDCl}_3$ , 600 MHz, 298 K.



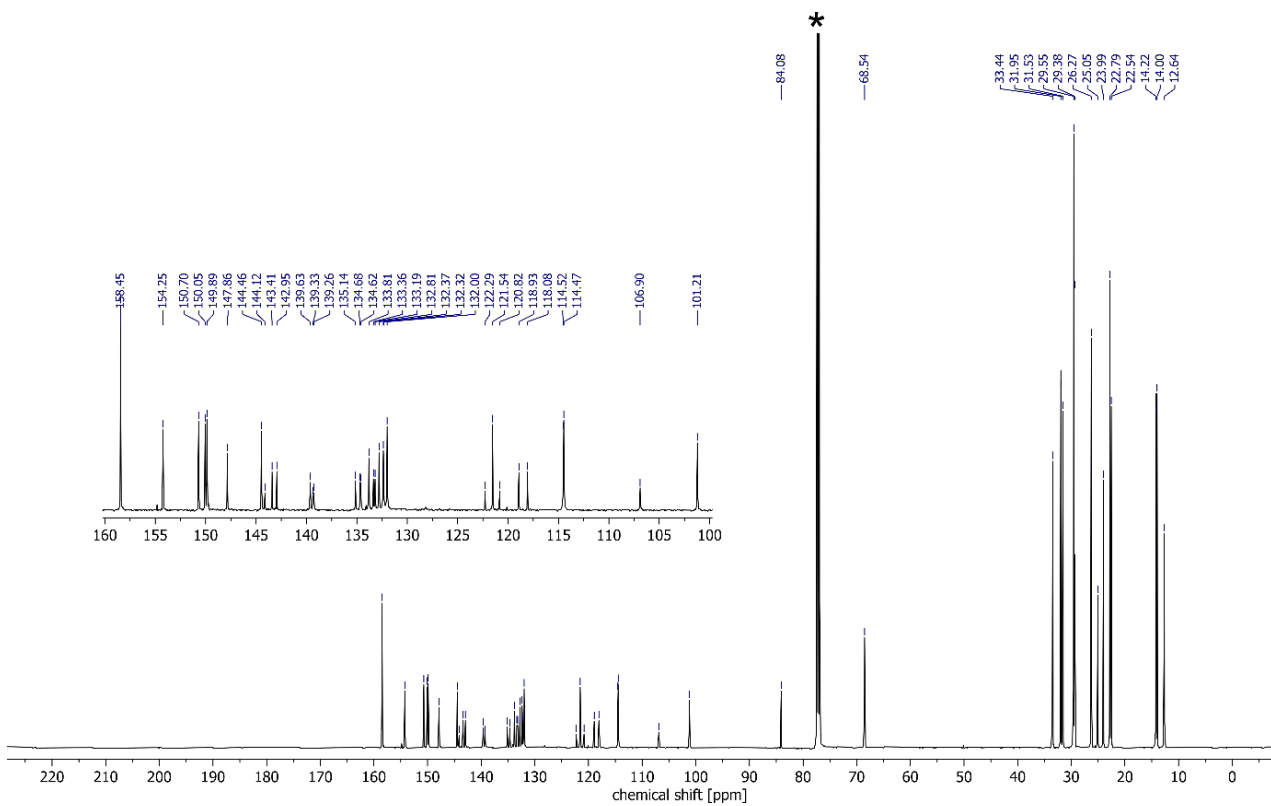
**Figure S10.**  $^{13}\text{C}$  NMR spectrum of **S6**,  $\text{CDCl}_3$ , 151 MHz, 298 K.



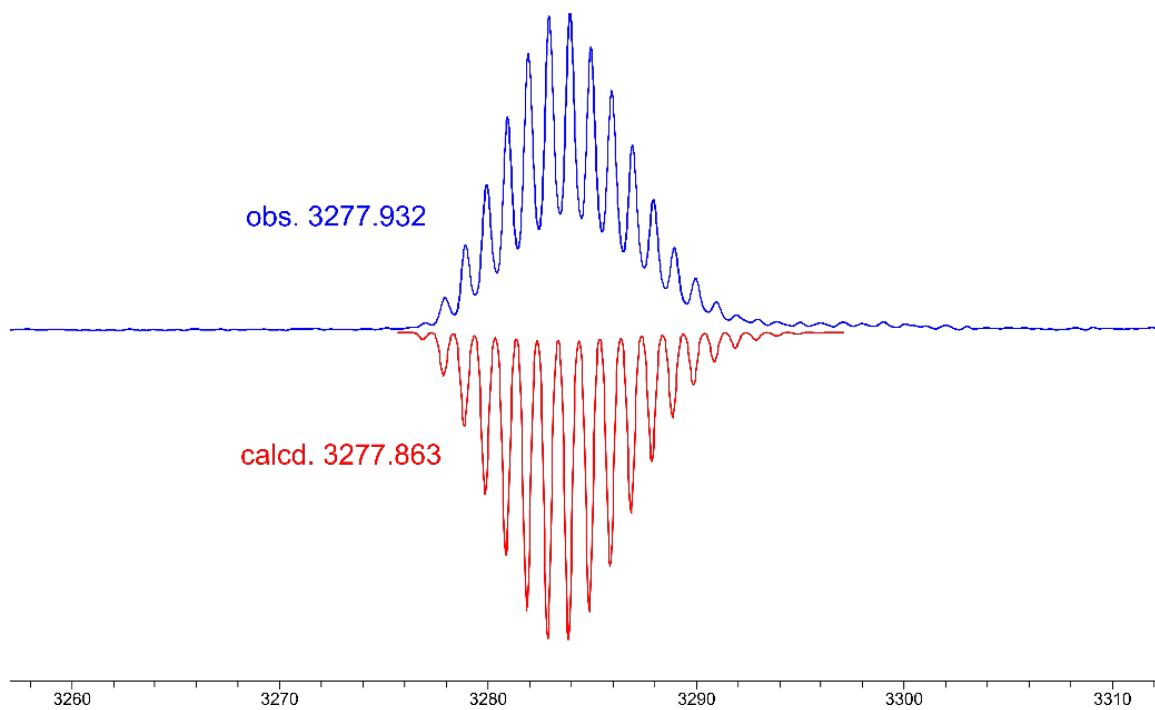
**Figure S11.** Selected region of calculated (red) and recorded (blue) MALDI mass spectra of **S6**, DCTB matrix.



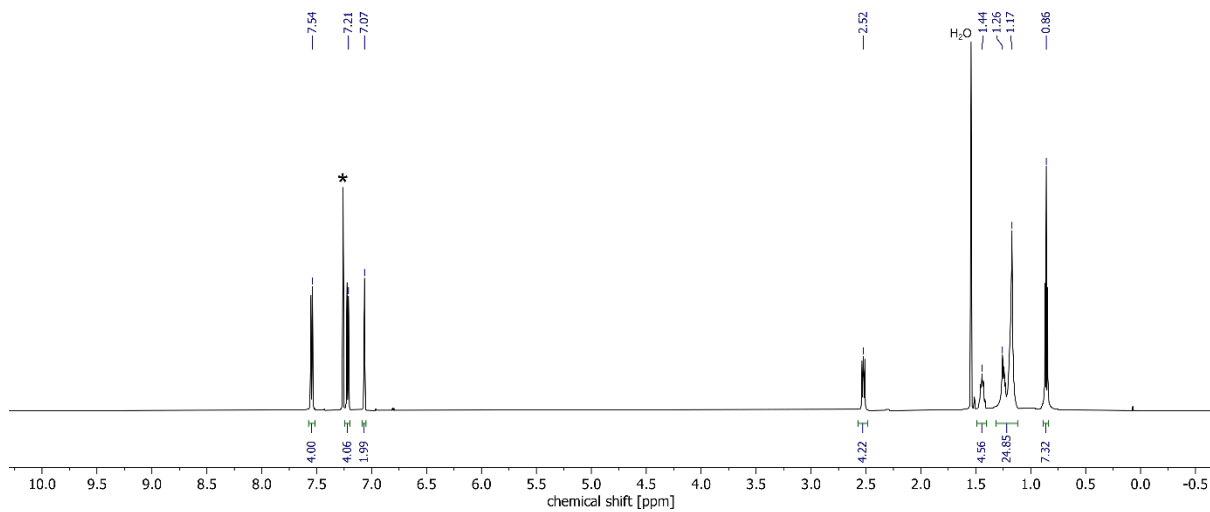
**Figure S12.**  $^1\text{H}$  NMR spectrum of **6**,  $\text{CDCl}_3$ , 600 MHz, 298 K.



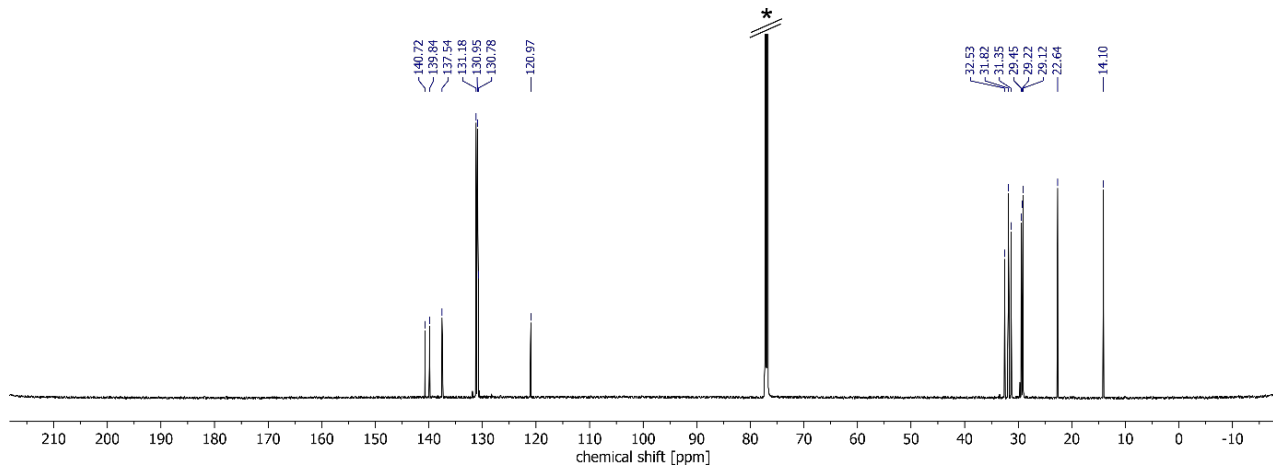
**Figure S13.**  $^{13}\text{C}$  NMR spectrum of **6**,  $\text{CDCl}_3$ , 151 MHz, 298 K.



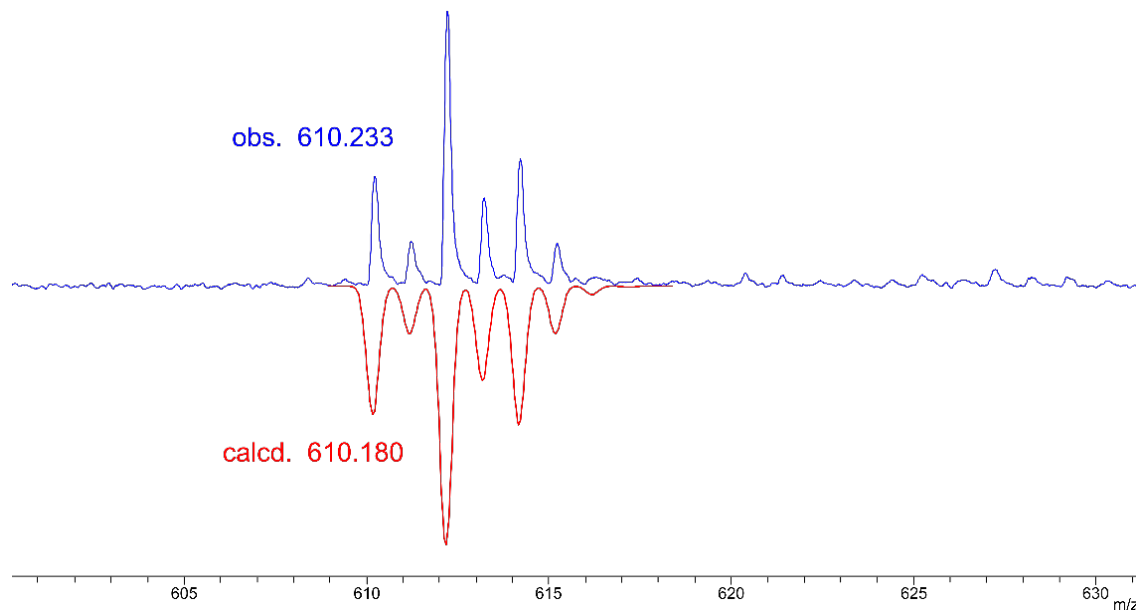
**Figure S14.** Selected region of calculated (red) and recorded (blue) MALDI mass spectra of **6**, DCTB matrix.



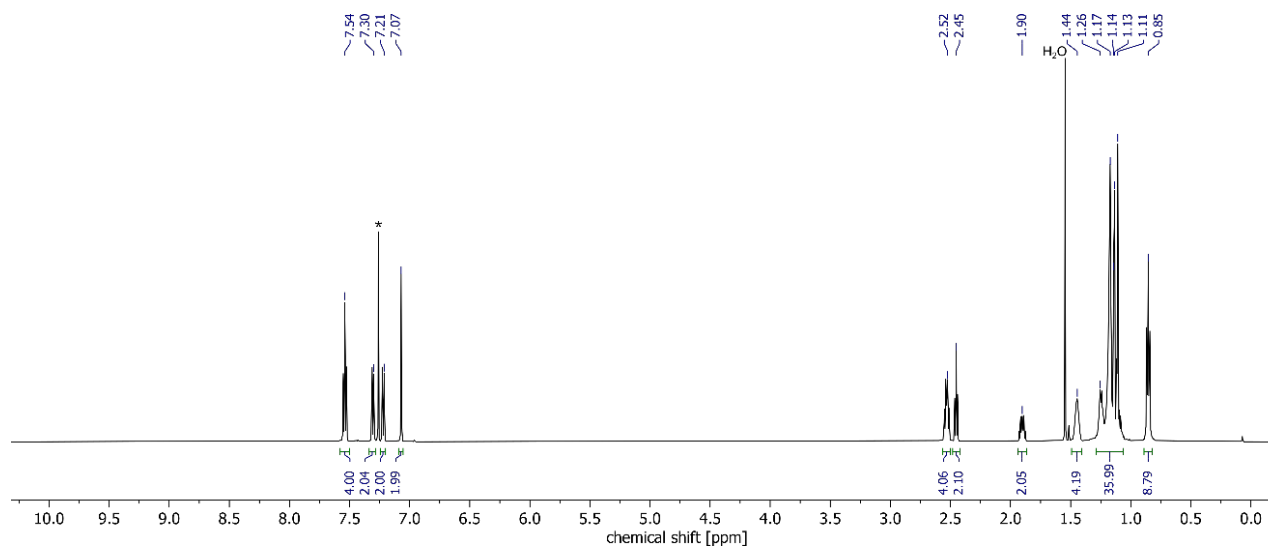
**Figure S15.**  $^1\text{H}$  NMR spectrum of **S2**,  $\text{CDCl}_3$ , 600 MHz, 298 K.



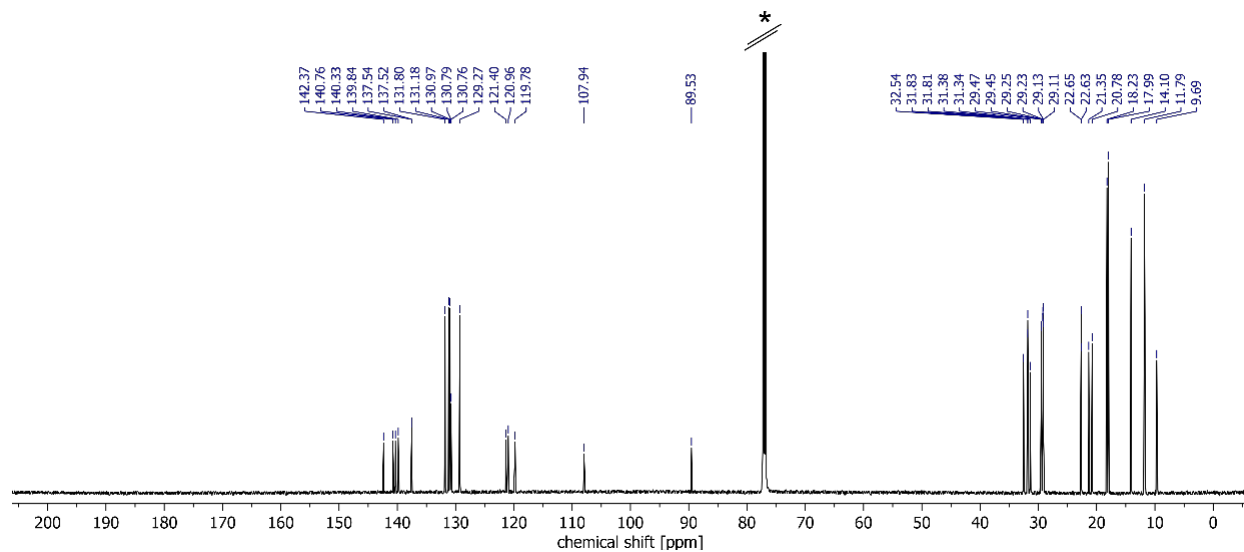
**Figure S16.**  $^{13}\text{C}$  NMR spectrum of **S2**,  $\text{CDCl}_3$ , 151 MHz, 298 K.



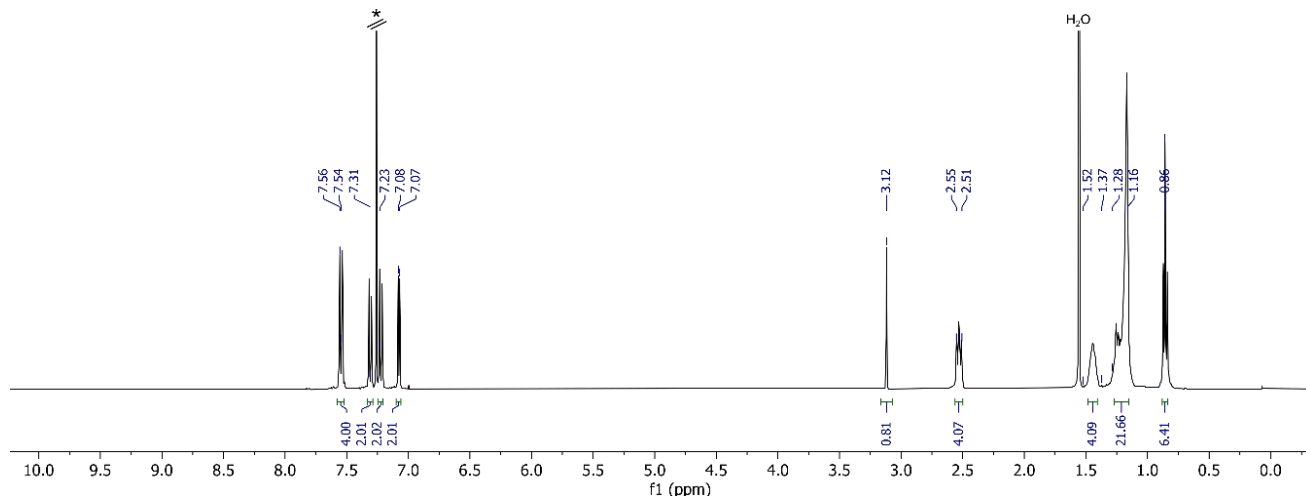
**Figure S17.** Selected region of a calculated (red) and recorded (blue) MALDI mass spectra of **S2**, DCTB matrix.



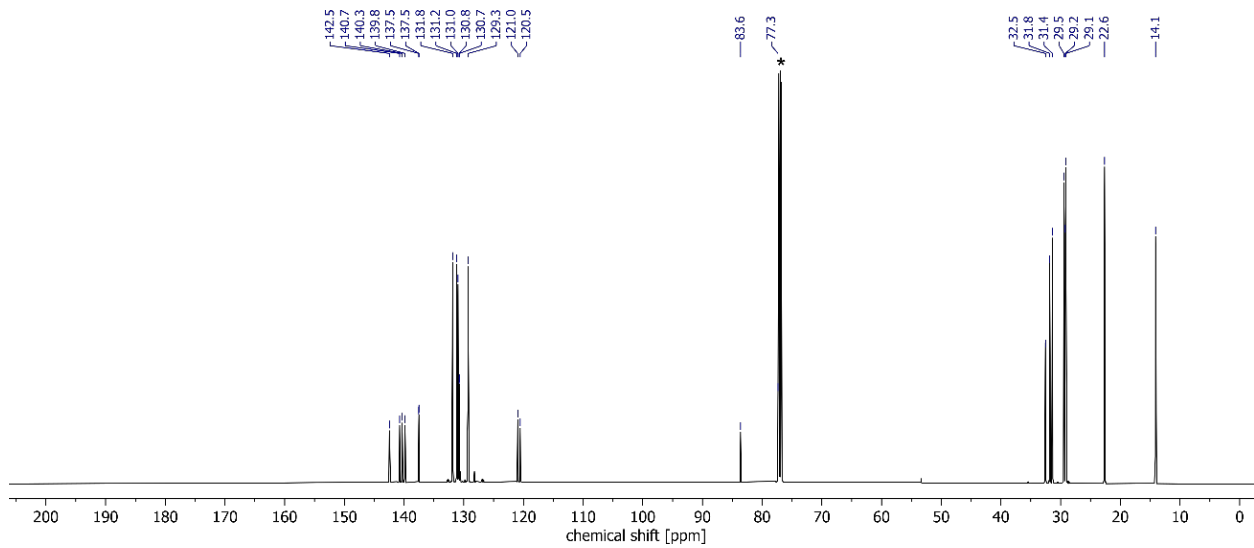
**Figure S18.**  $^1\text{H}$  NMR spectrum of **S3**,  $\text{CDCl}_3$ , 600 MHz, 298 K.



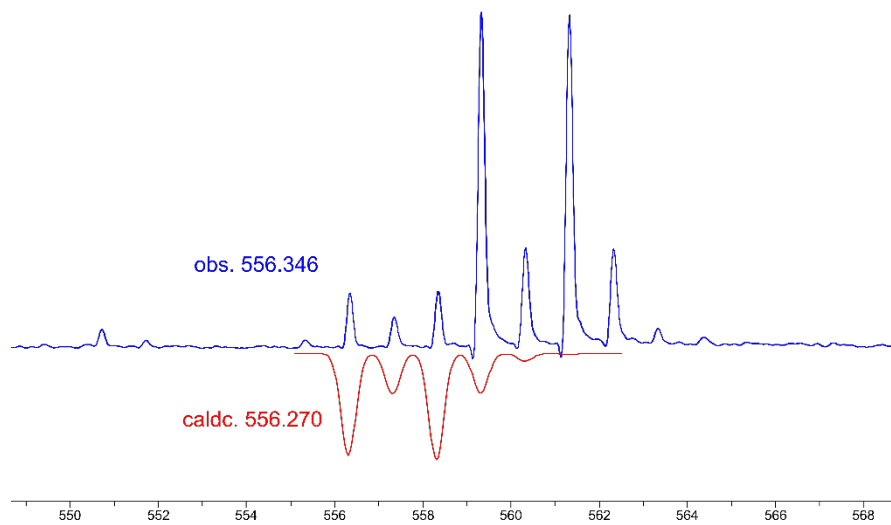
**Figure S19.**  $^{13}\text{C}$  NMR spectrum of **S3**,  $\text{CDCl}_3$ , 151 MHz, 298 K.



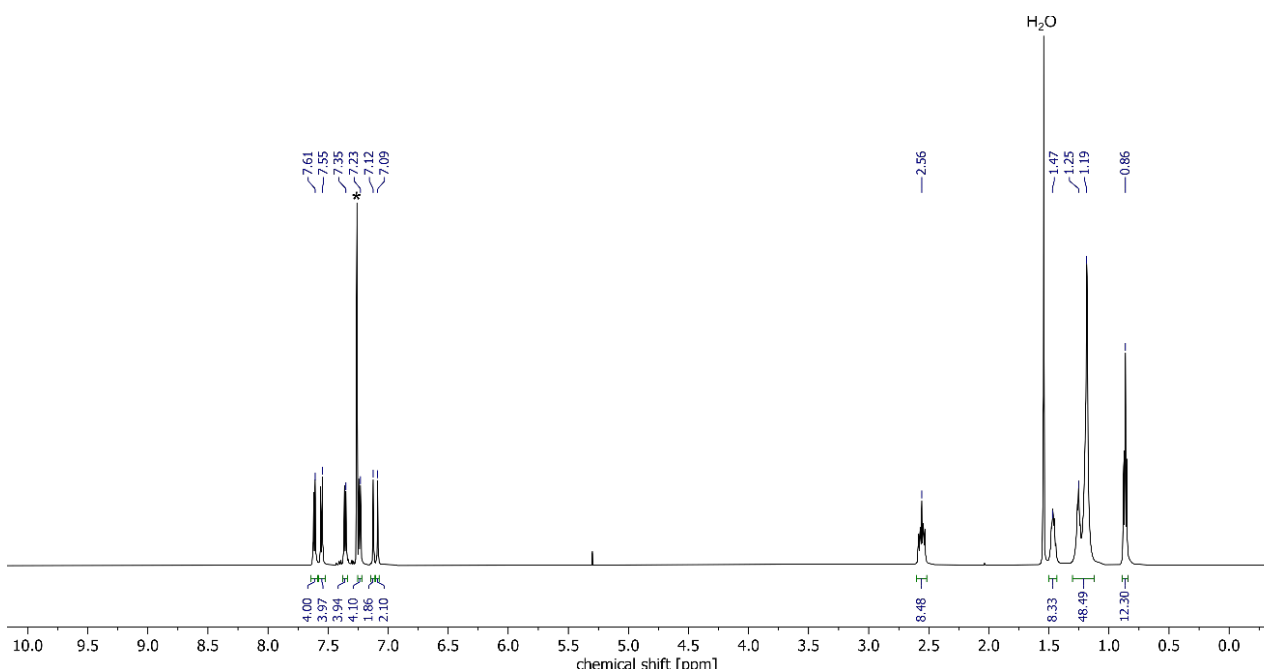
**Figure S20.**  $^1\text{H}$  NMR spectrum of **S4**,  $\text{CDCl}_3$ , 600 MHz, 298 K.



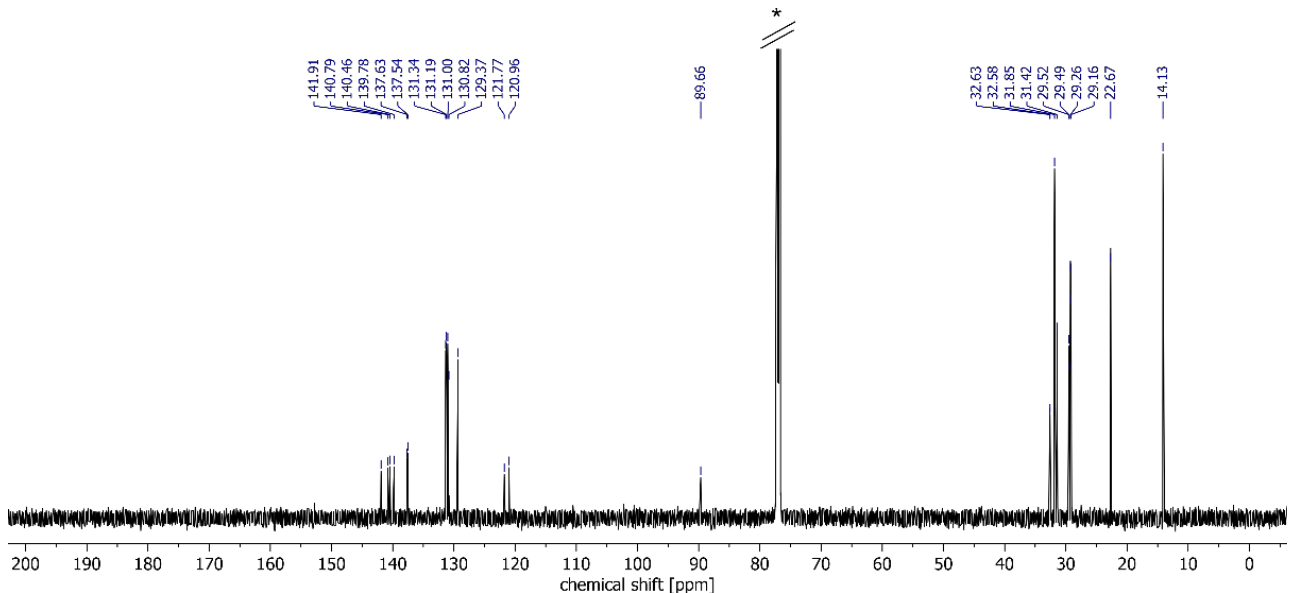
**Figure S21.** <sup>13</sup>C NMR spectrum of **S4**, CDCl<sub>3</sub>, 151 MHz, 298 K.



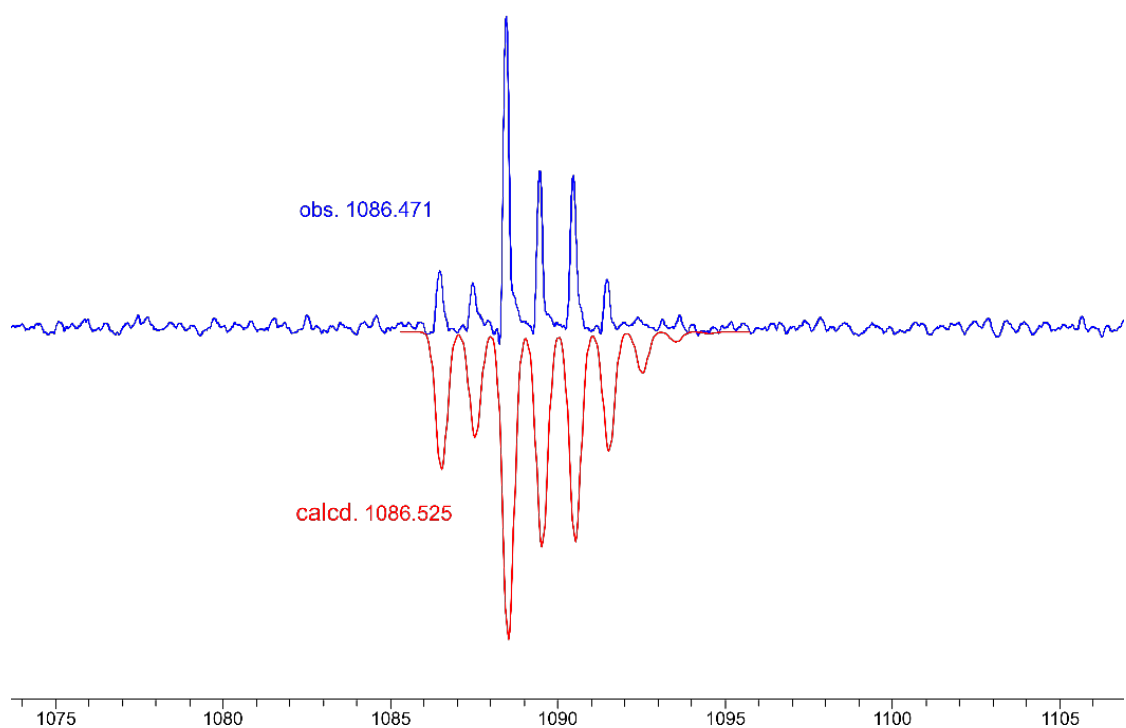
**Figure S22.** Selected region of calculated (red) and recorded (blue) MALDI mass spectra of **S4**, DCTB matrix.



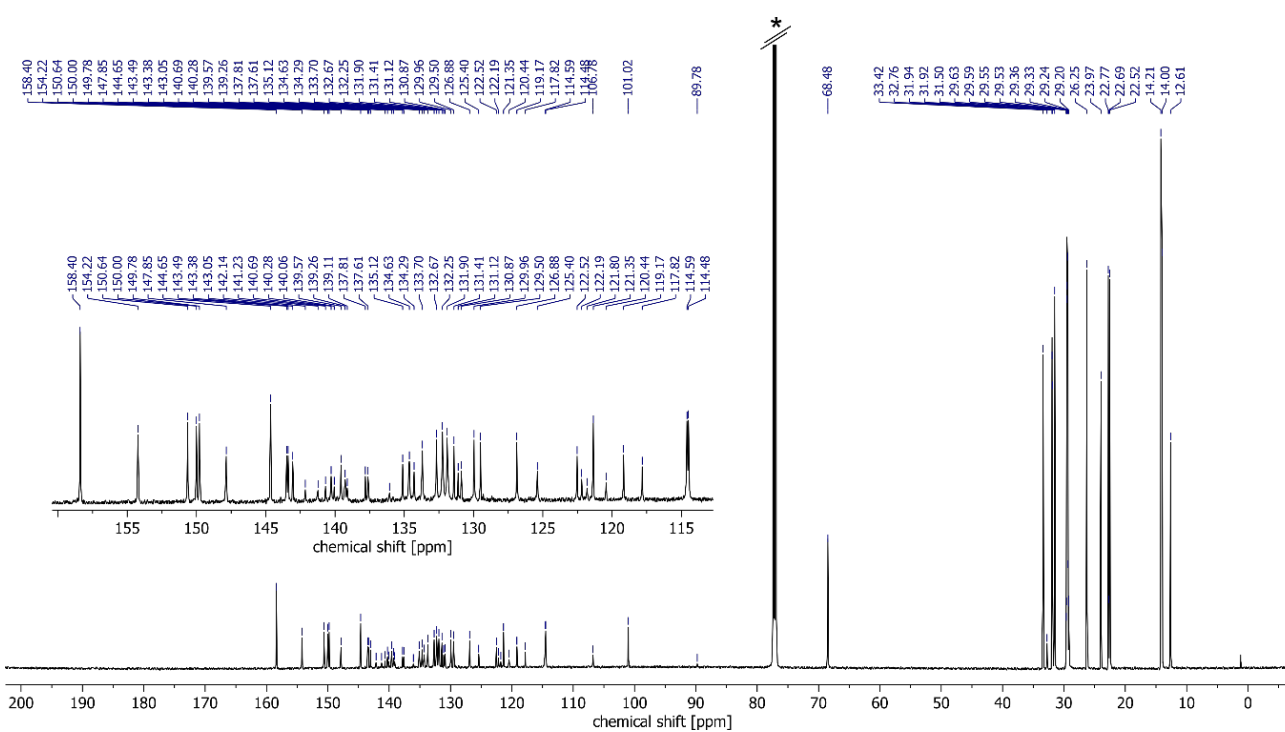
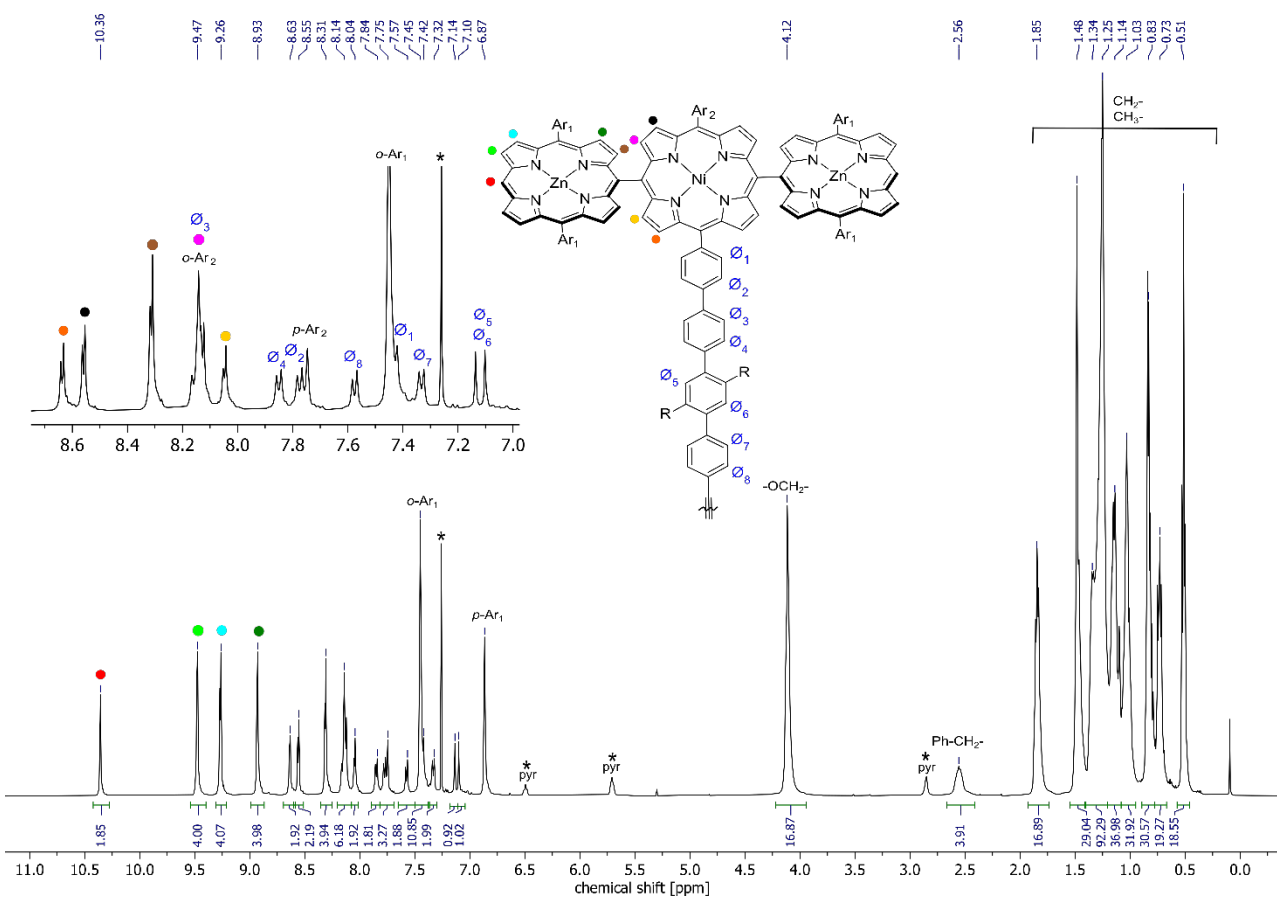
**Figure S23.** <sup>1</sup>H NMR spectrum of **7**, CDCl<sub>3</sub>, 600 MHz, 298 K.

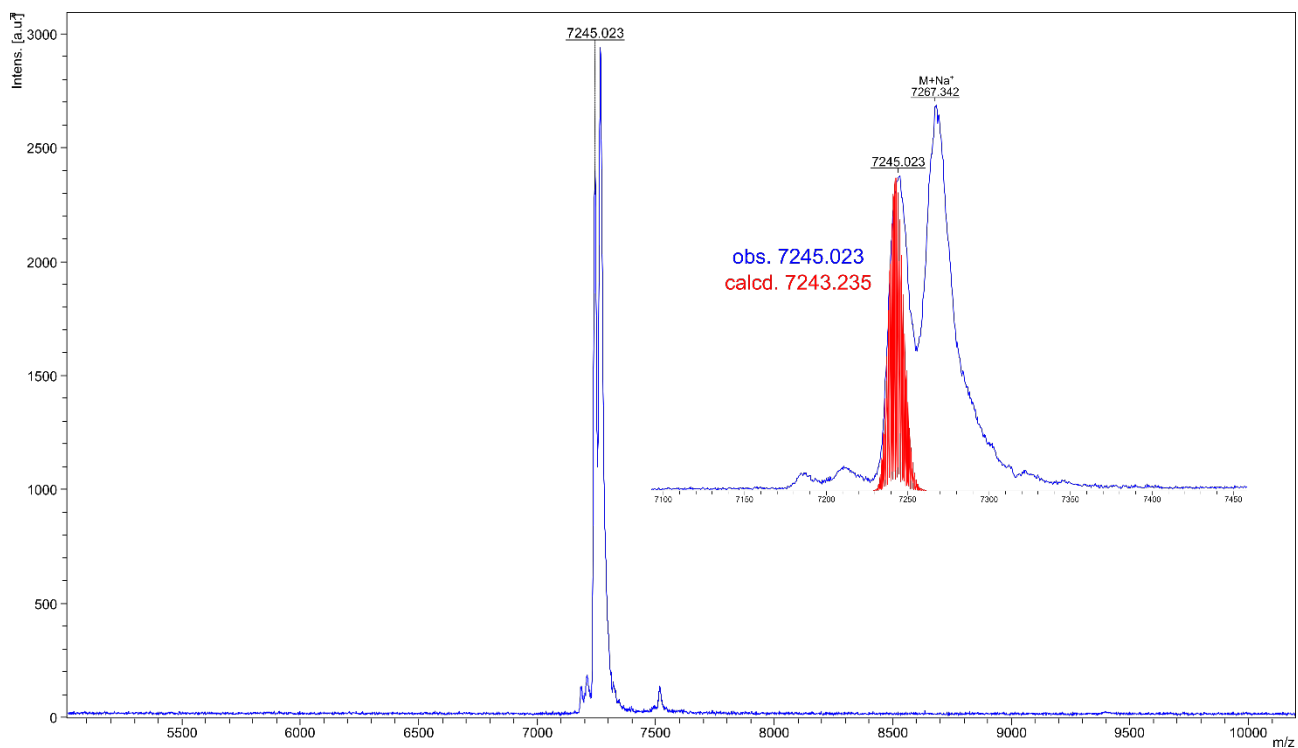


**Figure S24.**  $^{13}\text{C}$  NMR spectrum of **7**,  $\text{CDCl}_3$ , 151 MHz, 298 K.

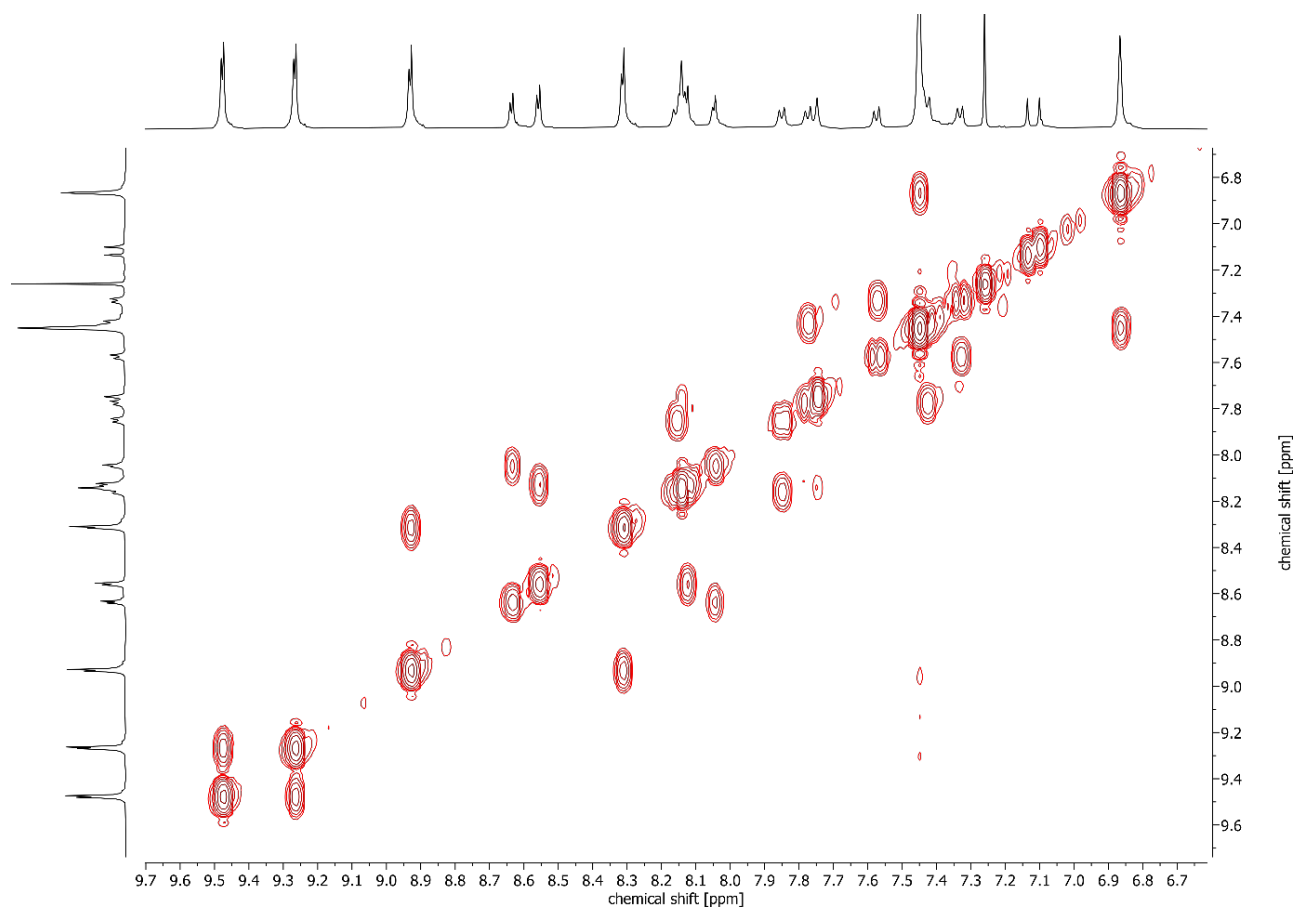


**Figure S25.** Selected region of calculated (red) and recorded (blue) MALDI mass spectra of **7**, DCTB matrix.

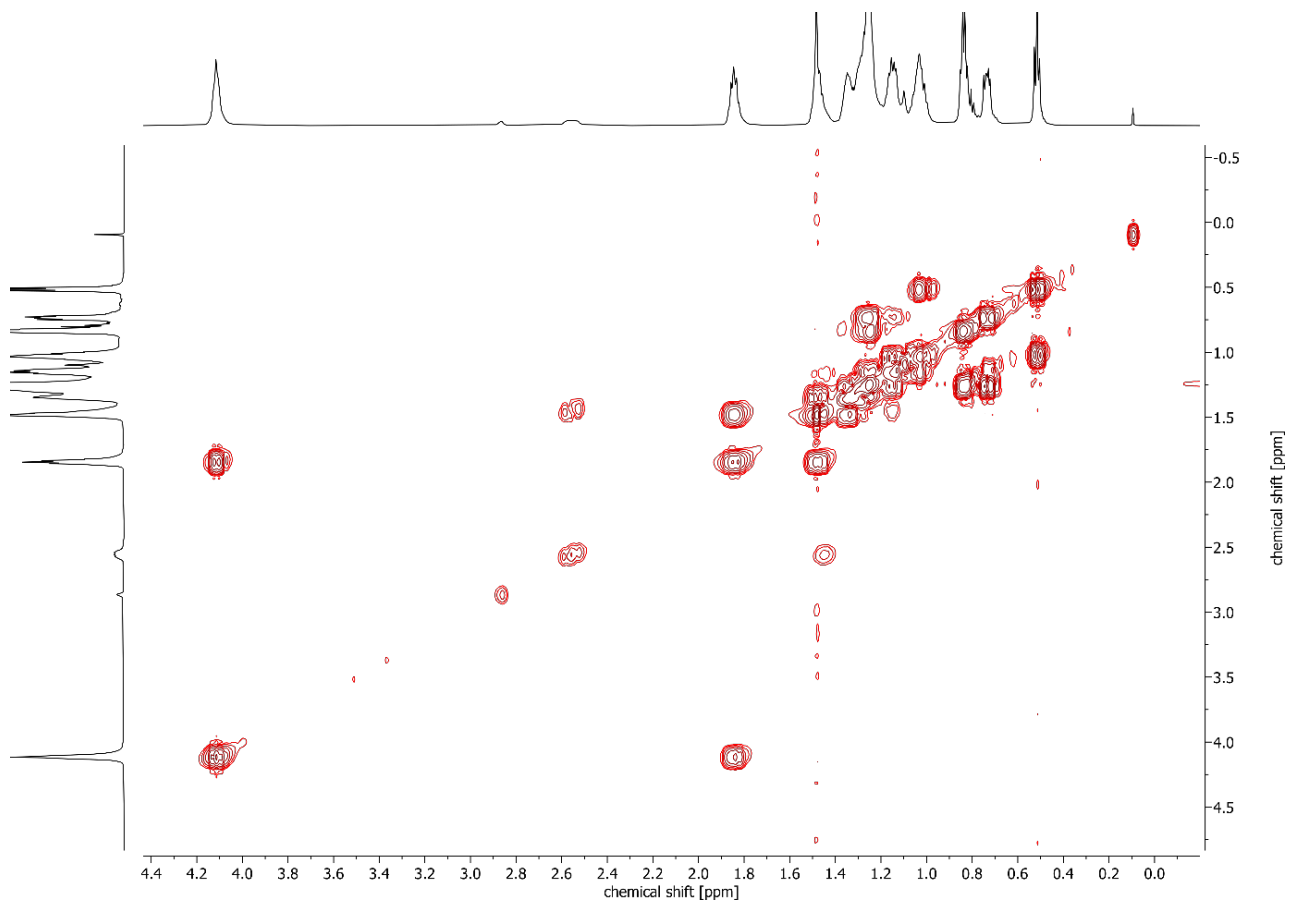




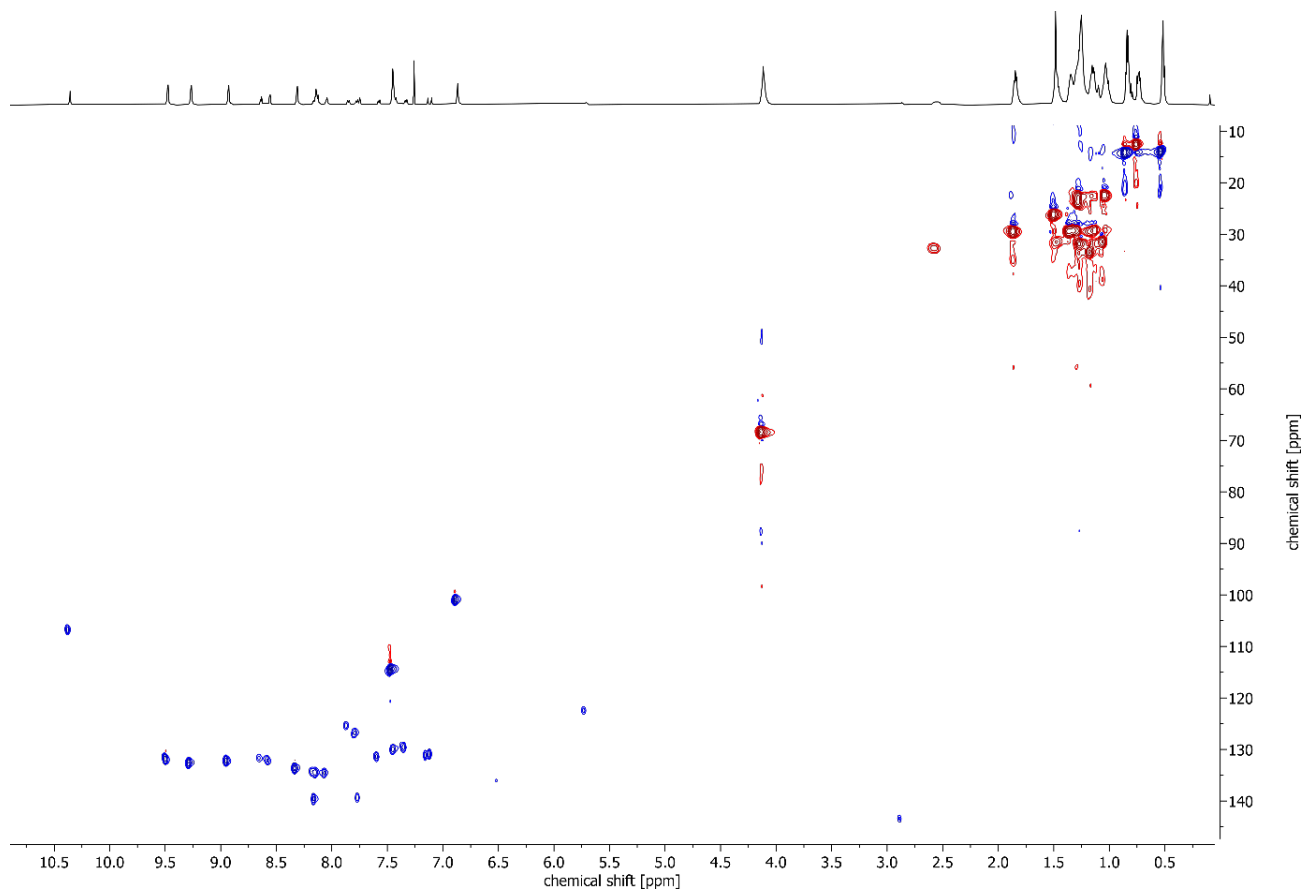
**Figure S28.** Selected region of calculated (red) and recorded (blue) MALDI mass spectra of **3**, DCTB matrix.



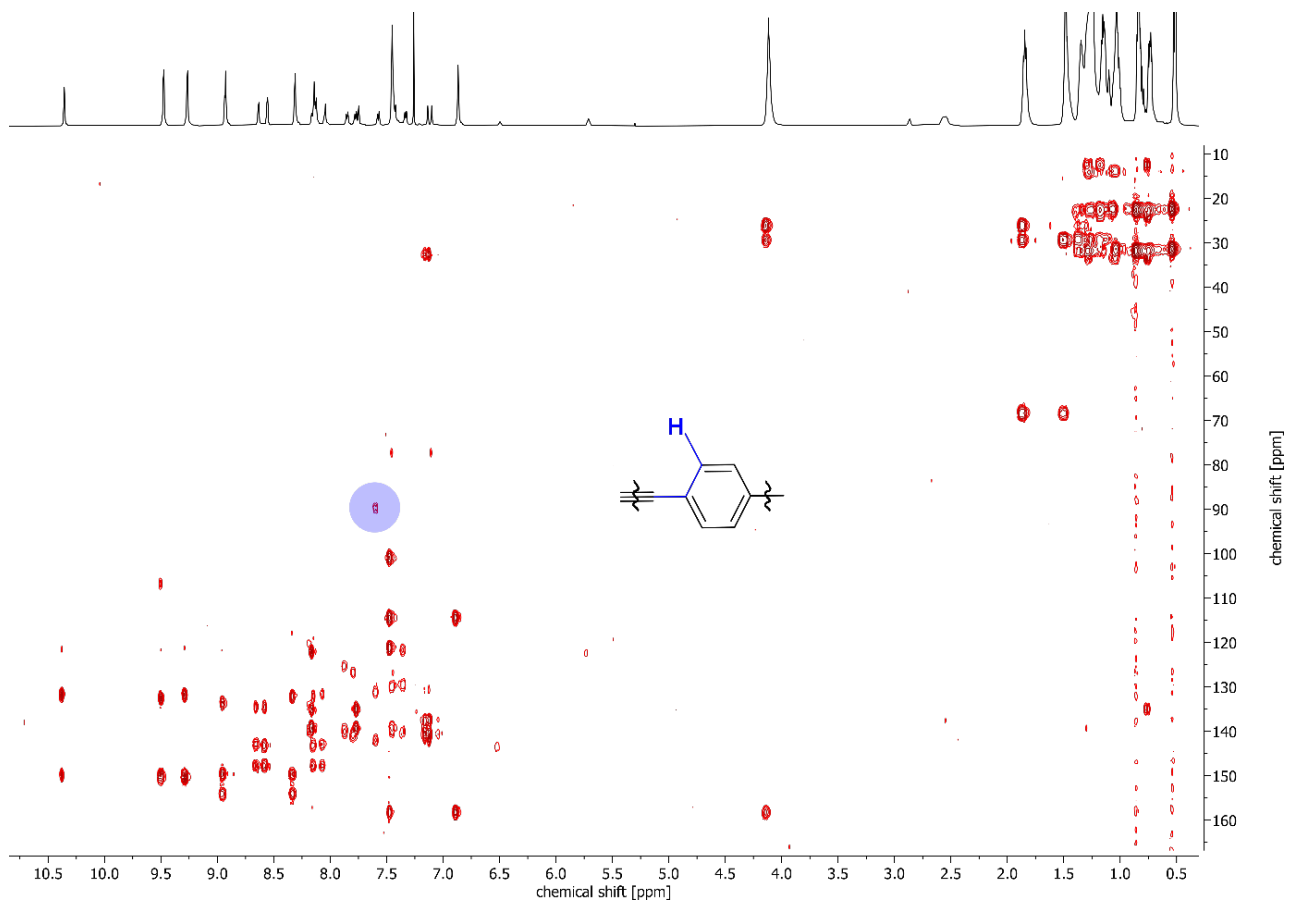
**Figure S29.** Selected aromatic region of a  $^1\text{H}$ - $^1\text{H}$  COSY NMR spectrum of **3**,  $\text{CDCl}_3$ , 600 MHz, 298 K.



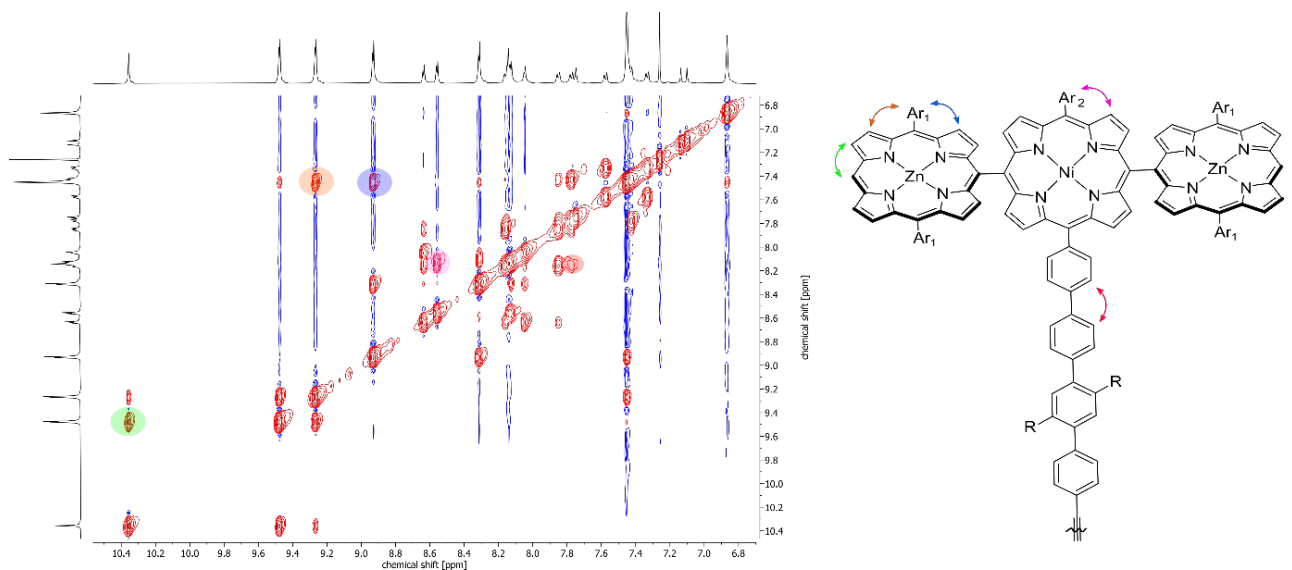
**Figure S30.** Selected alkyl region of a  $^1\text{H}$ - $^1\text{H}$  COSY NMR spectrum of **3**,  $\text{CDCl}_3$ , 600 MHz, 298 K.



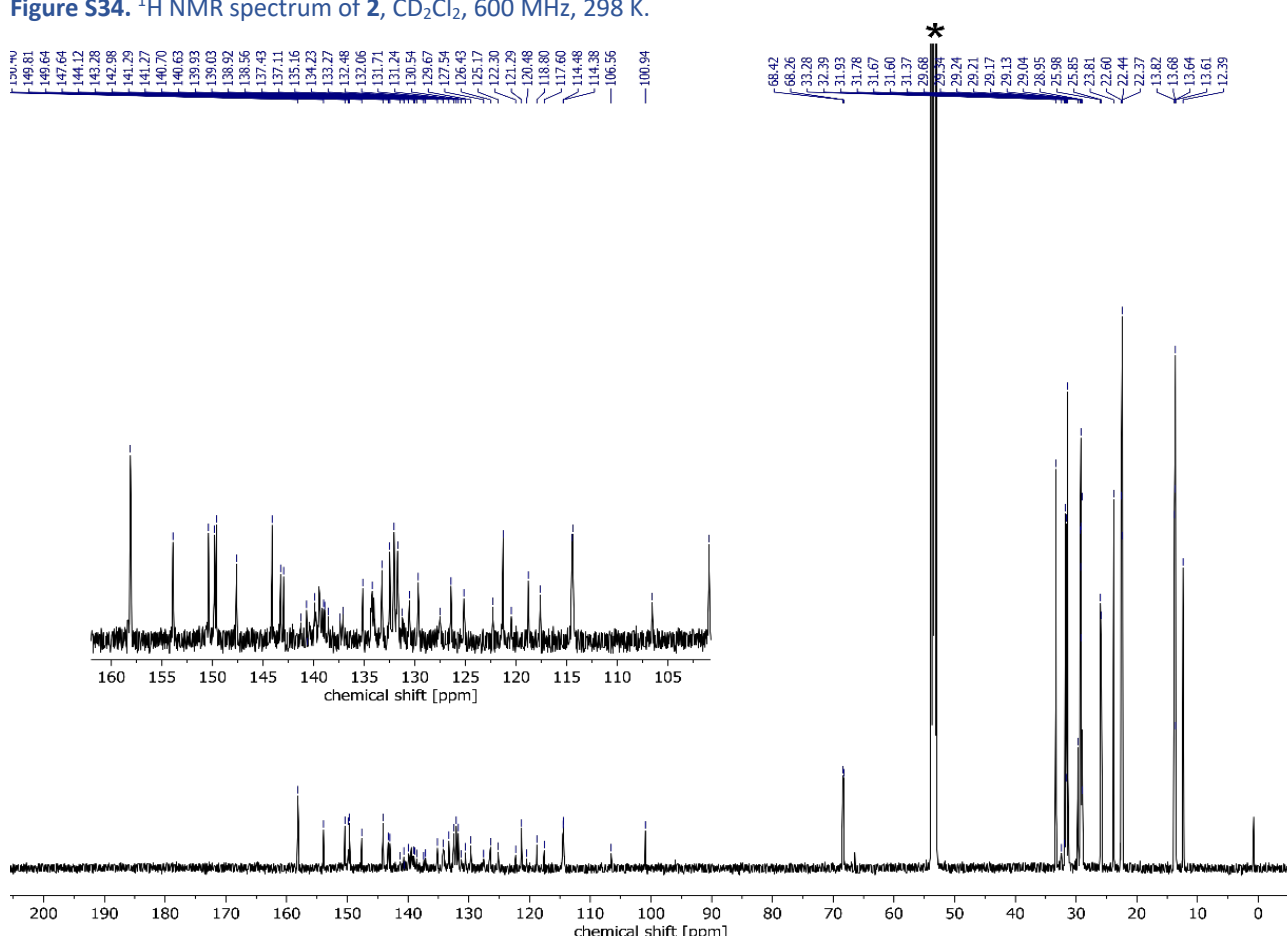
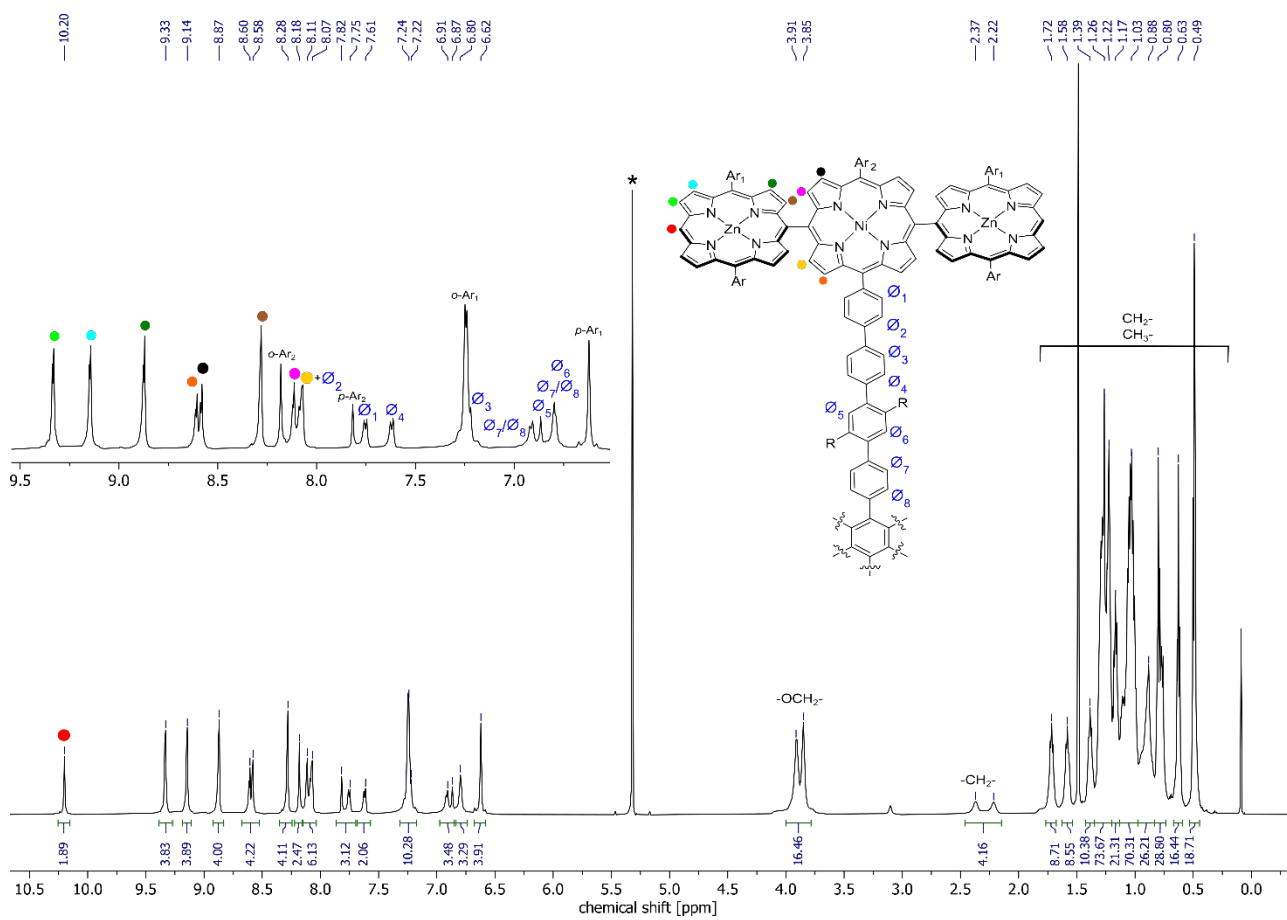
**Figure S31.**  $^1\text{H}$ - $^{13}\text{C}$  HSQC NMR spectrum of **3**,  $\text{CDCl}_3$ , 600 MHz, 298 K.



**Figure S32.**  $^1\text{H}$ - $^{13}\text{C}$  HMBC NMR spectrum of **3**,  $\text{CDCl}_3$ , 600 MHz, 298 K. Correlation between acetylene carbon and neighboring phenyl proton is marked in blue.



**Figure S33.** Selected aromatic region of a  $^1\text{H}$ - $^1\text{H}$  NOESY NMR spectrum of **3**,  $\text{CDCl}_3$ , 600 MHz, 298 K with assigned correlations crucial for signal assignment.



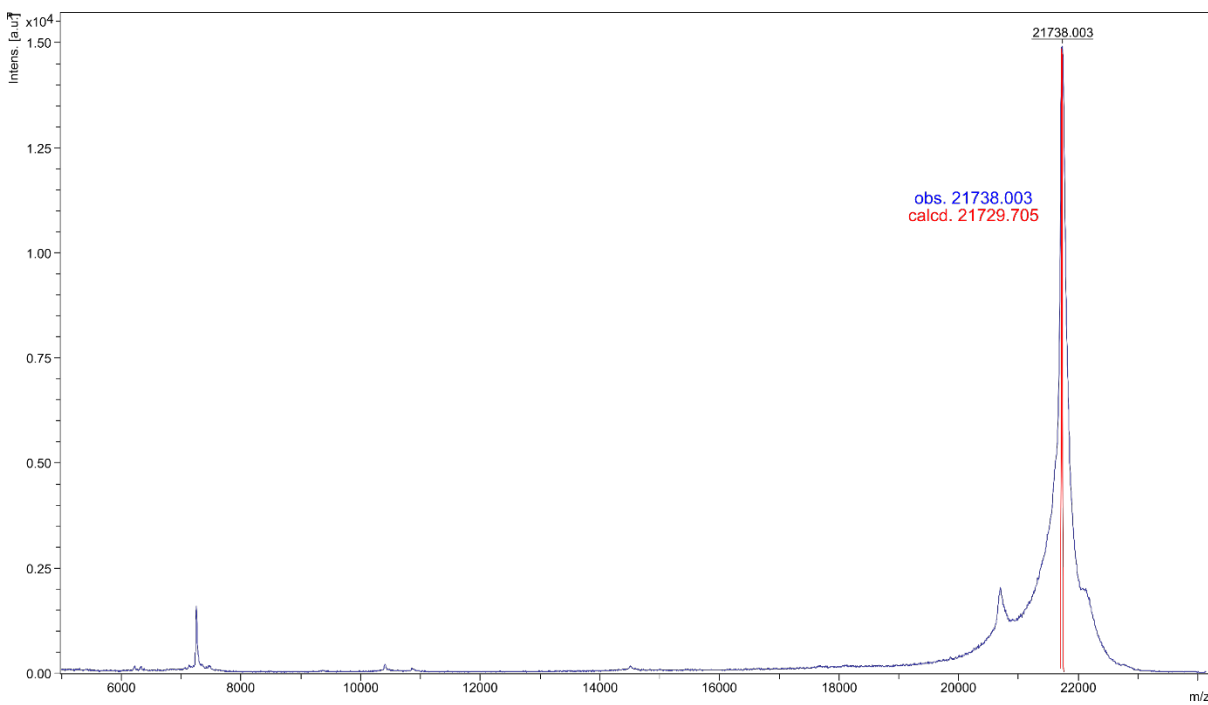


**Figure S36.** Calculated (red) and recorded (blue) MALDI mass spectra of **2**, DCTB matrix.

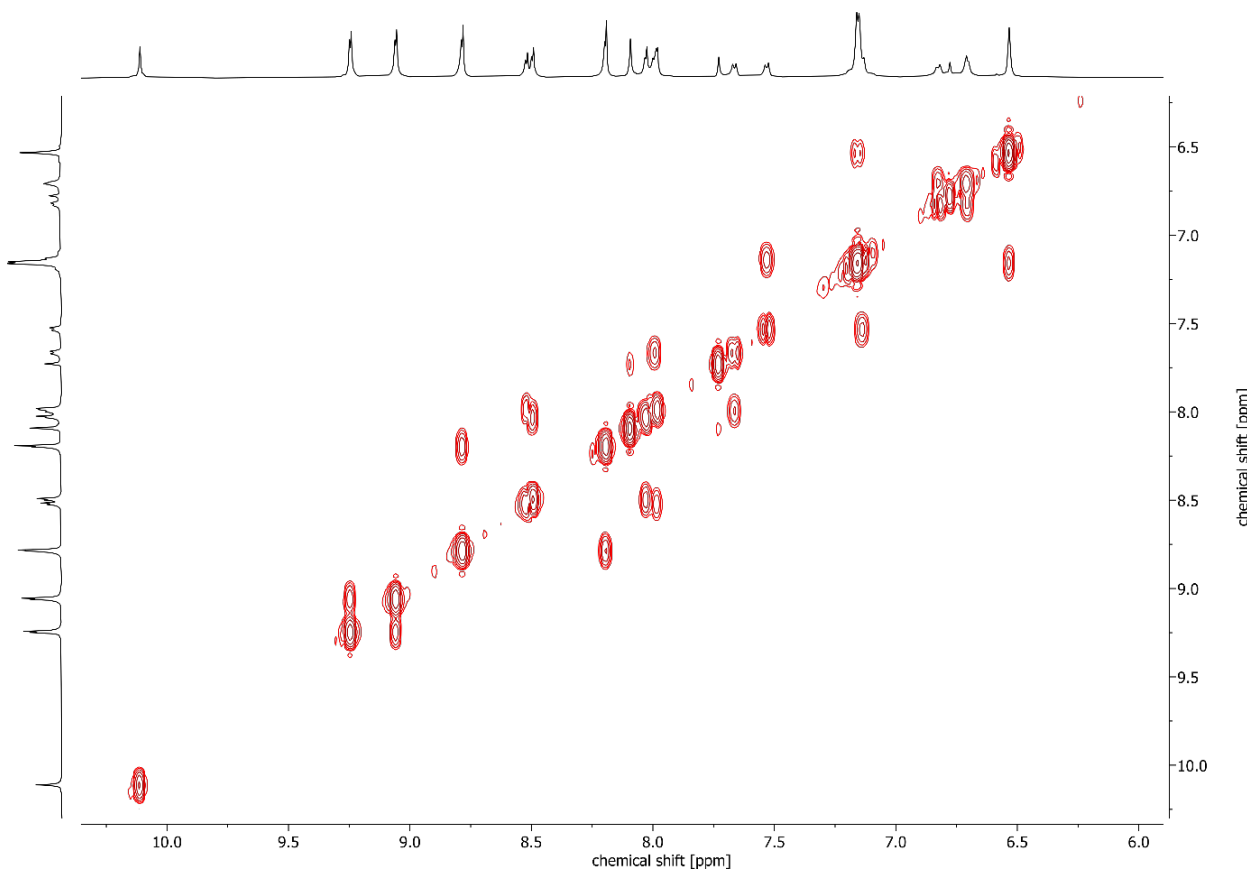


**Figure S37.** Selected aromatic region of a  ${}^1\text{H}$ - ${}^1\text{H}$  COSY NMR spectrum of **2**,  $\text{CD}_2\text{Cl}_2$ , 600 MHz, 298 K.

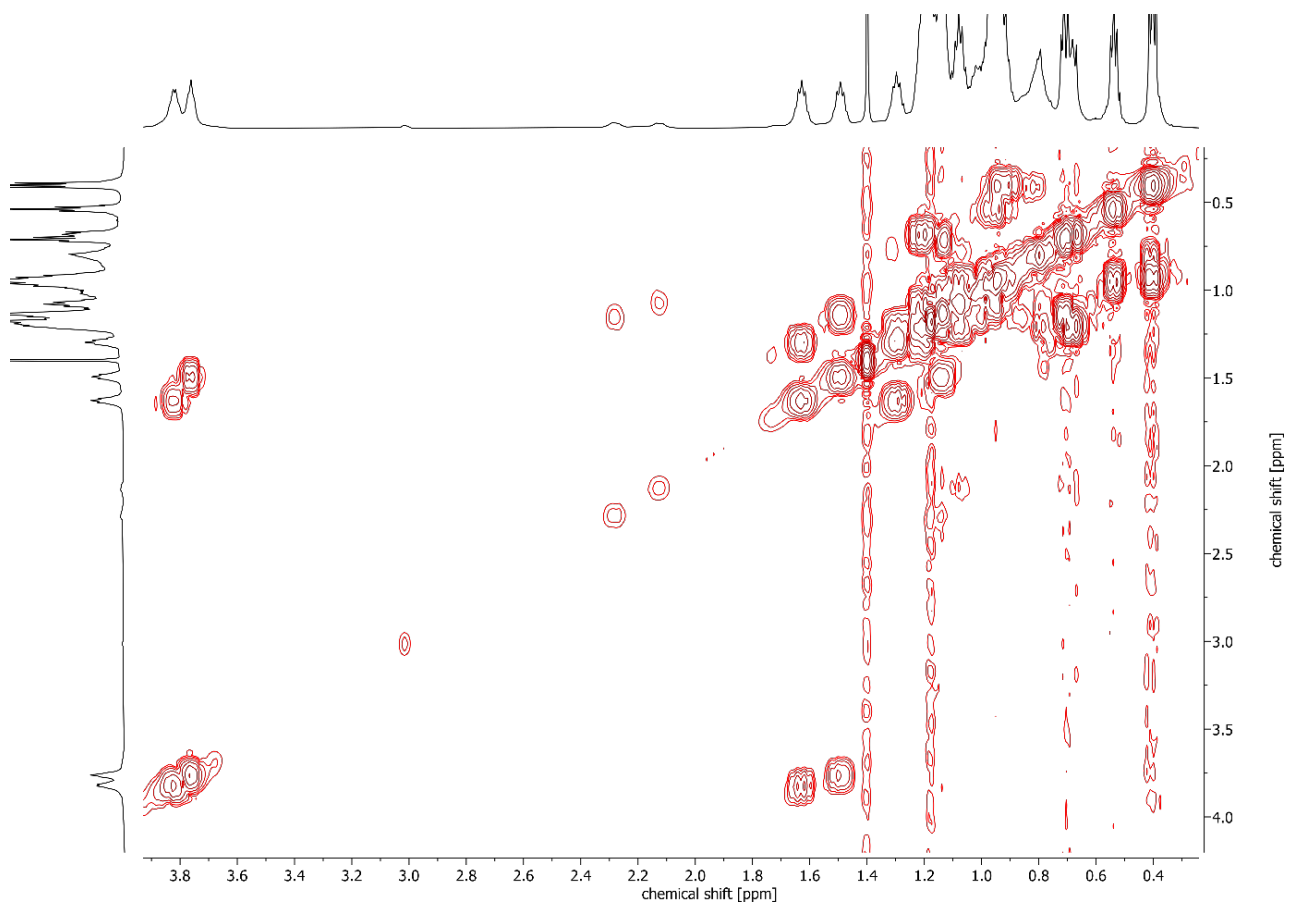


**Figure S38.** Selected alkyl region of a  $^1\text{H}$ - $^1\text{H}$  COSY NMR spectrum of **2**,  $\text{CD}_2\text{Cl}_2$ , 600 MHz, 298 K.

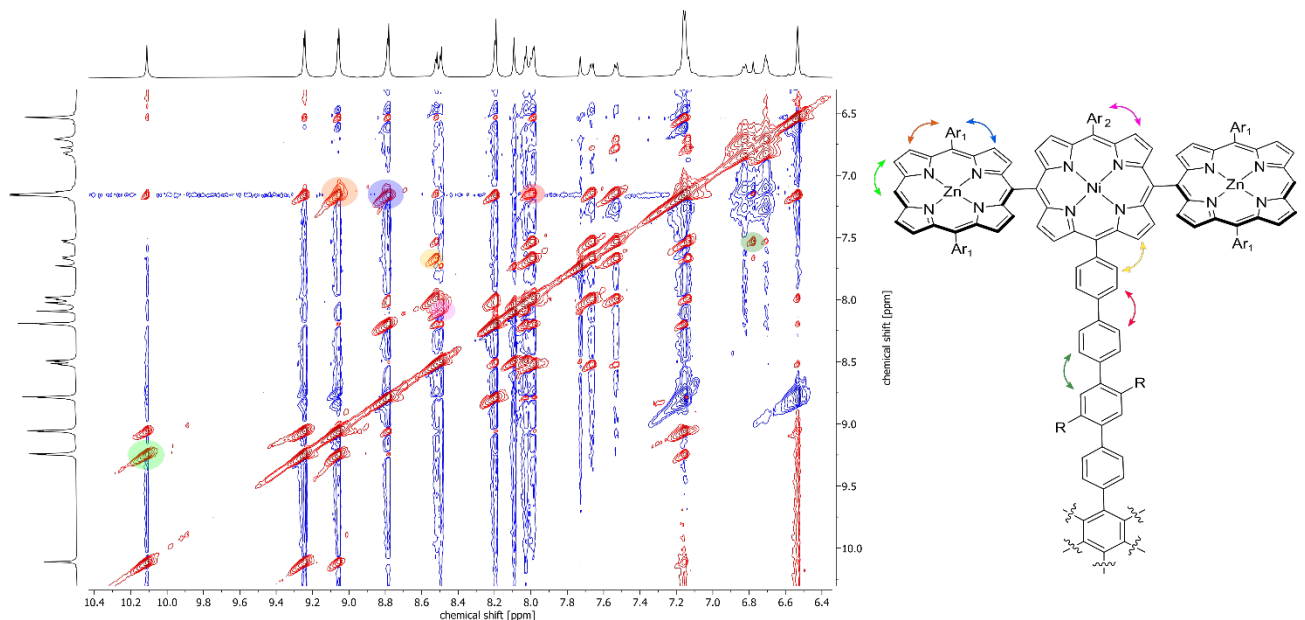


**Figure S39.** Selected aromatic region of a  $^1\text{H}$ - $^1\text{H}$  NOESY NMR spectrum of **2**,  $\text{CD}_2\text{Cl}_2$ , 600 MHz, 298 K with assigned correlations crucial for signal assignment.

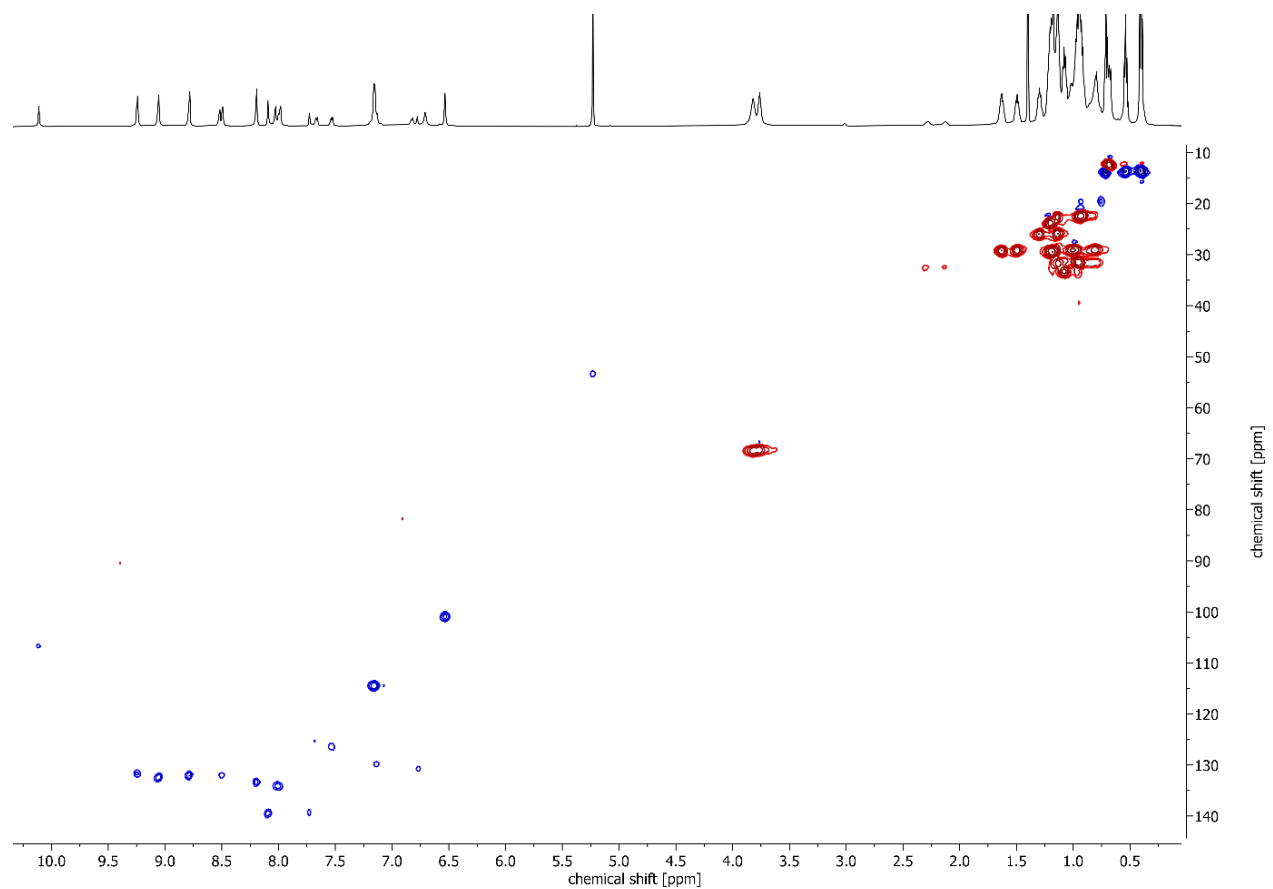


**Figure S40.**  $^1\text{H}$ - $^{13}\text{C}$  HSQC NMR spectrum of **2**,  $\text{CD}_2\text{Cl}_2$ , 600 MHz, 298 K.

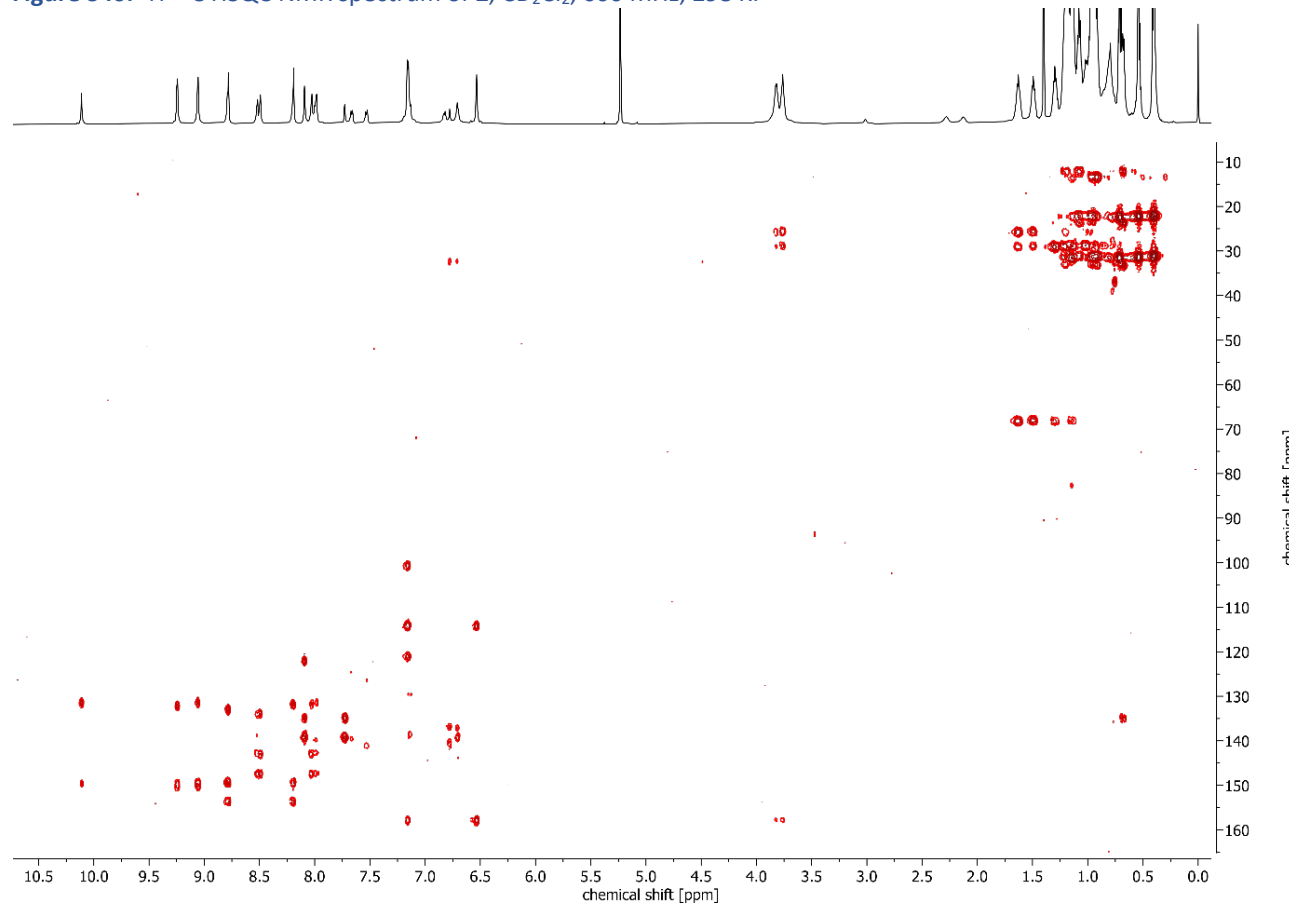


**Figure S41.**  $^1\text{H}$ - $^{13}\text{C}$  HMBC NMR spectrum of **2**,  $\text{CD}_2\text{Cl}_2$ , 600 MHz, 298 K.

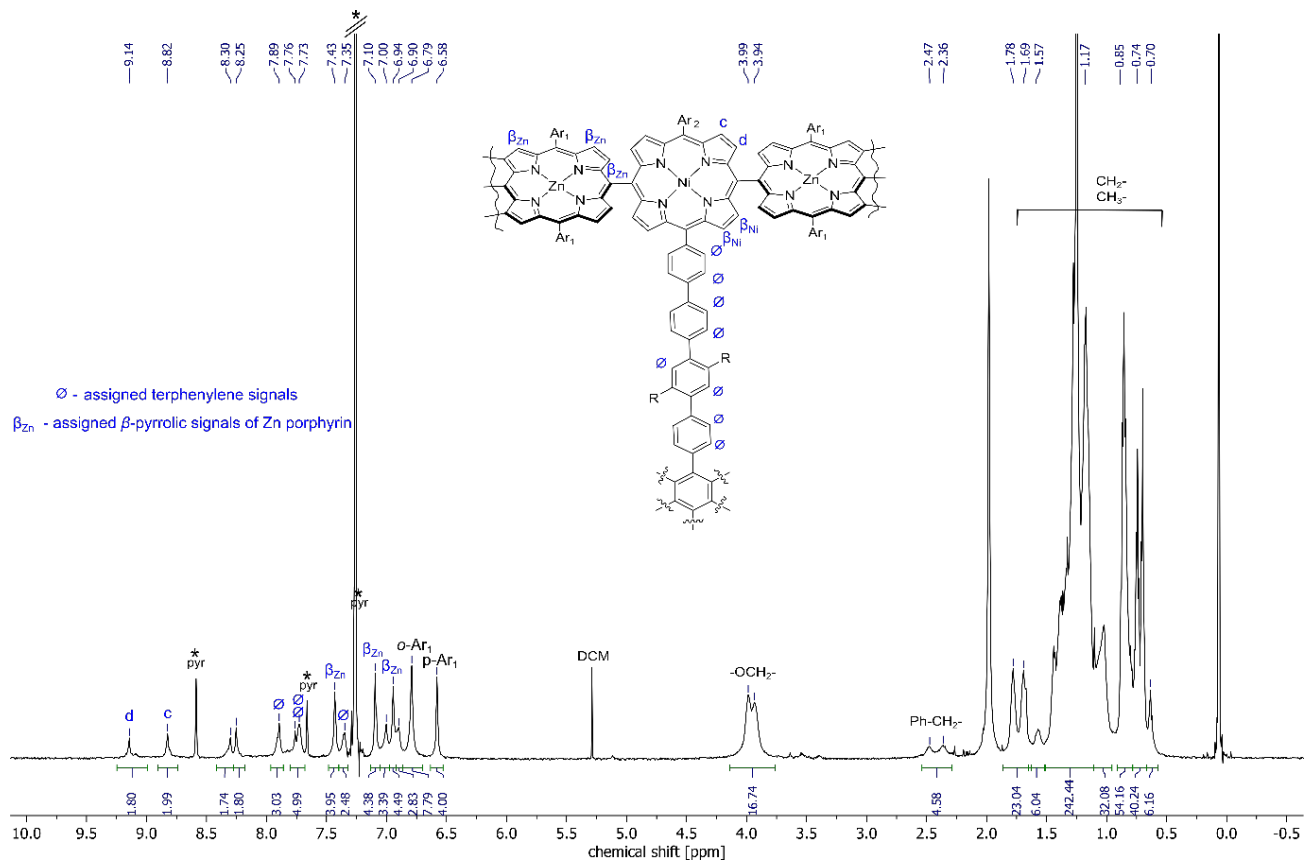


**Figure S42.**  $^1\text{H}$  NMR spectrum of **1** ( $\text{CDCl}_3 + 1\%$  pyridine- $d_5$ , 600 MHz, 298 K) with partial signals assignment.

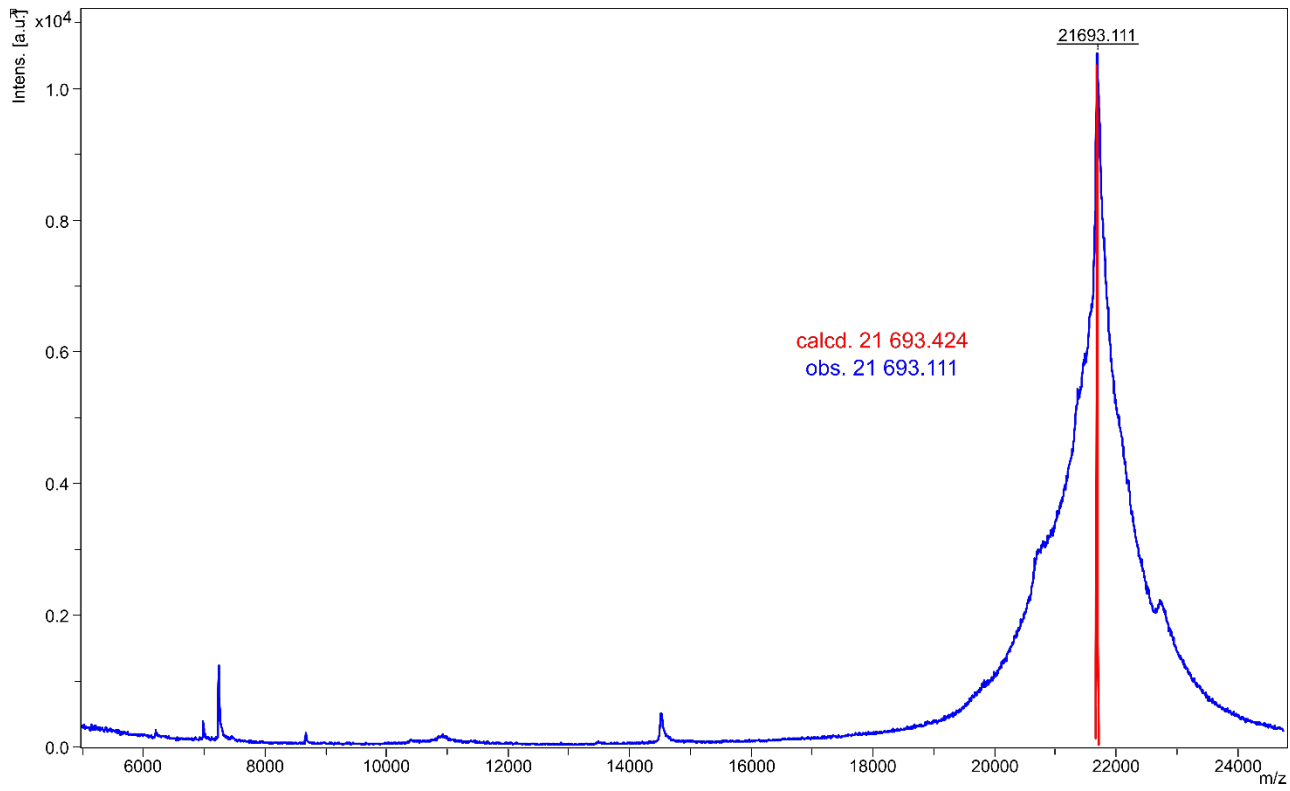


**Figure S43.** Calculated (red) and recorded (blue) MALDI mass spectra of **1**, DCTB matrix.

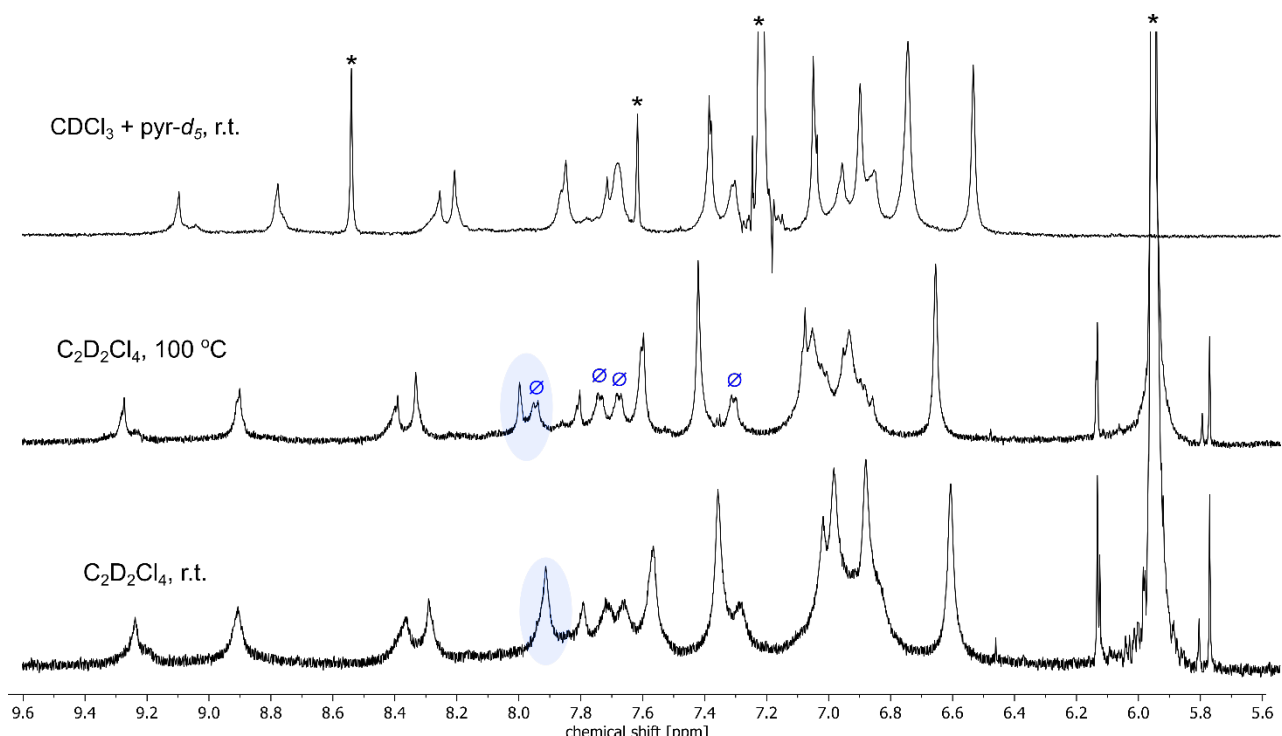


**Figure S44.** Comparison between NMR spectra of **1** recorded in chloroform at 25 °C with addition of pyridine-d<sub>5</sub> and in C<sub>2</sub>D<sub>2</sub>Cl<sub>4</sub> at 25 °C and 100 °C. Covalent core phenyl doublets become more resolved at higher temperature and it is possible to determine their coupling constants (ca. 8 Hz).

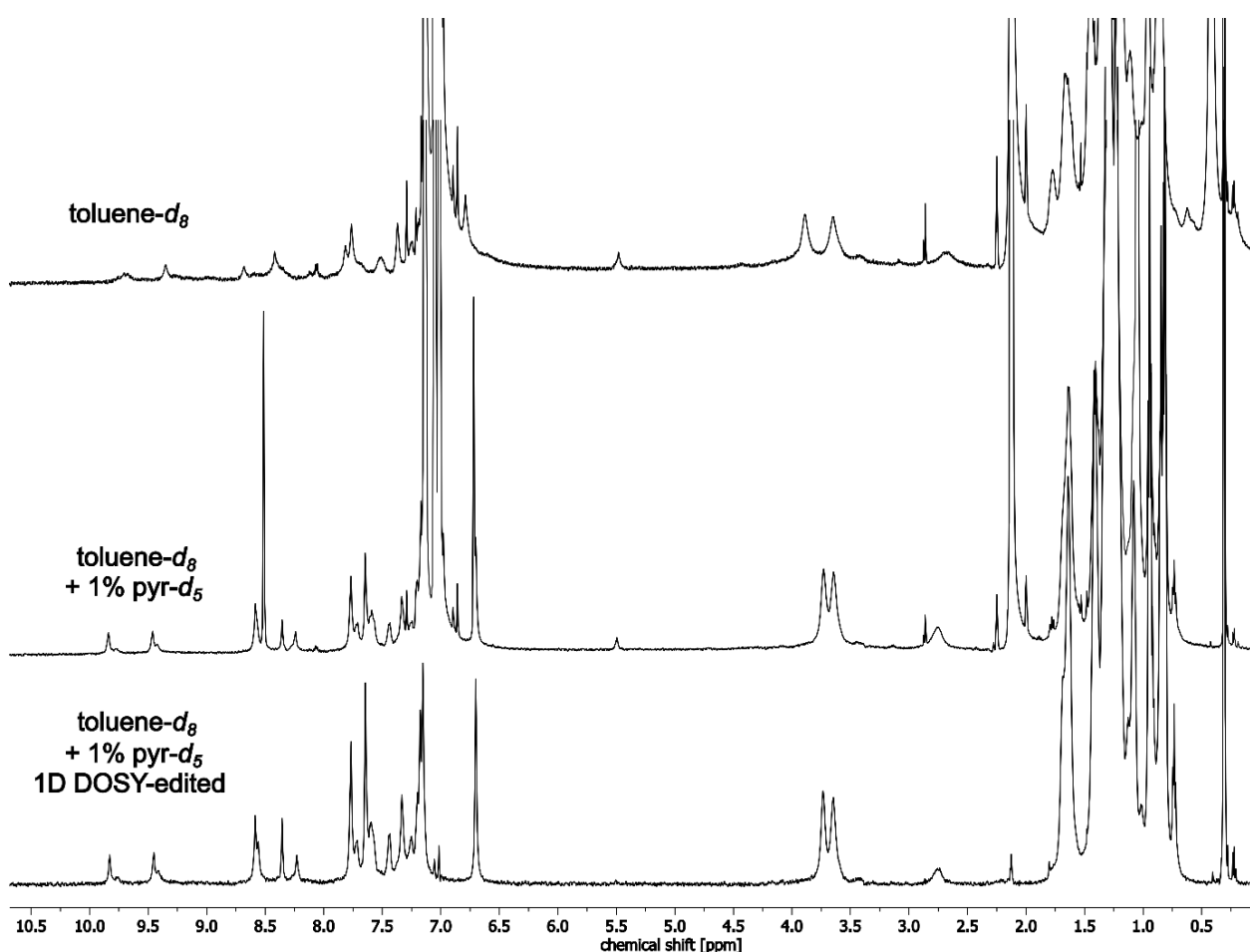


**Figure S45.** Comparison between <sup>1</sup>H NMR spectra of **1** recorded in toluene-d<sub>8</sub> before and after addition of pyridine and DOSY-edited spectrum (to remove the residual solvent peaks). Without pyridine, the sample aggregates strongly, whereas in the presence of pyridine, the peaks become sharper (600 MHz, 298 K).

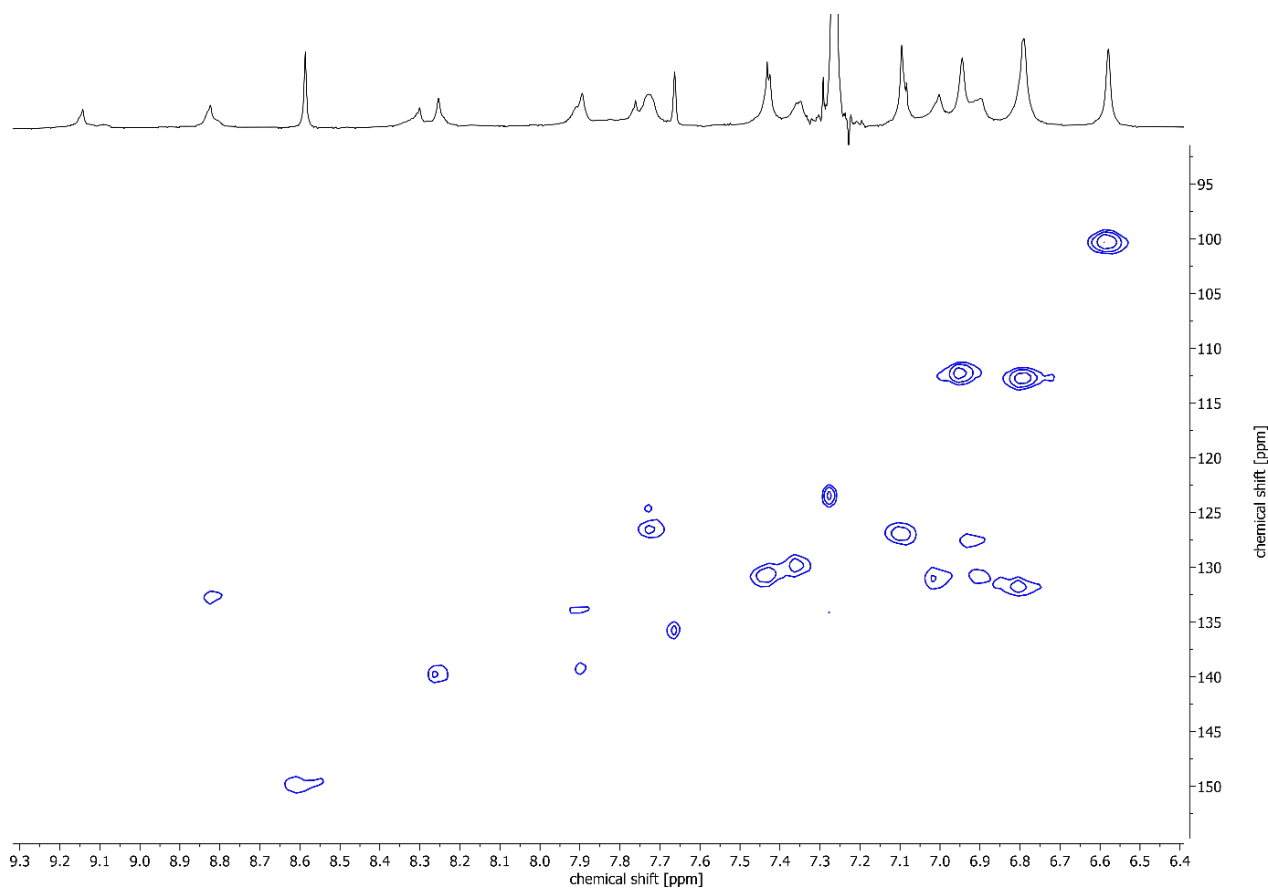


**Figure S46.** Selected aromatic region of a  $^1\text{H}$ - $^{13}\text{C}$  HSQC NMR spectrum of **1**,  $\text{CDCl}_3 + 1\%$  pyr- $d_5$ , 600 MHz, 298 K.

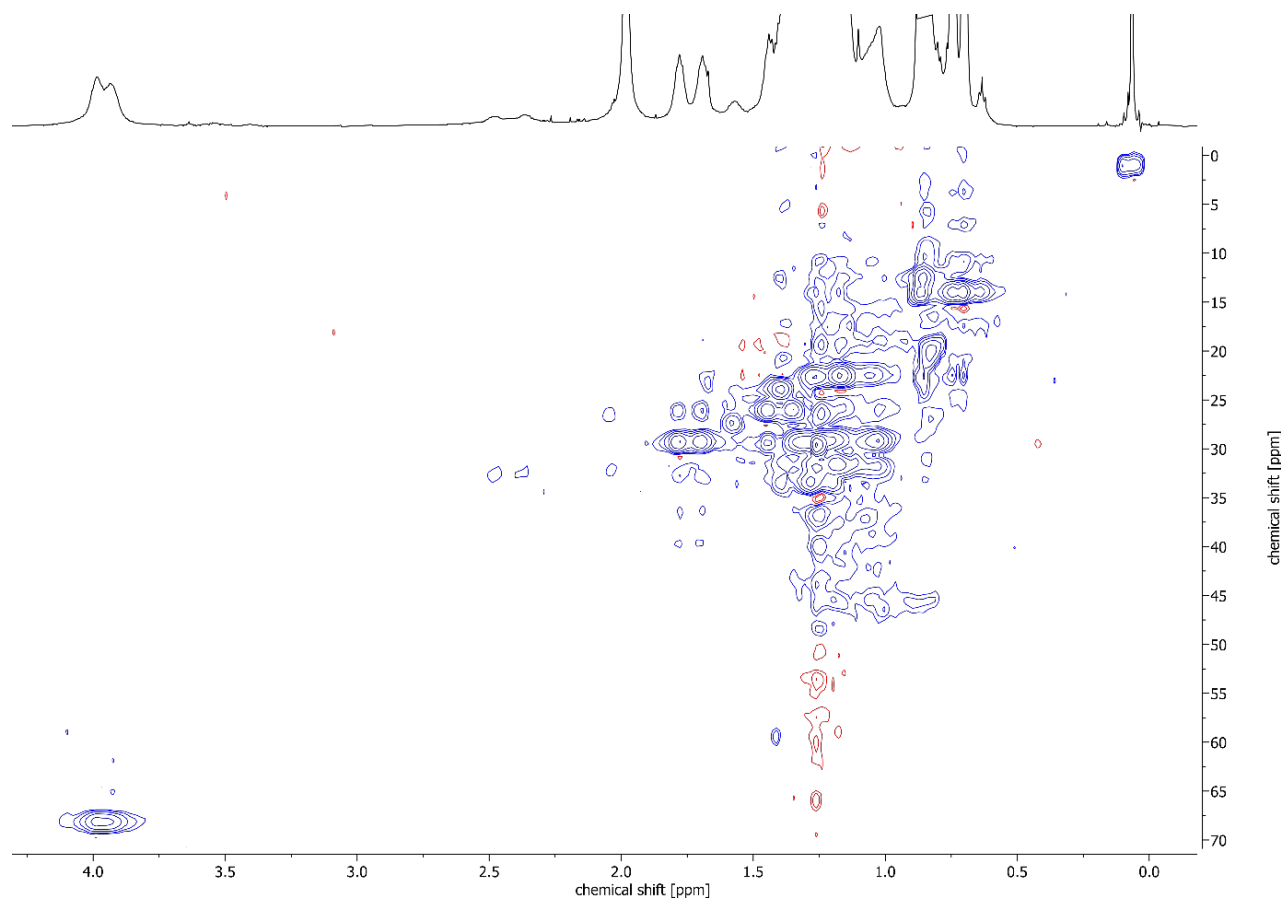


**Figure S47.** Selected alkyl region of a  $^1\text{H}$ - $^{13}\text{C}$  HSQC NMR spectrum of **1**,  $\text{CDCl}_3 + 1\%$  pyr- $d_5$ , 600 MHz, 298 K.

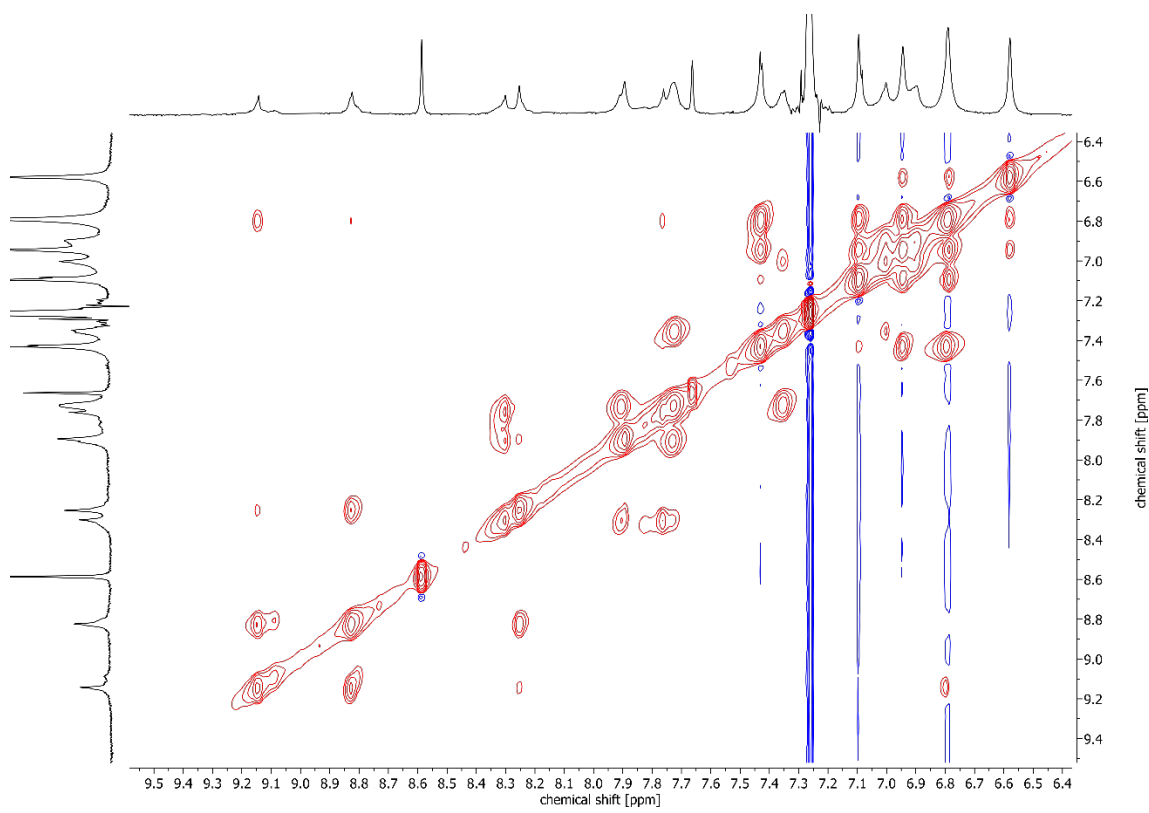


**Figure S48.** Selected aromatic region of a  $^1\text{H}$ - $^1\text{H}$  NOESY NMR spectrum of **1**,  $\text{CDCl}_3 + 1\%$  pyr- $d_5$ , 600 MHz, 298 K. Correlations crucial for signal assignment are marked in colors.

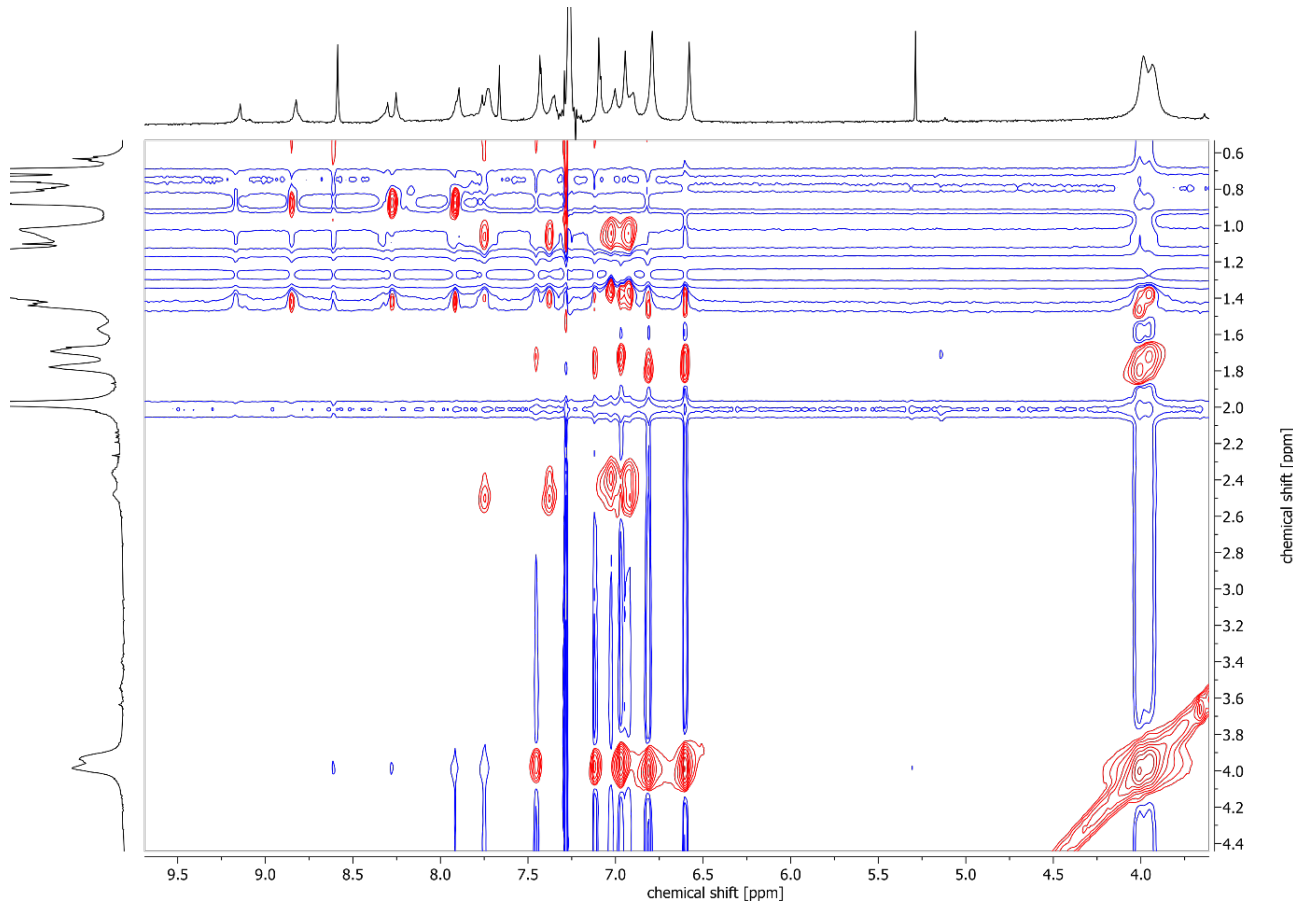


**Figure S49.** Selected region of a  $^1\text{H}$ - $^1\text{H}$  NOESY NMR spectrum of **1**,  $\text{CDCl}_3 + 1\%$  pyr- $d_5$ , 600 MHz, 298 K.

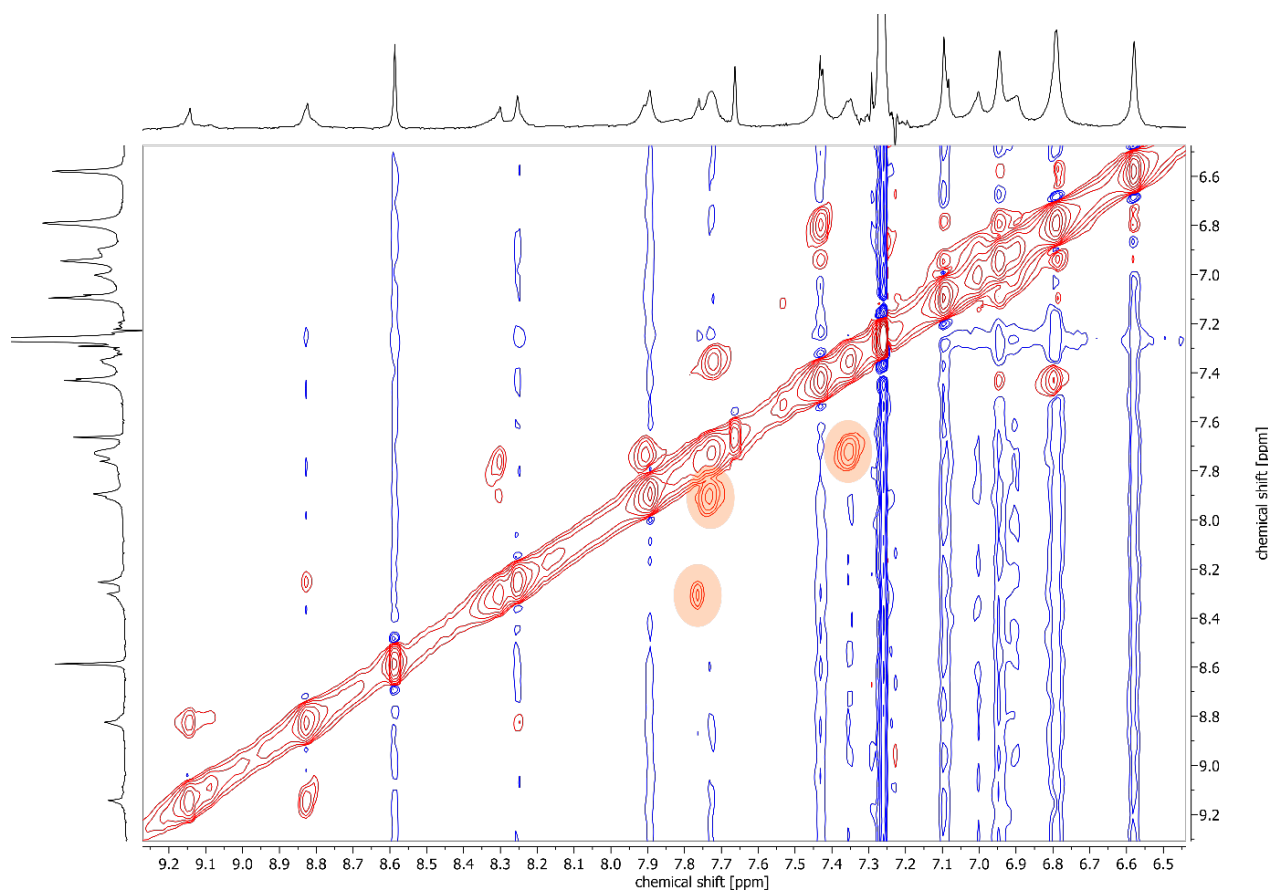


**Figure S50.** Selected aromatic region of a  $^1\text{H}$ - $^1\text{H}$  COSY NMR spectrum of **1**,  $\text{CDCl}_3 + 1\%$  pyr- $d_5$ , 600 MHz, 298 K.  
Correlations between the covalent core phenyls are marked in orange.

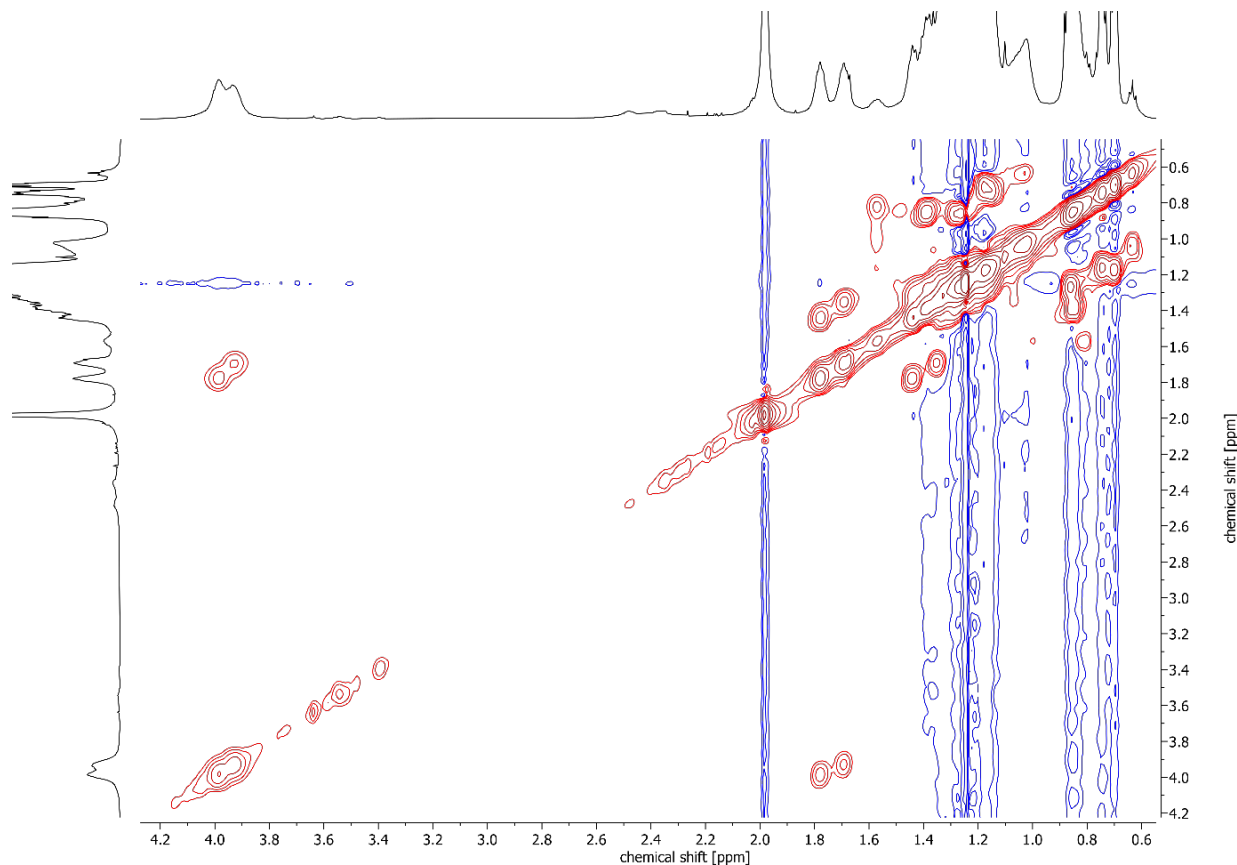


**Figure S51.** Selected aliphatic region of a  $^1\text{H}$ - $^1\text{H}$  COSY NMR spectrum of **1**,  $\text{CDCl}_3 + 1\%$  pyr- $d_5$ , 600 MHz, 298 K.

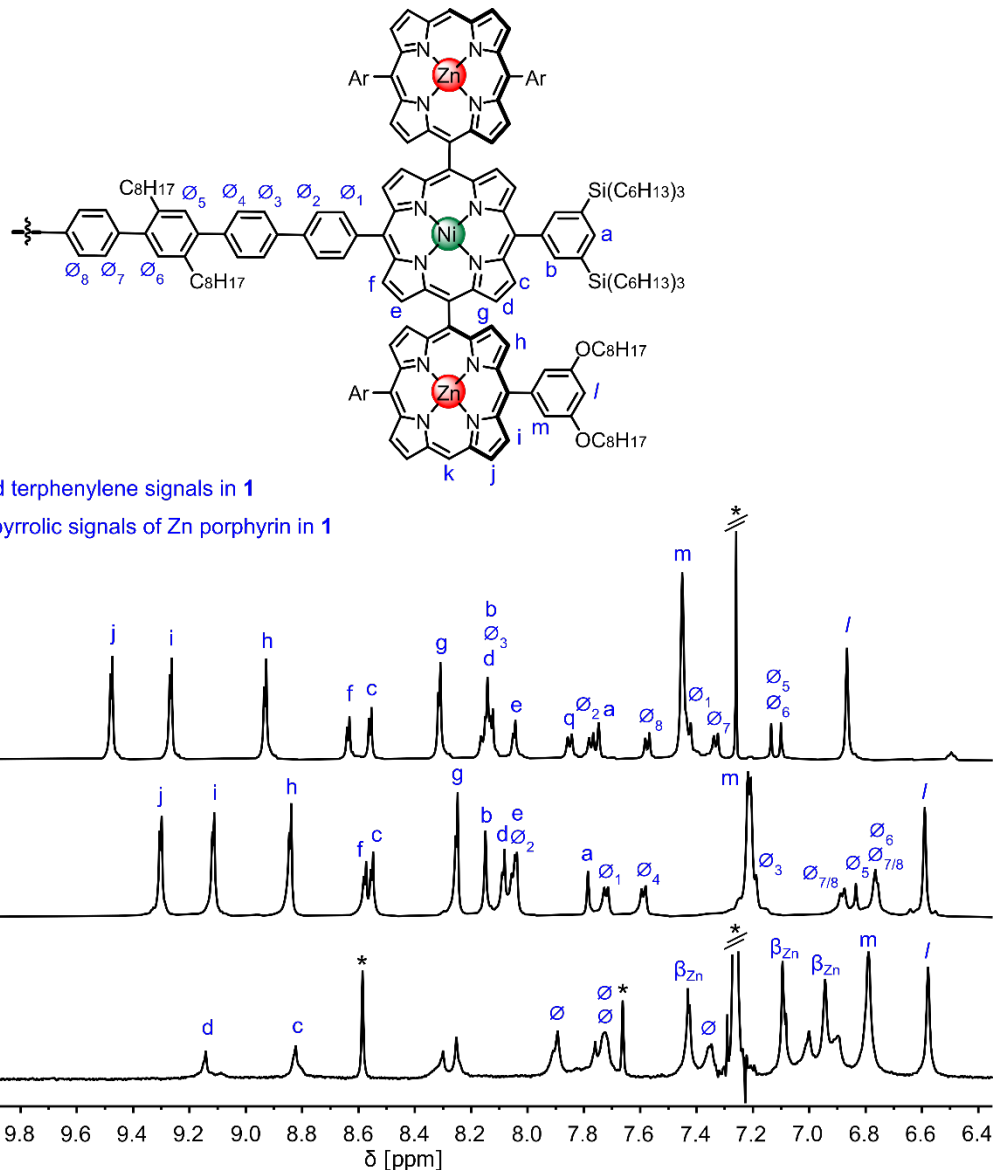


**Figure S52.** Comparison between NMR spectra of **3, 2, 1** and signals assignment. The signals for **1** can only be partially assigned due to substantial overlap and broadening. The positions of  $\beta_{\text{Ni}}$  protons after *meso-meso* coupling and edge-fusion of Zn porphyrins are consistent with a literature example of a linear tetramer<sup>[4]</sup> in which the  $\beta_{\text{Ni}}$  protons resonate in a region  $> 8.5$  ppm (molecule shown on Fig. S51). On the other hand, during edge-fusion the  $\beta_{\text{Zn}}$  protons tend to move to lower chemical shifts, also consistently with the observed loss of one type of  $\beta_{\text{Zn}}$  protons and high-field shift of the three remaining ones.<sup>[4]</sup> Integration of aromatic peaks matches the expected values.

## 5. STM Studies

### 5.1. Experimental Methods

All scanning tunnelling microscopy (STM) images were acquired with an Omicron STM-1 system operating under ultra-high vacuum (UHV) conditions with a base pressure of  $2 \times 10^{-9}$  mbar. Images were acquired at room temperature in constant current mode using electrochemically etched tungsten tips, coated in gold during tip optimisation. Image acquisition parameters (sample bias and current set-point) are stated within figure captions. Au(111) on mica surfaces (Georg Albert PVD GmbH) were prepared by cycles of argon ion sputtering (0.76 keV for 20 minutes at a pressure of  $9 \times 10^{-6}$  mbar) and annealing ( $\sim 500$  °C, 20 minutes). Samples were transported between the STM and x-ray photoelectron spectroscopy (XPS) UHV systems using a vacuum suitcase with a base pressure of  $< 1 \times 10^{-10}$  mbar. Porphyrin 18-mers **1** and **2** were deposited upon a clean Au(111) substrate via electrospray ionization with a Molecularspray UHV4i deposition source. 50 µg/mL solutions of **1** and **2** in toluene/methanol (3:1 ratio) were prepared. **1** was deposited with a solution flow rate of between 0.1 and 0.03 mL/hour for 20 minutes using a potential of 2 kV to initiate the electrospray event (pressure during deposition was  $2 \times 10^{-7}$  mbar). **2** was deposited with a solution flow rate of between 0.1 and 0.03 mL/hour for 40 minutes using a potential of 2 kV to initiate the electrospray event (pressure during deposition was  $2 \times 10^{-7}$  mbar). During the deposition of **2**, the electrospray spot was raster-scanned across the sample.

### 5.2. Details of Nanorings Characterization via STM

Nanoring dimensions were measured from line profiles acquired along the long- and short-axis of the rings; as shown in Fig S53. Peak-to-peak measurements were obtained, to determine the separation between the features corresponding to the position of the nanoring circumference. Measurements were performed on data acquired with both ‘forward’ and ‘backward’ scan directions. An average of the two measurements was taken, to minimize the effect of drift. The circumference of the rings was estimated using the Ramanujan approximation for the circumference of an ellipse:

$$C \approx \pi[3(a + b) - \sqrt{(3a + b)(a + 3b)}],$$

where  $C$  is the circumference of the ellipse, with  $a$  and  $b$  being the radii of the long- and short-axis of the ellipse, respectively.

Using the method previously described, the dimensions of **1** and **2** were obtained following deposition onto Au(111); as demonstrated in Figure S54 (Fig. S54a shows **1**, and Fig. S54b **2**). The average dimensions of the two were measured as follows: **2** circumference =  $15 \pm 1$  nm, long axis =  $5.5 \pm 0.3$  nm, short axis =  $4.3 \pm 0.2$  nm. **1** circumference =  $12 \pm 1$  nm, long axis =  $4.1 \pm 0.3$  nm, short axis =  $3.7 \pm 0.3$  nm. Due to difficulties in obtaining stable imaging conditions, the number of **2** rings suitable for measuring was limited, with a total sample size of 8. The sample for **1** consisted of 60 individual rings.

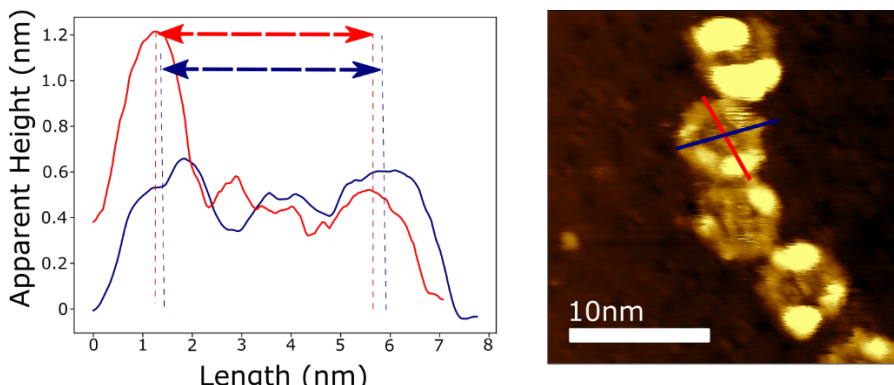


**Figure S53.** Line profiles acquired for the long- and short-axis of **1** deposited on an Au(111) surface (line-profile locations are indicated within the STM image). The peak-to-peak separation on the red and blue line profiles are 4.3 nm and

4.4 nm, respectively. The STM topograph shows **1** on Au(111) following electrospray deposition (sample bias = -2 V, set-point current = 15 pA).

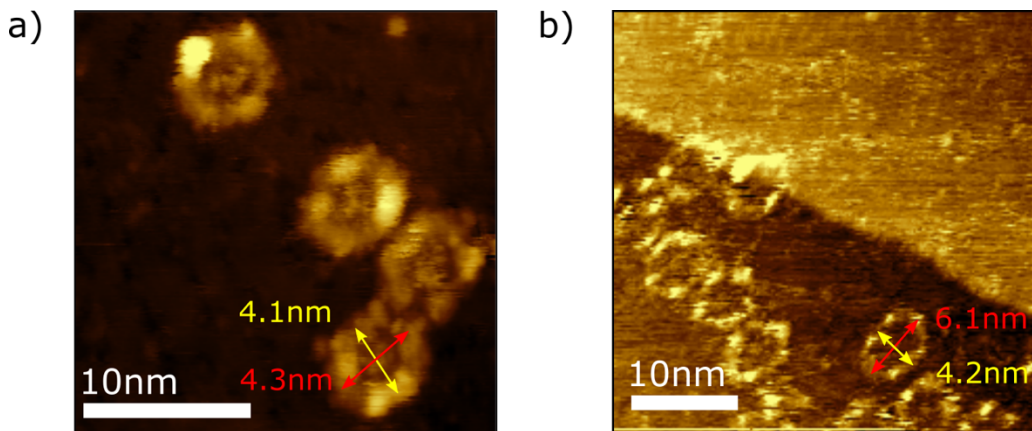


**Figure S54.** STM topographs of (a) **1** and (b) **2** following electrospray deposition onto Au(111) substrates. Measurements of the ring dimensions were acquired from this type of image (measurement positions indicated by red and yellow arrows). Image parameters: (a) sample bias = -2 V, set-point current = 15 pA. (b) sample bias = -1 V, set-point current = 20 pA.

### 5.3. Characterization of nanoring internal scaffold

The internal scaffold of **1** is observed in STM imaging. Figure S55 shows an STM topograph of several **1** adsorbed at the Au(111) surface; the associated line-profile reveals the presence of a topographic feature at the center of the ring which is assigned to the presence of the covalent template. Such features were not observed previously during measurements of a template-free 24-porphyrin nanoring.<sup>[5]</sup>

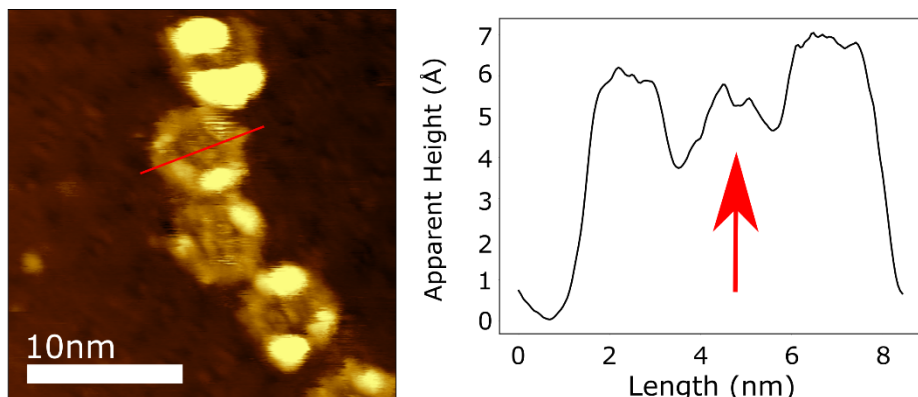


**Figure S55.** STM image of **1** deposited onto Au(111), with a line profile taken across the center of the ring (sample bias = -2 V, set-point current = 15 pA). The location of the line profile is indicated by the red line. The red arrow points to the raised feature in the center of the ring; assigned to the presence of the template.

### 5.4. Characterization of **1** and **2**

The dimensions of the long- and short-axis of **1** and **2** were acquired for both species following electrospray deposition onto two separate Au(111) substrates. Figure S56 displays the measured dimensions as well as the average circumference (as estimated by the Ramanujan approximation) for each species and black solid/dashed lines representing flattening factor,  $f$ :

$$f = \frac{a-b}{a},$$

where  $a$  and  $b$  are the long and short, respectively, radii of the ellipse defined for each nanoring species. The majority of **1** species have a flattening factor of  $f < 0.2$  (indicating a limited deviation from circularity) with **2** species showing increased flattening ( $f < 0.4$ ). This is attributed to the increased rigidity of **1** due to the fusing of the Zn porphyrin species.

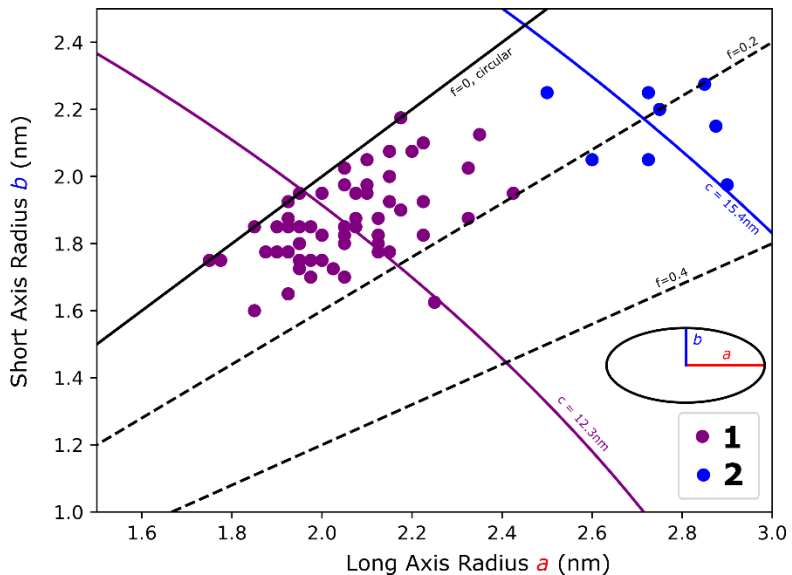


**Figure S56.** Graph showing experimentally measured long- and short-axis for **1** and **2** nanorings deposited onto Au(111). The blue and purple arcs correspond to an ellipse of fixed circumference; equivalent to the average circumference obtained for each nanoring deposition (circumference = 12.3 nm for **1**, 15.4 nm for **2**). The solid black line represents a flattening ratio of 0, indicating a circular ring shape. The dotted lines represent flattening ratios of 0.2 and 0.4, the shape becoming more elliptical with increasing *f* value. The dataset for **1** and **2** is based upon 60 and 8 rings, respectively.

### 5.5. Overview of surface following electrospray deposition

Sub-monolayer coverages of **1** and **2** were obtained following electrospray deposition. Large-area STM topographic images showing the presence of individual molecules and small clusters of **1** and **2** are shown in Figure S57.

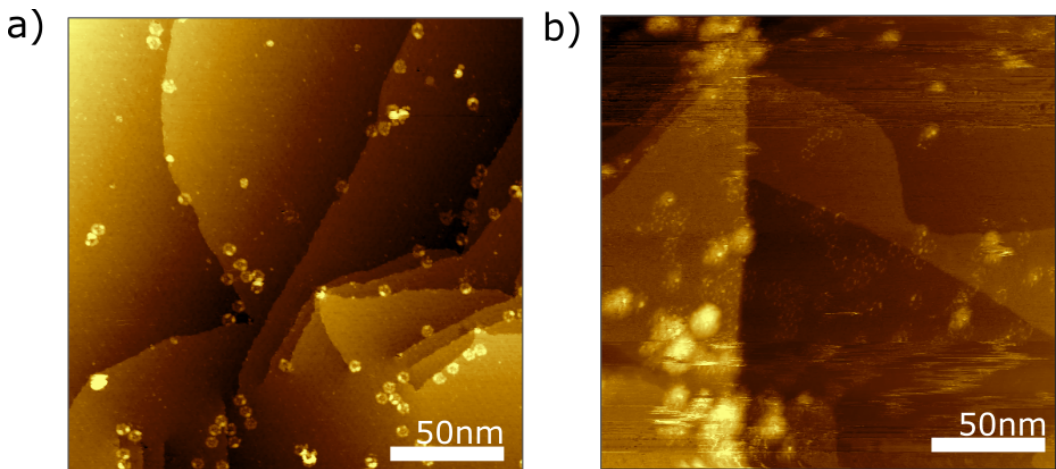


**Figure S57.** STM topographic images showing the distribution of (a) **1** (sample bias = -2.0 V, set-point current = 15 pA) and (b) **2** (sample bias = -1.0 V, set-point current = 20 pA) on Au(111) following electrospray deposition.

### 5.6. X-ray photoelectron spectroscopy (XPS) characterization

X-ray photoelectron spectroscopy (XPS) was acquired using a SPECS DeviSim near ambient pressure XPS (NAP-XPS) instrument operating in ultra-high vacuum (UHV) mode at a pressure  $< 1 \times 10^{-9}$  mbar. Spectra were measured using a Phoibos 150 NAP hemispherical analyzer with 20 eV pass energy and monochromatic Al  $K\alpha$  X-rays (1486.7 eV). All spectra are calibrated with respect to the Au 4f<sub>7/2</sub> peak at 83.95 eV.

Analysis of the Ni 2p and Zn 2p<sub>3/2</sub> regions reveals features consistent with the presence of Ni- and Zn-porphyrin species. For **1** the Ni 2p<sub>3/2</sub> peak is observed at a binding energy (BE) of 855.3 eV, consistent with a Ni(II) oxidation state<sup>[6]</sup> and clearly distinct from the expected BE of metallic Ni (852.6 eV);<sup>[7]</sup> for **2** the Ni 2p<sub>3/2</sub> peak is observed at a similar position 855.1 eV. The Zn 2p<sub>3/2</sub> region reveals peaks at 1022.1 eV and 1021.4 eV,

for **1** and **2** respectively; definitive identification of the Zn(II) state, compared to Zn(0), is non-trivial.<sup>[8]</sup> The shift to higher BE, of **1** relative to **2**, is assigned to the conformational differences between the two species. The ‘non-fused’ structure of **2** provides greater flexibility and facilitates an increased interaction with, and proximity to, the Au surface, as compared to **1**; we therefore assign this shift to higher BE to a reduced screening effect from the Au surface.

The ratio of Zn to Ni species was obtained by comparing the ratio of the fitted peak areas of Ni 2p<sub>3/2</sub> and Zn 2p<sub>3/2</sub> [normalized to the relevant photoionization cross-sections]. The calculated Zn:Ni ratio is 2:1, in agreement with the expected ratio of Zn- to Ni-porphyrins in both **1** and **2**.

For both **1** and **2** the N 1s region shows a feature which can be fitted to a single peak (BE 398.6 eV and 398.3 eV for **1** and **2**, respectively). A single peak N 1s is indicative of metallated porphyrin species,<sup>[9]</sup> and the calculated N:Zn ratio of 6:1 (obtained from the fitted peak areas of N 1s and Zn 2p<sub>3/2</sub> - normalized to the photoionization cross-sections), is in excellent agreement of the expected ration of N to Zn in **1** and **2**.

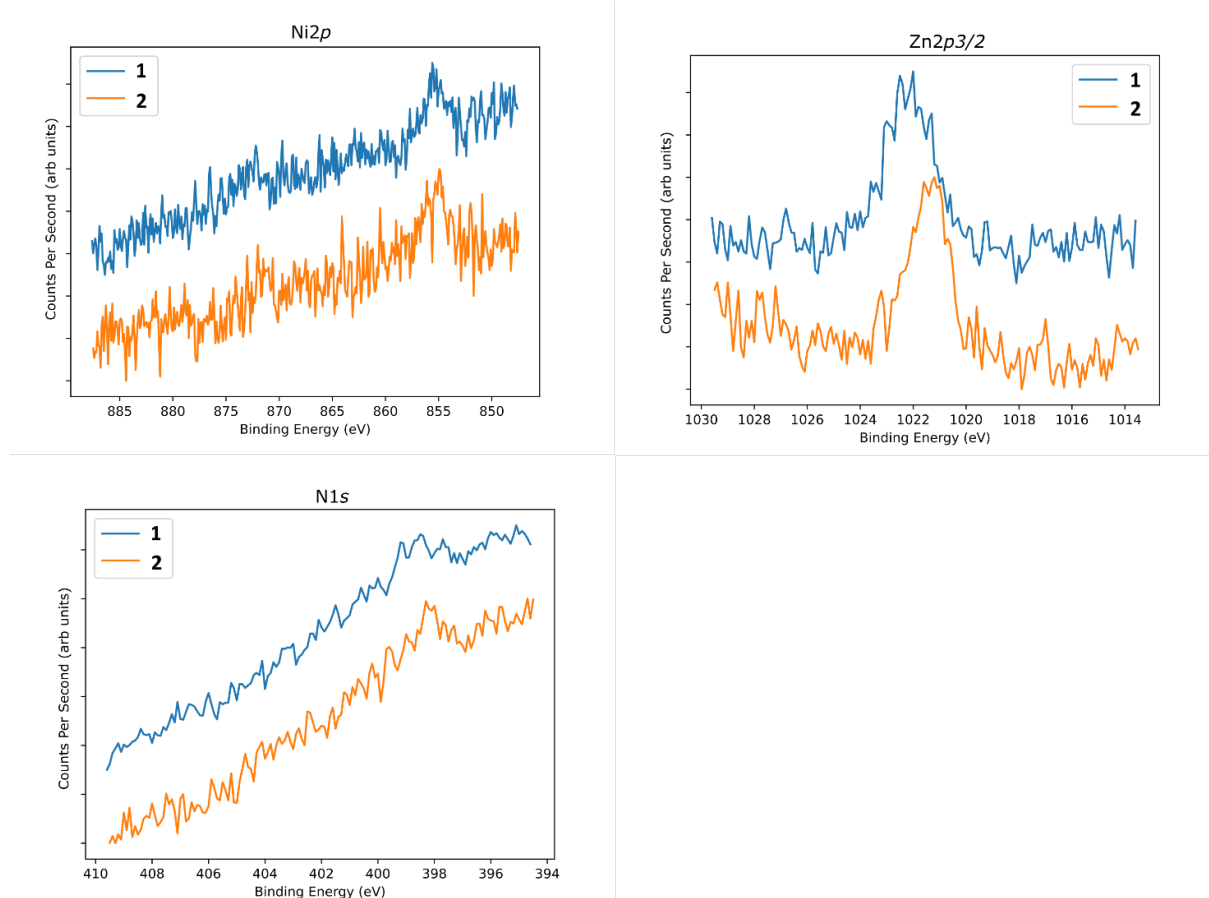


**Figure S58.** XPS analysis of the Ni 2p, N 1s and Zn 2p<sub>3/2</sub> regions. The N 1s spectra indicate a single nitrogen environment, and the presence of Ni and Zn suggests deposition of metallated porphyrins. Note: **2** spectra are for ‘as-deposited’ samples. **1** spectra were acquired following anneal (to remove excess solvent)

## 6. Calculated Molecular Geometries

Geometries were optimized using semiempirical tight binding *xTB* software (version 6.4.1) using *GFN1* parameters.<sup>[10]</sup> We calculated all the vibrational frequencies and none of them were imaginary. Alkyl and aryl solubilizing groups were replaced by hydrogen atoms to simplify the calculations.

### 5.1. Optimized geometries

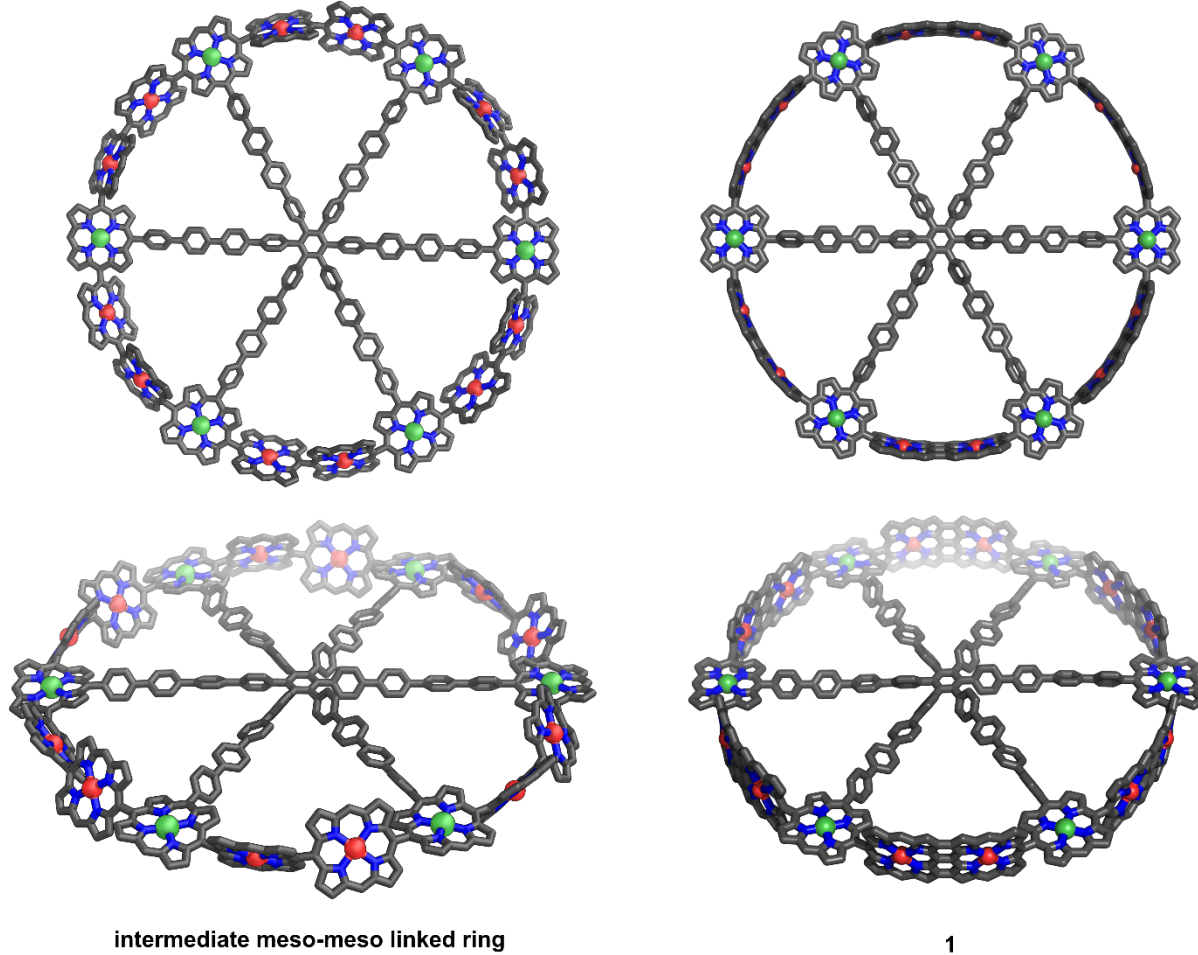


**Figure S59.** Optimized geometries of an intermediate *meso-meso* linked nanoring (not isolated, left) and **1** (*xTB gfn1*, right).

### 6.2. Cartesian coordinates

#### Meso-meso linked intermediate nanoring

total E = -1488.109640273214 Ha

```

C  -21.06182012125783  -3.32011068025697  0.57996485725008
C  -20.84960738355983  -3.88938678646352  -0.72514975478910
C  -20.25615352337072  -3.22345525259072  -1.80732798798097
C  -19.93204023414346  -3.80553305766126  -3.03751646148943
C  -19.27183012012685  -3.14830775460759  -4.13479693479310
C  -19.13800834415476  -4.06385049701707  -5.12684185822233
C  -19.74811778229369  -5.28062468994155  -4.66426118903151
N  -19.70438786857076  -5.09416364100144  -3.39253539658350
C  -21.66524866724693  -4.26984687635990  1.33746213885290
C  -21.84734773925024  -5.42282027811207  0.49956879980284
N  -21.31815337289633  -5.16849636063169  -0.73396832679961
C  -22.53849684111650  -6.57345024232706  0.85768646254165
C  -22.84600253341167  -7.65235751689262  0.03643869592351
N  -22.42763993844694  -7.81838684886352  -1.25269094507948
C  -23.00877111295170  -8.95559232153662  -1.73306789334684
C  -23.83922857013660  -9.52547675802147  -0.70356538037952
C  -23.71881488967487  -8.73590201999255  0.39252183419362
N  -21.30621143844158  -7.75662508641962  -3.90562232772708
C  -20.62806720527067  -7.57322817889020  -5.07669274259963
C  -19.90176393463867  -6.43790617822442  -5.41994149507493
C  -20.86124733305557  -8.70125113426414  -5.93641916661944
C  -21.70906413423699  -9.53331292565153  -5.28056957709876
C  -21.99119875072338  -8.93184344343664  -4.00399248860442
C  -22.83258882633272  -9.47356416288971  -3.02418057483861
H  -20.77102081410258  -2.32404992085486  0.87358603027479
H  -18.94861725643294  -2.11963058400247  -4.13491881517828
H  -18.68812399911396  -3.93163715523332  -6.09849840201446
H  -21.97599723072025  -4.20248187748263  2.36834226243266
H  -22.93444549319886  -6.60621279228414  1.86806133275707
H  -24.19344077147774  -8.85437132622622  1.35406647601473
H  -19.45472005820147  -6.43170085912775  -6.40937713102586
H  -20.43436732974602  -8.82448462993215  -6.91953966991505
N  -39.19488854948825  -21.01032439351591  -3.63949465428548
C  -37.26665082189309  -19.87946252956641  -2.63074473230500

```





















